

Unbundling Quantitative Easing: Taking a Cue from Treasury Auctions*

Michael Droste Yuriy Gorodnichenko
Harvard University UC Berkeley and NBER

Walker Ray
London School of Economics

December 3, 2021

Abstract

We study empirically and theoretically the role of preferred habitat in understanding the economic effects of the Federal Reserve’s quantitative easing (QE) purchases. Using high-frequency identification and exploiting the structure of the primary market for U.S. Treasuries, we isolate demand shocks that are transmitted solely through preferred habitat channels, but otherwise mimic QE shocks. We document large “localized” yield curve effects when financial markets are disrupted. Our calibrated model, which embeds a preferred habitat model in a standard New Keynesian framework, can largely account for the observed financial effects of QE. We find that QE is modestly stimulative for output and inflation, but alternative policy designs can generate stronger effects.

Keywords: quantitative easing, monetary policy, market segmentation, treasury auctions

JEL Classification: E52, E43, E44

*We thank Harald Uhlig, anonymous referees, Michael Bauer, Rhys Bidder, Michael Fleming, Ed Knotek, Matteo Maggiori, Eric Swanson, Michael Weber, Milena Wittwer, and seminar participants at Berkeley, New York Fed, Cleveland Fed, San Francisco Fed, Chicago Fed, ASU, DEC, CMC, Bilkent, GWU, Texas A&M, and Northwestern for comments on an earlier version of the paper. We are grateful to Maxime Sauzet for excellent research assistance.

1 Introduction

Demand for safe assets, and U.S. Treasuries in particular, plays a central role in the macro-financial landscape. The past decade saw the introduction of a new feature: large-scale asset purchases (LSAPs) implemented by central banks, representing a sharp increase in demand for safe assets. The most salient of these are the quantitative easing (QE) programs carried out by the Federal Reserve, which originated during the global financial crisis and reemerged during the COVID-19 crisis.

While evaluating the first rounds of QE, then-Fed chair Ben Bernanke observed, “The problem with QE is it works in practice but it doesn’t work in theory.” Indeed, QE was successful in reducing short- and long-term interest rates, but the mechanisms behind these effects are still not well-understood. For instance, standard models imply that Treasury demand is determined solely by economic agents’ intertemporal consumption decisions, which does not capture the sources of demand shifts initiated by the Fed.

Although workhorse macroeconomic models cannot readily explain the workings of QE, several explanations have been put forth. For instance, QE could have signaled to financial markets that the Fed was committed to keeping short-term interest rates low for a long time (forward guidance). Or, perhaps the Fed exploited financial market frictions (limited arbitrage and market segmentation) by purchasing securities in a particular segment. Alternatively, large-scale asset purchases by the Fed could signal a poor state of the economy, pushing interest rates down (“Delphic effect”).¹ Given the paucity of QE events, it has been difficult to provide clear empirical evidence for (and to assess the relative contributions of) the proposed channels. Moreover, QE policies have been implemented as responses to severe macroeconomic conditions, which further confounds identification and interpretation.

The objective of this paper is to unbundle the effects of QE by focusing on a specific channel: market segmentation and *preferred habitat*, which posits that certain investors have preferences for specific maturities. To this end, we take the following approach. First, we identify shifts in *private* demand for Treasuries that mimic QE, but are independent of all other plausible channels of QE. Next, we analyze the propagation of these demand shocks across financial markets. In particular, we assess the ability of preferred habitat theory to rationalize the observed responses, and we confirm key predictions regarding pass-through of demand shocks in and out of financial crises. Informed by our empirical analysis, we then develop a general equilibrium macroeconomic model designed to study QE policies. Our model suggests that the preferred habitat channel accounts for the bulk of the observed response to QE in financial markets. Finally, while QE has modest stimulative effects on output and inflation in our model, we explore counterfactual alternative

¹See, [Campbell et al. \(2012\)](#), [Martin and Milas \(2012\)](#) and [Bhattarai and Neely \(2020\)](#) for surveys of the literature.

QE implementations that can help improve the design of future asset purchases.

Our analysis starts with the key insight that the mechanism through which market segmentation and preferred habitat forces operate is not the source of Treasury quantity shocks *per se*, but rather how marginal investors in the market for Treasury debt absorb these shocks. We utilize the primary market for Treasuries to identify demand shifts that are independent of all QE propagation mechanisms besides preferred habitat. Although the primary market is the venue through which the Treasury issues debt (a supply-side action), the institutional structure of Treasury auctions has a number of desirable features for identifying shocks on the demand-side of the market. Crucially, the Treasury announces all features of the auction (e.g. maturity, the amount of newly offered and outstanding securities) many days before each auction. Because all of the supply information is known before the close of each auction, the release of the auction results reveal unexpected shifts in demand alone, allowing us to rule out a host of confounding factors. By utilizing high-frequency (intraday) changes in Treasury yields around the close of Treasury auctions, we are able to construct a novel measure of private demand shocks.

We document that demand shocks are reasonably large and persistent, with effects on yields typically lasting for many weeks following the auction. Furthermore, the surprise movements in demand are driven by institutional investors such as foreign monetary authorities, investment funds, insurance companies and the like. We show that these shocks are not driven by market-wide changes in expectations about inflation, output, or other general macroeconomic and financial conditions. Therefore, variation in Treasury yields around the release of Treasury auction results can help us to isolate the effect of *idiosyncratic* purchases in specific asset segments on the level and shape of the yield curve, which is difficult to achieve by examining only QE events. Because Treasury auctions are frequent and information spans many decades, we can study state dependence in the effect of targeted purchases of assets (e.g., crisis vs. non-crisis states), which is instrumental for understanding how QE-like programs can work in normal times. Importantly, because Treasury auctions for specific maturities are spread over time, we can identify changes in demand for government debt of specific maturities and trace the effect of these changes on other parts of the yield curve. In this sense, we have natural experiments which can mimic targeted purchases of the Fed during QE programs.

We use our auction demand shocks to empirically evaluate the “localization hypothesis,” a characteristic prediction of preferred habitat theory and a key input into our subsequent quantitative analyses. After deriving a simple regression specification informed by theory, we document strong evidence in favor of localized yield curve effects during financial crisis periods (i.e., the location of the demand shock in maturity space matters and the effects on the yield curve are larger for bonds of similar maturities), suggesting potentially powerful effects of QE on yields in crises. We cannot reject the null of no localization effects during normal times, which suggests a limited use of QE as a conventional

policy tool.

Building on [Vayanos and Vila \(2021\)](#) and [Ray \(2019\)](#), we develop a general equilibrium model with risk-free and risky debt to rationalize the empirical responses of the yield curve to shocks in demand for Treasury securities and to better understand the effects of QE on financial markets and the broader economy. We calibrate the model to match a variety of moments for yields and macroeconomic variables as well as the responses of yields to surprise movements in *private* demand during Treasury auctions in “crisis” and “non-crisis” times. When fed a shock mimicking QE1 in size and duration, our model generates movements in the yield curve remarkably close to those observed in the data. This result is consistent with the view that QE works mainly via market segmentation and preferred habitat, and that the *net* effect of other channels is small. Because the financial sector is embedded in a New Keynesian general equilibrium model, we can also study the macroeconomic effects of QE1. In our calibrated model, QE1 in “crisis” stimulates output and inflation approximately as much as a persistent 25-50 b.p. rate cut in “non-crisis” times.

Our policy experiments in the model indicate that these relatively modest macroeconomic effects are sensitive to the implementation details of QE. In particular, holding the securities on the balance sheet longer (and making this clear to markets on announcement) boosts the stimulative power of QE significantly. We also show that QE may have unintended consequences: uncertainty surrounding the Fed’s asset purchases themselves may lead to excess macroeconomic volatility, thus calling for policy guidance. The expansionary effects of QE fall precipitously when undertaken during periods when bond markets are relatively healthy. Finally, QE programs tilted towards risky assets (e.g., mortgage-backed securities) are more effective in stimulating the economy when these assets are more volatile. Taken together, these results suggest that QE should remain in policymakers’ toolkit, but must be utilized with caution.

Our paper makes three primary contributions. First, we develop a novel, high-frequency measure of demand shocks for Treasuries by exploiting the institutional structure of Treasury auctions. A well-identified shock series is crucial for improving our understanding of a wide range of quantity-driven macro-finance theories, and we hope our measure will be analyzed and extended in future work in a fashion similar to the high-frequency monetary shocks pioneered by [Kuttner \(2001\)](#), [Bernanke and Kuttner \(2005\)](#), [Gürkaynak et al. \(2007\)](#), and others. Our approach is a natural next step to complement existing empirical approaches estimating affine term structure models ([Hamilton and Wu \(2012\)](#), [Kaminska and Zinna \(2020\)](#)) or demand systems ([Kojen et al. \(2021\)](#)) using lower frequency data.

Second, we provide strong empirical evidence for *state-dependent* localization effects in the spillovers across maturities of surprise movements in Treasury demand. This new finding confirms one of the characteristic predictions of preferred habitat theory, and

thus our paper shows that these mechanisms are crucial in understanding the Treasury market. While there is extensive research on how QE purchases impacted the yield curve (e.g. [D’Amico and King \(2013\)](#), [Li and Wei \(2013\)](#), [Cahill et al. \(2013\)](#), [King \(2019b\)](#)), our approach allows us to isolate and confirm the role of preferred habitat in explaining localization effects. Hence, our results clarify one of the key channels through which QE purchases affect yields. Put differently, in the spirit of [Fieldhouse et al. \(2018\)](#) and [Di Maggio et al. \(2020\)](#), we use QE-like events (rather than QE directly) and rich cross-sectional variation in order to obtain sharp identification and precise estimates.

Third, we embed a financial model of the entire term structure of interest rates within a dynamic model of the macroeconomy and thus can provide an integrated analysis of QE. This is important because previous studies of QE largely focus separately on either financial variables or macroeconomic variables. For example, [Krishnamurthy and Vissing-Jorgensen \(2012\)](#) and [Chodorow-Reich \(2014\)](#) study the effects of QE announcements on financial markets, but do not quantify the macroeconomic effects of QE. Papers such as [Vayanos and Vila \(2021\)](#), [Greenwood and Vayanos \(2014\)](#), [Greenwood et al. \(2016\)](#), [King \(2019a\)](#) and related work explore the financial market implications of preferred habitat theory, but are silent on any potential effects on output or inflation. On the other hand, recent developments in macroeconomic theory (e.g., [Sims and Wu \(2020\)](#), [Gertler and Karadi \(2011\)](#), [Karadi and Nakov \(2020\)](#), [Cúrdia and Woodford \(2011\)](#), [Carlstrom et al. \(2017\)](#), and [Chen et al. \(2012\)](#)) concentrate on aggregate variables, but are unable to capture the rich dynamics in bond markets which we document. Moreover, many of these theories rely on reserve requirements or moral hazard/enforcement constraints on banks as the key channel through which QE works. In contrast, we focus on the interaction of preferred habitat with limited risk-bearing capacity in bond markets as the core mechanism behind QE effects. Our quantitative model merges these literatures: we utilize financial data and high-frequency identification to discipline our model, which we then use to quantify the macroeconomic effects of QE. Relative to the model of [Ray \(2019\)](#), we introduce risky assets (which provides a more realistic modeling of QE1 and households’ borrowing rates) and provide quantitative analysis of different designs of QE policy experiments (e.g., we shed light on how the allocation of QE across risky and risk-free assets can affect the macroeconomy).

Our paper is related to a broad set of papers studying Treasury auctions, investigating how yields move around Treasury auctions (e.g., [Lou et al. \(2013\)](#), [Fleming and Liu \(2016\)](#)) and respond to variation in demand (e.g., [Cammack \(1991\)](#), [Beetsma et al. \(2016, 2018\)](#), [Forest \(2018\)](#)). However, our focus is not Treasury auctions in and of themselves; rather, we exploit the institutional structure of the primary market for Treasuries to better understand the mechanisms behind QE. More broadly and in contrast to this literature, we *structurally* link demand shocks identified from Treasury auctions to a general equilibrium preferred habitat model.

2 Data and Institutional Details

In this section we describe the primary sources of our data and present basic statistics. First, we describe the U.S. Treasury auctions for U.S. government notes and bonds (coupon-bearing nominal securities). Second, we describe the details of the data regarding intraday secondary-market Treasury prices.

2.1 Primary Market for Treasury Securities

The Treasury sells newly issued securities to the public on a regular basis through auctions. In recent years, 2-, 3-, 5- and 7-year notes are auctioned monthly. 10-year notes and 30-year bonds are auctioned in February, May, August and November with reopenings in the other 8 months. The frequency of auctions has changed over time. For example, 30-year bonds were not issued between 1999 and 2006 and were issued only twice a year between 1993 and 1999; and 20-year bonds were auctioned in May 2020, the first time since 1986.

There are two types of bids: noncompetitive and competitive. Noncompetitive bidders agree to accept the terms settled at the auction, and are typically limited to \$5 million per bidder. Competitive bidders submit the amount they would like to purchase, not exceeding 35% of the amount offered at auction, and the price (the interest rate) at which they would like to make the purchase.

Auction participants include primary dealers, other non-primary brokers and dealers, investment funds (for example, pension, hedge, mutual), insurance companies, depository institutions, foreign and international entities (governmental and private), the Federal Reserve System Open Market Account (SOMA), and individuals. These participants are classified into three groups: primary dealers, direct bidders, and indirect bidders. Primary dealers (brokers and banks) trade on their account with the Federal Reserve Bank of New York; they are required to participate in every Treasury auction, and typically buy the largest share of auctioned debt. Direct bidders are non-primary dealers who submit bids for their own proprietary accounts. Indirect bidders submit competitive bids via a direct submitter, including foreign and international monetary authorities placing bids through the Federal Reserve Bank of New York.²

Additionally, the Treasury divides investors into the following classes: Investment Funds (mutual funds, money market funds, hedge funds, money managers, and investment advisors); Pension and Retirement Funds and Insurance Companies (pension and retirement funds, state and local pension funds, life insurance companies, casualty and liability insurance companies, and other insurance companies); Depository Institutions

²Starting in 1997, the SOMA amount was changed from being listed within the announced offering amount to being additions to the announced offering amount. That is, if the Treasury auctions \$15 billion in bonds and the Federal Reserve would like to purchase \$1 billion in the auction, the Treasury issues \$16 billion in bonds. This change was made so that the Treasury would be able to provide better information to the market about the amount of securities actually available for sale to the public.

(banks, savings and loan associations, credit unions, and commercial bank investment accounts); Individuals (individuals, partnerships, personal trusts, estates, non-profit and tax-exempt organizations, and foundations); Dealers and Brokers (primary dealers, other commercial bank dealer departments, and other non-bank dealers and brokers); Foreign and International (private foreign entities, non-private foreign entities placing tenders external of the Federal Reserve Bank of New York (FRBNY), and official foreign entities placing tenders through FRBNY); Federal Reserve System; Other (categories not specified in investor class descriptions above). [Fleming \(2007\)](#) describes the breakdown by types and class of bidders in greater detail.

As detailed in [Figure 1](#), there are four stages of a Treasury auction:³

1. *Announcement*: The Treasury releases all pertinent information regarding an upcoming auction a few days prior to the auction date. An announcement includes security information (maturity, CUSIP identifier, schedule of coupon payments, etc.) as well as the amount offered, the bidding closing times, which class of bidders can participate, and other information describing the rules of the auction.

[Figure 2a](#) presents a typical announcement. At this auction, the Treasury offers \$16 billion in 30-year bonds. This is a new auction (the Treasury does not reopen a previous auction) with a maximum award (maximum allocation to a bidder) of \$5.6 billion.

2. *Bidding*: After the announcement, individuals and institutions may submit bids up until the auction closing time. The announcement in [Figure 2a](#) stipulated that non-competitive bids should be submitted by 12:00 p.m., while the deadline for competitive bids is 1:00 p.m.
3. *Results*: Most Treasury note and bond auctions close at 1:00 p.m. Competitive bids are accepted in ascending order (in terms of yields) after the auction closes until the quantity meets the amount offered minus the amount of non-competitive bids. All bidders receive the same yield as the highest accepted bid. Once the auction closes and the winning bids are determined, the information regarding the results is released immediately. Besides the winning yield, the Treasury announces various aggregate statistics regarding the bidding. Beginning in the early 2000s, auction results are released within minutes of the close of the auction (see [Garbade and Ingber \(2005\)](#)).

[Figure 2b](#) presents a typical announcement about auction results, which corresponds to the auction announcement presented in [Figure 2a](#). The demand (tendered) for the security was \$33.3 billion. Primary dealers account for most bids (\$23.7 billion), \$489.9 million was bought by the Federal Reserve (SOMA), and a relatively low amount was bought via non-competitive bids (\$14.8 million). The “bid-to-cover,” the ratio

³See [Driessen \(2016\)](#) for details on the design of Treasury auctions. [Garbade \(2007\)](#) provides historical details regarding the manner in which the Treasury has conducted auctions.

of all bids received to all bids accepted, was $\$33.3/\$16.0=2.08$. The interest rate, corresponding to the winning yield, was set at 3.75 percent per year.

4. *Issuance:* A few days after the close of an auction, the Treasury delivers the securities and charges the winning bidders for payment of the security. At this point the winning bidders can hold the security to maturity and receive coupon payments, or sell the security on the secondary market.

Data from the announcements and results of every auction since late 1979 are available from TreasuryDirect.gov. Data regarding amounts accepted and tendered by bidder type (primary dealer, direct, and indirect) are available starting in 2003. The Treasury provides information regarding allotment by investor class starting in 2000.

2.2 Intraday Treasury Yields

Once a Treasury security auction is complete, the security is issued to the winning bidders and the security is free to trade on the secondary market. Treasuries trade in the over-the-counter market, the largest and most active debt market in the world. Following the announcement of an auction but before issuance, there is a forward market for newly auctioned Treasuries. The forward contracts mature on the same day as the securities are issued, and hence this market is referred to as the “when-issued market.” Our data on secondary-market yields (including when-issued yields) comes from GovPX, which provides comprehensive intraday coverage of all outstanding U.S. Treasuries for the period 1995-2017. We use changes in intraday Treasury yields in order to construct market-based measures of demand surprises occurring during Treasury auctions.⁴

2.3 Summary Statistics

Our analysis focuses on Treasury note and bond auctions. We exclude inflation-protected securities (TIPS) and floating rate notes because these securities have different structural arrangements than simple coupon-bearing nominal securities. We also exclude Treasury bills (zero-coupon securities with maturity one year or less) because the QE programs mainly bought long-maturity nominal U.S. government debt.

Table 1 presents summary statistics for note and bond auctions from 1995-2017 for which we have intraday Treasury yields (Appendix Figure B1 plots the number and size

⁴An earlier draft of this paper used Treasury futures to construct auction demand shocks. Treasury futures provide a natural market-based measure of unexpected shifts in Treasury prices; however, secondary-market Treasury yields around auctions contain essentially no predictable movements. In addition, Treasury futures cannot be tied directly to a specific CUSIP-level bond issue, and the futures markets are less liquid than the secondary over-the-counter Treasury market. For these reasons, we focus our analysis on demand shocks constructed using secondary-market Treasury yields. Our results are robust to using futures. See [Gorodnichenko and Ray \(2017\)](#).

of note and bond auctions split by maturity). Since 1995, a typical offering of \$20 billion generates more than \$50 billion in demand. Primary dealers account for the largest source of demand (bid-to-cover ratio ≈ 2), but other types of bidders also account for a large fraction of auction offerings. Primary dealers purchase approximately 60 percent of auctioned Treasuries, with the rest split between investment funds and foreign buyers. There is considerable variation in the offered amounts (standard deviation $\approx \$9$ billion) as well as the level and composition of demand (standard deviation for the bid-to-cover ratio ≈ 0.5 , and the standard deviation of bid-to-cover ratio for primary dealers is 0.35). In our sample of Treasury note and bond auctions, the median maturity is 5 years. The winning yield (“high yield”) is on average close to 3% per year with standard deviation of 1.9 percentage points.

3 Quantifying Demand Shocks

In this section, we describe how we measure the surprise movements in Treasury yields around Treasury auctions and document properties of these surprises. Our key assumption is that within small enough windows around the release of Treasury auction results, shifts in Treasury yields reflect unexpected changes in market beliefs about the demand for Treasuries with a specific maturity. Indeed, the Treasury announces an offered amount well before an auction happens, thus fixing supply in advance of investor bidding. Hence, between the announcement and close of the auction, Treasury yields should move only in response to unexpected changes in demand conditions. By focusing our analysis on a narrow window around the close of an auction and the release of the auction results, we aim to isolate variation only due to unexpected shifts in demand for this specific auction. As a result, we can identify a demand shock for a specific maturity and then use this shock to trace the reaction of Treasury yields for the given maturity and for other maturities as well as reactions for other prices in financial markets.

3.1 Shock Construction

Let $y_{t,pre}^{(m)}, y_{t,post}^{(m)}$ be the Treasury yields before and after the close of the auction on date t with maturity m . We measure the surprise movements in Treasury yields as:

$$D_t^{(m)} = y_{t,post}^{(m)} - y_{t,pre}^{(m)}. \quad (1)$$

For all auctions, $y_{t,pre}^{(m)}$ is the last yield observed 10 minutes before the close of the auction, while $y_{t,post}^{(m)}$ is the first yield observed 10 minutes following the release of the auction results. If the date t auction is a re-opening of a previously issued security, we use secondary market yields to construct our shocks. If the date t auction is instead a newly issued security, we use yields from the “when-issued” market. In our sample, auctions

typically close at 1:00PM, or less frequently at 11:30AM. However, the time between the close of the auction and the release of the results is a function of how long it takes the Treasury to compile the results. The Treasury began releasing results much faster in the early 2000s, but in the 1990s auction results frequently took over an hour after the close of the auction to be released. Unlike the close of the auction, the time at which the results are released is not reported by the Treasury. However, wire reports from Bloomberg allow for an upper bound on the release time. Note that we use small symmetric windows around the events to eliminate predictable movements in prices identified in [Lou et al. \(2013\)](#) and [Fleming and Liu \(2016\)](#). Indeed, [Fleming and Liu \(2016\)](#) show that these predictable movements extend to the hours before and after the auction, but near the close of the auction and release of the results (30-minute window) the price movements are reactions to the surprises regarding the demand observed at the auction. Hence, the use of small intraday windows (10-minute in our case) is key to identifying unanticipated demand shocks.

Figure 3 plots the time series of our constructed shock measures, with summary statistics presented in Table 2. Panels A and B of Table 2 report summary statistics for $D_t^{(m)}$ shocks during auction dates, both pooling across maturities as well as separately by maturity. The mean values of the shocks are close to zero (and statistical tests do not reject the null of zero means). Moreover, there is essentially no serial correlation in $D_t^{(m)}$ ($\rho = -0.03$). In sum, these summary statistics indicate that surprises are not systematic and do not contain predictable movements.⁵ In our sample period, the standard deviation of $D_t^{(m)}$ increases in maturity m and ranges from 1.3 basis points for 2-year maturity to 3.3 basis points for 30-year maturity. For comparison, [Chodorow-Reich \(2014\)](#) estimates that the largest intraday movements in yields following a QE announcement occurred after the Fed announced its purchases of Treasuries on March 18, 2009, whereby Treasury rates (five-year maturity) fell by 23 basis points. Panels C and D present statistics separately for periods of expansion/recession, and for periods of a binding/non-binding ZLB. Demand shocks appear to be more volatile during busts compared to booms.

To verify that these shocks are not spurious, we also report (Panel E of Table 2) movements in Treasury yields on non-auction days (for days without auctions, the same “pre” and “post” windows are used as auctions in the same period). In all cases, the variance of the shocks on auction dates is larger than on non-auction dates. This pattern further suggests that surprise auction results influence secondary-market Treasury yields.

⁵There is evidence that the when-issued market systematically trades at lower yields than the winning yield at the auction (see e.g. [Fleming and Liu \(2016\)](#)). However, as evidenced by Table 2, our demand shocks do not contain any such systematic biases because we focus exclusively on the changes in secondary-market yields. Additionally, Appendix Figure B2 compares auction shocks constructed using Treasury futures and yields. The two shock series are highly correlated, showing that secondary-market yield movements in these small windows around auctions do not contain any predictable movements.

3.2 Narrative Evidence

To provide a better understanding of what forces are behind these surprise movements, Figure 4 plots the 30-year Treasury yields during two 30-year Treasury bond auctions. The first is from December 9, 2010. This auction was a reopening of previously issued 30-year bonds from the month prior. The 30-year Treasury yields are relatively stable in the lead up to the close of the auction. After the auction closes and results are released, yields dropped sharply and immediately. The Financial Times [wrote](#):

“Large domestic financial institutions and foreign central banks were big buyers at an auction of 30-year US Treasury bonds on Thursday. ‘Investors weren’t messing around...You don’t get the opportunity to buy large amounts of paper outside the auctions and ‘real money’ were aggressive buyers.’”

The second is from an auction of newly issued bonds on August 11, 2011. Once again, when-issued yields were relatively stable in the lead up to the close of the auction, but after the close and release of the auction results, yields immediately rose. The Financial Times [wrote](#):

“An auction of 30-year US Treasury bonds saw weak demand...bidders such as pension funds, insurers and foreign governments shied away. ‘There’s not too many ways you can slice this one, it was a very poorly bid auction.’”

We interpret the two example auctions as follows. Before the auction closes, the market information set consists of all the supply information, both for outstanding securities as well as the amount on offer for the current 30-year auction. The 30-year Treasury yields reflect beliefs about the expected path of short-term interest rates, inflation expectations, and demand for long-maturity Treasury securities. After the auction closes and the results are released, the only update to the information set is the news regarding the bidding that took place in the auction, which solely reflects demand for Treasury debt. The change in the 30-year yields reflects this unexpected shift in beliefs about Treasury demand. The contemporaneous articles in the financial press further suggest that the important driver of the demand shifts arise from foreign and domestic institutional investors.

The narrative evidence from the financial press also highlights why auctions can have important elements of price discovery: when investors wish to purchase large amounts of Treasuries to meet their needs, they may prefer to use auctions rather than attempting to make large transactions on the secondary market. As a result, auctions reveal new information about demand for government debt that is not already reflected in over-the-counter secondary market trades.

3.3 Demand Determinants

We assume that $D_t^{(m)}$ captures unexpected shifts in the demand for Treasuries. We hypothesize that these shocks are particularly driven by demand shifts arising from institutional investors. Figure 4 and the corresponding reporting in the financial press provided some narrative evidence in this direction. However, $D_t^{(m)}$ is a market-based measure and hence is an equilibrium response to the underlying shifts in demand. The mapping from shifts in demand to changes in Treasury yields may be complex, so it is important to establish that the market interpretation of changes in demand is related to observable movements in demand.

The bid-to-cover ratio is a natural measure of demand in a given auction: a higher bid-to-cover indicates higher demand relative to the amount of Treasuries offered. The binned scatter plot in Figure 5 shows that the bid-to-cover ratio (after controlling for its four own lags) is a strong predictor of our measure of demand shocks. Table 3 presents formal evidence by regressing our shocks on measures of demand reported at the auction:

$$D_t^{(m)} = \alpha^{(m)} + \beta^{(m)} X_t^{(m)} + \varepsilon_t^{(m)}. \quad (2)$$

We present estimates separately for auctions of different maturities in columns (1)-(6). Column (7) reports results when we pool across maturities and impose that $\beta^{(m)}$ is the same across maturities m . Consistent with our interpretation of our intraday yield changes as a measure of unexpected demand shocks, the results show that the bid-to-cover ratio is strongly negatively associated with $D_t^{(m)}$. That is, a higher bid-to-cover ratio predicts a larger intraday fall in Treasury yields following the close of the auction.

These results also show that the effect of typical surprise increases in demand is economically large. For example, a one standard deviation (0.46) increase in the bid-to-cover ratio in a Treasury auction for 10-year notes leads to a $3.05 \times 0.46 \approx 1.4$ basis point decline in 10-year Treasury yields. We can back out a simple estimate for the sensitivity of yields as a function of the change in quantity demanded (in terms of dollars). A typical offering amount in a 10-year Treasury note auction is between \$20 and \$30 billion. Hence, our estimates imply that an increase in demand for 10-year Treasuries by \$10 billion decreases 10-year yields by $3.05 \times (\frac{10}{30}, \frac{10}{20}) \approx (1.02, 1.53)$ basis points.

Panel B repeats the regressions from Panel A, but explicitly decomposes the bid-to-cover ratio into “expected” and “surprise” components. For these regressions, we first estimate a univariate AR(4) model of the bid-to-cover ratio separately for each maturity group. This AR(4) model helps us to filter out predictable, low-frequency variation in demand for Treasuries in the primary market. We then construct the fitted (expected) and residual (surprise) values of the bid-to-cover ratio, and regress $D_t^{(m)}$ on these expected and surprise components. We find that the variation in our demand shocks is determined by the surprise component of the bid-to-cover ratio, and is unaffected by expected movements

in the bid-to-cover ratio.

In order to assess sensitivity of our demand shocks to changes in demand by bidder type, Panel C reports estimates of equation (2) using the bid-to-cover ratio of indirect bidders, direct bidders, and primary dealers. The sensitivity of surprises $D_t^{(m)}$ to unexpected demand of indirect bidders increases with maturity. For example, a unit increase in the bid-to-cover ratio for indirect bidders decreases the yields of 2-year Treasuries by 4.7 basis points, and the yields of 30-year Treasuries by 15.8 basis points. Direct bidders exhibit the same pattern, although the coefficients are smaller. The sensitivity to changes in the bid-to-cover ratio coming from primary dealers is smaller still. When we pool across maturities, demand of direct and especially indirect bidders generates *ceteris paribus* more variation in Treasury yields than demand of primary dealers, although for all bidder types an increase in bidder demand implies a decline in intraday yields $D_t^{(m)}$.

Panel D uses additional investor allotment data from the Treasury to break down the amount accepted by types of bidders: Investment Funds, Foreign, Dealers, and remaining smaller investors classes (which we aggregate into a “Miscellaneous” category). Since the fractions by group add up to one, we set Dealers as the leave-out category. The estimated coefficients suggest that as the fraction accepted for investment funds and foreign buyers increases, $D_t^{(m)}$ declines. The coefficients for the Miscellaneous category are generally smaller and less robust.

These results indicate that movements in demand conditions, as proxied by the bid-to-cover ratio, are a key determinant of $D_t^{(m)}$. Furthermore, we observe that the demand from institutional investors is important in accounting for variation in $D_t^{(m)}$. We stress that our identifying assumption only relies on observing the changes in *yields* immediately following the close and release of auction results. Our empirical approach does not require a measure of the unanticipated movement in quantity demanded. Hence, our empirical analysis in the remainder of the paper only relies on our constructed measure $D_t^{(m)}$.

3.4 Comovement Across Markets

We now turn to analyzing how our demand shocks for Treasuries propagate across other financial markets. We measure the impact of demand shocks on other assets by estimating simple regression specifications of the form:

$$y_t = \gamma + \phi D_t + u_t, \quad (3)$$

where y_t is the change in the price or yield of some asset on auction date t and D_t is our auction demand shock. We pool across all auction maturities to simplify presentation, but our results are robust to estimating equation (3) separately by maturity groups.

Where available, we use intraday changes within the same time window as our shocks D_t . However, we also examine changes at the daily frequency, partly due to data limita-

tions but also because daily changes may pick up responses in other asset markets that do not occur immediately. A strong correlation between D_t and y_t signals either that D_t and y_t have a common determinant (e.g., changes in inflation expectations alter the behavior of bids in Treasury auctions and change prices of inflation swaps) or that y_t is a channel of propagation for D_t shocks (e.g., unexpected prices in an auction result in repricing of Treasuries in the secondary market). To preserve space, we focus on OLS estimates of equation (3).⁶

Panel A of Table 4 reports results for debt markets. The dependent variable in the first row is the intraday change in the price (co-moves negatively with the yield) of the Exchange Traded Fund (ETF) “LQD,” which tracks the iBoxx Liquid Investment Grade Index. The estimated coefficient $\hat{\phi}$ is interpreted as the impact in log points of a one basis point increase in D_t . We observe a strong reaction to the Treasury demand shock, accounting for more than 50 percent of variation observed in corporate bond ETF prices during the short windows around the close and release of the Treasury auction results.

The next rows report the results for the daily change in corporate bond yields, as measured by Moody’s Aaa, Moody’s Baa, and Bank of America’s C corporate yield indices. Consistent with the intraday results, our demand shocks have a strong effect on safe (Aaa) corporate bonds. Moreover, the pass-through of our demand shocks to corporate bond yields is nearly one-to-one. However, using daily rather than intraday changes as the dependent variable leads to a decline in R^2 , which underscores the benefits of using intraday data. While our demand shocks still have large effects on moderately safe debt (Baa), there appears to be much smaller transmission to highly risky corporate debt (C), though the coefficient is estimated imprecisely.

As expected, yields in the secondary market react strongly to the demand shock. Furthermore, this reaction is persistent in spite of the fact that our shocks are constructed from intraday movements. Figure 6 plots the contemporaneous reaction of 10-year Treasury spot rates (top panel) and the Aaa corporate bond yields (bottom panel) to our shocks D_t , as well as the reactions up to 60 days in the future. The reaction remains strongly statistically significant over three weeks later, while the point estimate is quite stable even 2 months later. To provide a perspective on the magnitude of this persistence, Figure 6 also plots the change in yields following the QE1 announcement on March 18, 2009 (normalized such that the change on impact is equal to 1). Consistent with Wright (2012) and Greenlaw et al. (2018), yields had returned to roughly their starting point within a few months.

One may be concerned that these reactions in the bond market are driven by some omitted factor, rather than idiosyncratic changes in institutional investors’ demand for Treasuries. Our high-frequency identification goes a long way towards assuaging this

⁶We report very similar instrumental variable estimates (using unexpected changes in the bid-to-cover ratio as instruments) in Appendix Table B1.

concern but it is still possible that our demand shocks reflect changes in bidders’ expectations of macroeconomic or financial fundamentals. This is an issue for our interpretation if two conditions hold: (i) this information was not already reflected in market prices, and instead is only revealed at the auction; (ii) the market as whole updates their beliefs about fundamentals by observing the results of the auction. If this “information factor” is indeed the driver, one should see a strong co-movement of D_t and indicators capturing beliefs about current or future states of the economy and financial markets. Although the “information factor” can take any number of forms thus making it nearly impossible to rule out this channel beyond reasonable doubt, we focus on a battery of key indicators to assess the quantitative significance of this alternative explanation.

Panel B of Table 4 reports results for equities, a popular proxy for economic outlook. Rows 1 and 2 report the results for the intraday change in ETFs tracking the S&P 500 and the Russell 2000 indices. Rows 3 and 4 are for the daily changes in these indices. Although the estimated slope is generally positive, the estimate is typically insignificant. Moreover, the quantitative importance is small, as the auction demand shocks account for a tiny share of variation in equities.

Panel C of Table 4 presents results for inflation expectations and commodities. The dependent variable in row 1 is the intraday change in the ETF “GLD,” which tracks the price of Gold Bullion. Row 2 reports results for the daily change in the S&P Total Commodity Index. For the Commodity Index we do not find a significant correlation with D_t . For Gold, while the relationship is statistically significant, the R^2 is very low. Rows 3 and 4 report the results for the daily change in inflation expectations implied by inflation swaps at the 10-year and 2-year horizon. We observe that demand shocks for Treasuries do not generate significant movements in inflation expectations.⁷ Hence, our high-frequency demand shocks do not appear to impact inflation expectations.

Panel D of Table 4 reports results for various bond spreads and credit default swaps. Row 1 reports results for the daily change in the Moody’s Baa-Aaa corporate yield spread. Rows 2 and 3 use daily changes in two CDS indices from Credit Market Analysis that track the automotive industry (a highly cyclical industry) and banks (a proxy for the financial sector). These three measures proxy for expectations about future output and market conditions. We find that surprise movements D_t have no tangible effect on these measures, consistent with the view that D_t shocks do not capture superior information of Treasury auction bidders about future recessions and the like. Row 4 documents that D_t shocks are not associated with VIX (a measure of market perceptions about future volatility). Hence, it is unlikely that there is a common force that moves D_t and volatility or that D_t shocks propagate via volatility. In short, as with the case of inflation expectations,

⁷To further explore the robustness of this finding, we plot reactions of inflation swap rates at all available maturities in Appendix Figure B3. We find that the change in the inflation expectation term structure exhibits little reaction to D_t .

these null results provide further evidence that our demand shocks are not being driven by changes in expectations regarding output, liquidity, default risk, or volatility.⁸

As a final test, Panel E of Table 4 reports results with expected federal funds rates, which are derived from federal funds futures contracts. We view this as a “catch-all” test of the “information factor” story: if our demand shocks reflect changes in market expectations of fundamentals, then the market will also expect a Fed response (to the extent these fundamentals matter for the macroeconomy). We find that our demand shocks are not associated with changes in expected federal funds rates: the estimated coefficients on our demand shocks are very close to zero in these specifications, and demand shocks explain virtually none of the variation in federal funds futures in our sample.⁹

The results of Tables 3 and 4 allow for some broad observations. First, given our high-frequency approach and the institutional structure of Treasury auctions, our constructed shocks are likely only driven by new information regarding the demand side of the market. Second, these shifts are largely driven by shifts in the demand arising from institutional investors. Third, these demand shocks from the primary market for Treasuries propagate to the corporate debt market. Finally, these demand shifts are unlikely to be driven by some underlying shift in macroeconomic expectations (e.g., flight to quality or inflation expectations) that may move demand for Treasuries at all maturities.

4 Channels of Treasury Demand Shocks

Although one should not interpret $D_t^{(m)}$ as structural shocks, the properties of $D_t^{(m)}$ shocks allow us to study how unexpected demand interventions at specific maturities propagate to other maturities. We aim to answer two related questions: Does the location of the demand shock in maturity space matter? Are the impacts state-dependent? Building on recent theoretical work, we develop a model of the propagation mechanisms of Treasury demand shocks and test (and confirm) key implications of the theory.

4.1 Spillovers

To provide some examples of spillovers across the yield curve, Figure 7 plots the changes in the entire the yield curve following auctions of 30-year and 10-year Treasuries for four dates. Each panel of the figure plots the intraday yield changes (as estimated from local mean smoothing regressions, across all traded Treasuries) during small windows around specific auctions. On December 9, 2010 (Panel A), there was unexpectedly strong

⁸As a robustness exercise, we plot sensitivities for select asset prices estimated over rolling windows in Appendix Figure B4.

⁹We focus on short-horizon federal funds expectations because these futures contracts are more liquid than longer-horizon futures contracts. Appendix Figure B5 documents a series of rolling regressions for h -month ahead federal funds futures and their trade volume for h up to 12 months.

demand (as measured by changes in our demand shock $D_t^{(30y)}$) during an auction of 30-year Treasuries. We observe that, although the whole yield curve shifted down, the strongest reaction was for long maturities. Similarly, on August 11, 2011 (Panel B) there was unexpectedly weak demand during another 30-year auction. The entire yield curve shifts up, and the effect is increasing in magnitude as the maturity approaches 30 years.

We find a similar pattern following the 10-year auction on August 12, 2009 (Panel C). Unexpectedly weak demand at the auction is associated with increases in yields across the entire term structure, but the largest effects are observed for maturities of 10 years or greater. However, this contrasts with the pattern observed following another 10-year auction on January 11, 2017 (Panel D). In this case, unexpectedly strong demand puts downward pressure on the yield curve, but the largest effects are for intermediate maturities around 5 years; as the maturity increases, the effect becomes attenuated.

These cases provide suggestive evidence that the location can in fact matter. To systematically characterize the impact of these demand shocks, we now examine the impact on the term structure of Treasury rates through the lens of the *preferred habitat* model of investor demand.

4.2 A Macroeconomic Preferred Habitat Model

We now develop key testable predictions of preferred habitat theory regarding the propagation of demand shocks. Our analysis is based on the model originally proposed in [Vayanos and Vila \(2021\)](#) and embedded in a general equilibrium New Keynesian setting as in [Ray \(2019\)](#). We extend this framework to allow for the existence of risky assets (mortgage-backed securities, corporate debt, etc.) as well as risk-free Treasury bonds. The key idea is the existence of “clientèle” investors who have idiosyncratic demand (“preferred habitat”) for assets of specific maturities. For example, pension funds can have a preference for long-maturity Treasuries to better match the maturity structure of pension liabilities. The other side of the market are risk-averse arbitrageurs such as hedge funds and dealers, who smooth out these preferred-habitat demand shocks. Fluctuations in asset prices lead to changes in consumption due to the borrowing decisions of households. The model formalizes the interaction of preferred-habitat investors with arbitrageurs, and how these interactions have spillover effects in the real economy.

Financial markets: There are two sets of assets: riskless and risky zero coupon bonds with maturity $\tau \in (0, T)$, available in zero net supply. A τ -maturity riskless bond pays \$1 at maturity with certainty in period $t + \tau$, which we interpret as Treasuries. A risky τ -maturity bond instead pays $D_{t+\tau} \equiv e^{d_{t+\tau}}$ at maturity in period $t + \tau$, where D_t is a stochastic process. Formally, one can think of this as a portfolio of risky bonds, a fraction of which default at every period and therefore only make payments $D_{t+\tau}$ at maturity. More generally, these assets capture a wider range of assets subject to payoff uncertainty.

Arbitrageurs have mean-variance preferences and allocate their wealth W_t to holdings $X_t^{(\tau)}, \tilde{X}_t^{(\tau)}$ across τ riskless and risky bonds, respectively. Their budget constraint is:

$$\max_{\{X_t^{(\tau)}, \tilde{X}_t^{(\tau)}\}_{\tau=0}^T} E_t dW_t - \frac{a}{2} Var_t dW_t \quad (4)$$

$$\text{s.t. } dW_t = \left(W_t - \int_0^T X_t^{(\tau)} d\tau - \int_0^T \tilde{X}_t^{(\tau)} d\tau \right) r_t dt + \int_0^T X_t^{(\tau)} \frac{dP_t^{(\tau)}}{P_t^{(\tau)}} d\tau + \int_0^T \tilde{X}_t^{(\tau)} \frac{d\tilde{P}_t^{(\tau)}}{\tilde{P}_t^{(\tau)}} d\tau, \quad (5)$$

where $P_t^{(\tau)}$ is the price of a τ -maturity riskless bond, $\tilde{P}_t^{(\tau)}$ is the price of a τ -maturity risky bond, and r_t is the short rate set by the monetary authority. Denote by $y_t^{(\tau)}, \tilde{y}_t^{(\tau)}$ the yield to maturity of the τ riskless and risky bonds, respectively. The parameter a governs the risk-return trade-off that arbitrageurs face. This parameter can be taken literally as a risk aversion parameter, or more generally can be thought of as a proxy for factors that lead to the imperfect risk-bearing capacity of arbitrageurs. For tractability, we take a as time-invariant, although one would expect a to increase in periods of financial distress; we will analyze (in a comparative statics sense) how the predictions of the model depend on the risk-bearing capacity of arbitrageurs.¹⁰

On the other side of the market is a continuum of habitat investors, who specialize in (riskless and risky) bonds of specific maturities. These investors are assumed to respond to prices through the following demand curves:

$$Z_t^{(\tau)} = -\alpha(\tau) \log P_t^{(\tau)} - \sum_{k=1}^K \theta^k(\tau) \beta_t^k, \quad (6)$$

$$\tilde{Z}_t^{(\tau)} = -\tilde{\alpha}(\tau) \log \tilde{P}_t^{(\tau)} - \sum_{k=1}^{\tilde{K}} \tilde{\theta}^k(\tau) \tilde{\beta}_t^k. \quad (7)$$

The functions $\alpha(\tau), \tilde{\alpha}(\tau)$ are the semi-elasticities of a τ -habitat investor's demand for riskless and risky assets, respectively. Time-varying demand factors are given by $\{\beta_t^k, \tilde{\beta}_t^k\}$, and the functions $\{\theta^k(\tau), \tilde{\theta}^k(\tau)\}$ govern how these demand shocks lead to changes in demand from τ -habitat investors. Market clearing implies that in equilibrium, arbitrageurs take the opposite positions of habitat investors: $X_t^{(\tau)} + Z_t^{(\tau)} = 0, \tilde{X}_t^{(\tau)} + \tilde{Z}_t^{(\tau)} = 0$.

Macroeconomic dynamics: Inflation π_t , the output gap x_t , the central bank's policy rate r_t , and risky asset payoffs d_t are determined by a modified set of New Keynesian

¹⁰He and Krishnamurthy (2013), Kyle and Xiong (2001) and others show how risk aversion can be endogenously higher in times of crises. A model with (endogenous) switches in risk aversion would be a better description of the data but this modeling approach would make analysis intractable.

relationships:

$$d\pi_t = (\rho\pi_t - \delta x_t - z_{\pi,t}) dt, \quad (8)$$

$$dx_t = \varsigma^{-1} (\tilde{r}_t - \pi_t - \bar{r} - z_{x,t}) dt, \quad (9)$$

$$dr_t = -\kappa_r(r_t - \phi_\pi\pi_t - r^*) dt + \sigma_r dB_{r,t}, \quad (10)$$

$$dd_t = -\kappa_d(d_t - \psi_x x_t - d^*) dt + \sigma_d dB_{d,t}, \quad (11)$$

$$dz_{\pi,t} = -\kappa_{z_\pi} z_{\pi,t} dt + \sigma_{z_\pi} dB_{z_\pi,t}, \quad (12)$$

$$dz_{x,t} = -\kappa_{z_x} z_{x,t} dt + \sigma_{z_x} dB_{z_x,t}. \quad (13)$$

Equation (8) is a New Keynesian Phillips curve, relating inflation and the output gap, subject to a cost-push shock $z_{\pi,t}$. The parameter ρ is the discount rate, and δ governs the degree of price stickiness. Equation (9) is a modified New Keynesian IS curve, where the output gap depends on an “effective” borrowing rate $\tilde{r}_t \equiv \int_0^T \eta(\tau) E_t \frac{d\tilde{P}_t^{(\tau)}}{\tilde{P}_t^{(\tau)}} d\tau$, which depends on the entire term structure of risky borrowing rates. The function $\eta(\tau)$ is a weighting function, ς^{-1} is the intertemporal elasticity of substitution, \bar{r} is the “natural” real borrowing rate, and $z_{x,t}$ is an aggregate demand shock. Equation (10) is a Taylor rule, with persistence in the policy rate. The response of the policy rate to inflation is governed by ϕ_π , while κ_r is a mean-reversion parameter, and r^* is the central bank’s target policy rate (set such that the economy features a zero inflation and output gap steady state). Equation (11) governs the time-variation in the payoff of the risky assets, where the stochastic payoff process d_t depends on the output gap through the parameter ψ_x and the mean reversion to the steady state d^* depends on the parameter κ_d .¹¹ Equations (12) and (13) define the mean-reverting cost-push and aggregate demand processes, where $\kappa_{z_\pi}, \kappa_{z_x}$ govern the persistence in these processes. The terms $B_{r,t}, B_{d,t}, B_{z_\pi,t}, B_{z_x,t}$ are standard independent Brownian motions, with respective volatility terms $\sigma_r, \sigma_d, \sigma_{z_\pi}, \sigma_x$.

Our specification of the effective borrowing rate implies that households do not respond directly to the policy rate r_t . Instead, household borrowing is a function of risky borrowing rates (across all maturities). Under risk neutrality, expected returns are equalized and therefore $\tilde{r}_t = r_t$, and the model collapses to a standard New Keynesian model; this will be the case when arbitrageur risk aversion $a = 0$. Away from risk neutrality ($a > 0$), the predictions of our model depart from those of standard models. In particular, the pass-through of conventional monetary policy to household borrowing (and therefore, the pass-through to the broader macroeconomy) will depend on how conventional policy affects risky borrowing rates. In equilibrium, this pass-through depends on how arbitrageurs adjust their portfolio allocations in response to changes in the policy

¹¹Technically, in order to maintain the interpretation of the risky assets as a portfolio or risky bonds where D_t captures the fraction of defaulting risky bonds, we would have to add some bounds to ensure $D_t \leq 1$. However, this leads to a much less tractable model, and so we assume a linear specification. This can be interpreted as a local approximation of the true process; alternatively, one can interpret the model more broadly as capturing assets with uncertain payoff governed by the process D_t .

rate. Moreover, demand shifts for bonds and risky assets lead to changes in arbitrageurs' portfolio allocations, which in turn will lead to equilibrium changes in asset prices.

We show in Appendix A that despite this complexity, in equilibrium we have that bond and risky asset prices are an affine function of the state variables. Following Ray (2019), the dynamics of the economy are governed by

$$\begin{bmatrix} \mathbf{y}_t & \mathbf{x}_t \end{bmatrix}^\top \equiv \mathbf{Y}_t = -\boldsymbol{\Upsilon} (\mathbf{Y}_t - \bar{\mathbf{Y}}) dt + \boldsymbol{\sigma} d\mathbf{B}_t, \quad (14)$$

where the vector \mathbf{y}_t includes state variables (the habitat demand factors and the persistent policy rate) and \mathbf{x}_t includes the non-predetermined variables (inflation and the output gap), the matrix $\boldsymbol{\sigma}$ depends on structural parameters, and the dynamics matrix $\boldsymbol{\Upsilon}$ is determined as a fixed point that produces equilibrium dynamics in the bond market consistent with equilibrium dynamics of the macroeconomy and vice versa. Note that this formulation also allows for correlation of idiosyncratic habitat demand factors and the macro fundamentals.

This model of preferred habitat bond markets provides insights into the observations of Figure 4. In particular, one of the characteristic predictions of preferred habitat theory, first formalized in Vayanos and Vila (2021), is the *localization hypothesis*. When arbitrageur risk-bearing capacity is high, demand shocks have *global* effects on the yield curve. That is, the relative response of the interest rates across the yield curve does not depend on where in maturity space the demand shock occurs. However, as arbitrageur risk-bearing capacity declines, the spillovers of demand shocks become more *localized*. That is, the relative response of interest rates becomes more concentrated on parts of the yield curve that are closer in maturity space to where the demand shock occurs.

Intuitively, when arbitrageurs are nearly risk-neutral, macroeconomic fundamentals affecting the path of the short rate are by far the dominant factor in determining of the term structure of interest rates. Hence, when arbitrageurs hold bonds, the main source of risk to which they are exposed is short-rate fluctuations. Demand shocks that re-allocate bonds away from arbitrageurs reduce their exposure to short-rate risk, and hence decrease the compensation arbitrageurs require to hold bonds. Since all bonds are sensitive to short-rate risk, any such demand shock will push down yields of all bonds. Importantly, this mechanism is independent of the location (in maturity space) of the demand shock.¹²

As arbitrageur risk aversion increases, demand shocks become more prominent as additional sources of risk. Arbitrageurs try to limit their exposure to these sources of risk, leading to less propagation from the location of the demand shock to other parts of the term structure. Arbitrageurs become less willing to integrate bond markets across

¹²In this example, the location of a demand shock will impact the size of the effect on the yield curve, but not the shape of the response of the yield curve. Hence, the relative effect of a demand shock on the yield curve is independent of the location of the shock.

maturities, and hence the response of the yield curve becomes more localized around the location (in maturity space) of a given demand shock.

4.3 Localization Regression Specification

In order to formalize and derive an empirical test of the localization hypothesis, consider a version of the model with the following Treasury demand factors: a “short” maturity factor β_t^s and “long” maturity factor β_t^ℓ such that

$$\int_0^T \theta^s(\tau) d\tau = \int_0^T \theta^\ell(\tau) d\tau, \quad (15)$$

$$\exists \tau' : \theta^s(\tau) < \theta^\ell(\tau) \iff \tau > \tau'. \quad (16)$$

That is, the factors have the same overall magnitude across maturities (equation (15)), but the short factor is more concentrated in bonds of short maturities relative to the long factor (equation (16)). Note that this does not require the assumption that the long factor β_t^ℓ only affects demand for long maturities; indeed, changes in β_t^ℓ will shift demand for bonds of all maturities τ such that $\theta^\ell(\tau) \neq 0$. In other words, as long as $\theta^k(\tau) \neq 0$ for some maturity τ , we allow for a “hard-wired,” direct response of yields for this maturity to factor k . In this sense, the demand factors imply “correlated” changes in demand across the term structure: a short factor can directly move demand for short- and long-maturity bonds and a long factor can directly move demand for short- and long-maturity bonds. We only require (equation (16)) that, relative to the short factor β_t^s , the long factor has a larger direct effect on demand for bonds with long maturities.

In this context, the localization hypothesis involves the differential responses of the entire yield curve to movements in the short and long demand factors. We can formally state a version of the localization hypothesis as follows. When arbitrageur risk-bearing capacity is high ($a \approx 0$), the relative response of the yield curve is the same for both factors. On the other hand, when risk-bearing capacity is low ($a \gg 0$), then long demand shocks have relatively larger effects on long-maturity yields and *vice versa* for short demand shocks. This logic implies:

$$\text{if } a \approx 0 : \frac{\partial y_t^{(\tau)} / \partial \beta_t^s}{\partial y_t^{(\tau^*)} / \partial \beta_t^s} \approx \frac{\partial y_t^{(\tau)} / \partial \beta_t^\ell}{\partial y_t^{(\tau^*)} / \partial \beta_t^\ell}, \quad (17)$$

$$\text{if } a \gg 0 : \tau > \tau^* \iff \frac{\partial y_t^{(\tau)} / \partial \beta_t^s}{\partial y_t^{(\tau^*)} / \partial \beta_t^s} < \frac{\partial y_t^{(\tau)} / \partial \beta_t^\ell}{\partial y_t^{(\tau^*)} / \partial \beta_t^\ell}, \quad (18)$$

where τ^* is some arbitrary “baseline” maturity (and unrelated to τ) and $\partial y_t^{(\tau)} / \partial \beta_t^k$ is the

response of τ -maturity yields to the demand shock $k \in \{s, \ell\}$.¹³ Hence, these expressions make statements about the movements of the yield curve to short and long demand shocks, *relative* to movements in some fixed maturity τ^* . Specifically, equation (17) states that even if $\theta^k(\tau) \neq \theta^k(\tau^*)$ (i.e., direct responses are different across maturities for a given factor) and $\theta^s(\tau) \neq \theta^\ell(\tau)$ (i.e., direct responses for a given maturity are different across factors), arbitrageurs with low risk aversion ($a \approx 0$) ensure that the *equilibrium* scaled responses of yields are approximately the same for short and long factors. In contrast, equation (18) states that when risk aversion is high, arbitrageurs do not smooth out demand shocks and the scaled responses of yields depend on where the direct impact of a factor is concentrated. In particular, if the long factor has a larger direct effect on demand for long maturities than the short factor, then in equilibrium, the scaled response of yields for longer maturities is larger for the long factor than for the short factor.

In order to test the localization hypothesis, we need empirical analogues that are proportional to the model objects $\partial y_t^{(\tau)} / \partial \beta_t^s$ and $\partial y_t^{(\tau)} / \partial \beta_t^\ell$. That is, we require empirical measures of the conditional response of yields to demand factors for short-maturity and long-maturity Treasuries, holding all other state variables constant. As shown in Section 3, our high-frequency identification strategy is precisely designed to isolate the reactions of the yield curve to Treasury demand shocks alone, effectively ruling out any other shocks during these small windows around auctions. This insight allows us to arrive at a simple, theory-based regression specification that can test the localization hypothesis using only high-frequency changes in yields around auctions $D_t^{(\tau)} = y_t^{(\tau),post} - y_t^{(\tau),pre}$, which are data analogues proportional to $\partial y_t^{(\tau)} / \partial \beta_t^k$.¹⁴ Our localization specification is

$$D_t^{(\tau)} = \alpha^{(\tau)} + \gamma_s^{(\tau)} \mathbf{I}(m_t = short) D_t^{(\tau^*)} + \gamma_\ell^{(\tau)} \mathbf{I}(m_t = long) D_t^{(\tau^*)} + \varepsilon_t^{(\tau)}, \quad (19)$$

where $\mathbf{I}(m_t = short)$ is an indicator variable equal to one if there is an auction of short-maturity bonds on date t , $\mathbf{I}(m_t = long)$ is an indicator variable equal to one if there is an auction of long-maturity bonds on date t . We estimate equation (19) for all maturities τ , holding τ^* fixed.¹⁵

¹³Section C in the Appendix discusses in detail the sufficient conditions and formally derives the localization predictions of the model.

¹⁴One can make the connection between the data and the model tighter by working with a jump-diffusion process to better match the discrete timing of Treasury auctions and hence have a well-defined t^{pre} and t^{post} in the model. Our approach based on continuous processes introduces some slippage between the model and the data but it allows us to have a tractable model. To be clear, the discrepancy with auctions in the model are: *i*) The auction is just revealing the results (which we interpret as the demand shock), but in reality the actual change in holdings occurs a few days later. In the model, there is no “news about future change in portfolios,” just a contemporaneous change in demand. *ii*) We think of the auction as “scooping up” changes in demand leading up to the auction, which are only revealed when the auction closes. Again, the model only allows for contemporaneous changes in demand, which are observable by all agents.

¹⁵This approach does not require us to observe the underlying structural demand shocks β_t^k , and instead only relies on the change in yields conditional on an (unobserved) changes in demand factor β_t^k . The change in the bid-to-cover ratio is a proxy for structural demand shifts, but we do not have a high-

Coefficients $\hat{\gamma}_s^{(\tau)}$ and $\hat{\gamma}_\ell^{(\tau)}$ measure the relative effect of demand shocks for short-maturity and long-maturity auctions respectively. Now we can restate the localization hypothesis formally as a function of the coefficients $\gamma_s^{(\tau)}$, $\gamma_\ell^{(\tau)}$, and risk aversion a as follows: i) as risk aversion $a \rightarrow 0$, $|\gamma_s^{(\tau)} - \gamma_\ell^{(\tau)}| \rightarrow 0$ for all maturities τ ; ii) when risk aversion is high ($a \gg 0$), then $\gamma_s^{(\tau)} > \gamma_\ell^{(\tau)}$ if $\tau < \tau^*$ and $\gamma_s^{(\tau)} < \gamma_\ell^{(\tau)}$ if $\tau > \tau^*$.

4.4 Empirical Localization Results

To test the state-dependent localization hypothesis, we estimate specification (19) separately for two subsamples: a “non-crisis” period (risk aversion a is low), and a “crisis” period (risk aversion a is high). Testing for the equality of coefficients $\hat{\gamma}_s^{(\tau)}$ and $\hat{\gamma}_\ell^{(\tau)}$ in each subsample shows whether demand shocks have more localized effects when risk aversion is high. In our baseline estimates, we take the “crisis” period to be 2008-2012. We divide the auctions into short-maturity (maturity of 5 years or less) and long-maturity (maturity of 7 years or greater). The results are robust to alternative choices.

Since we construct $D_t^{(\tau)}$ from secondary-market yields, we do not have measures for all maturities τ at all times. Our approach is to run rolling regressions (across maturities), including yields for maturities within ± 2 years for each maturity $\tau \leq 20$ years and within ± 4 years for each maturity $\tau > 20$ year. Given that the choice of benchmark maturity τ^* is arbitrary, we set $\tau^* = 3$, with an eye towards applying our results to QE in order to focus on the differential effects of intermediate and long-maturity yields.

Panel A of Figure 8 plots the estimates of $\hat{\gamma}_s^{(\tau)}$ and $\hat{\gamma}_\ell^{(\tau)}$ for the non-crisis sample. The estimated responses follow a similar hump-shaped pattern peaking at intermediate maturities (around roughly 5-7 years), and then declining and stabilizing for longer term maturities (with a possible slight uptick for very long (20+ years) maturities). In general, we cannot reject equality of $\hat{\gamma}_s^{(\tau)}$ and $\hat{\gamma}_\ell^{(\tau)}$.

When we estimate specification (19) on the crisis sample, we observe a strikingly different pattern (Panel B of Figure 8). In response to shocks in demand for short- and long-maturity Treasuries, both $\hat{\gamma}_s^{(\tau)}$ and $\hat{\gamma}_\ell^{(\tau)}$ increase rapidly for $\tau < \tau^*$, with the $\hat{\gamma}_s^{(\tau)}$ estimates increasing somewhat more quickly than $\hat{\gamma}_\ell^{(\tau)}$. Once we move to maturities greater than τ^* , the estimates quickly diverge. Specifically, in response to shocks in demand for short-maturity Treasuries, the yields for maturities greater than τ^* fall relative to the yield response for τ^* (as shown by the estimates of $\hat{\gamma}_s^{(\tau)}$). On the other hand, in response shocks in demand for long-maturity Treasuries, yields for maturities $\tau > \tau^*$ continue to increase relative to the benchmark maturity τ^* (as shown by the estimates of $\hat{\gamma}_\ell^{(\tau)}$). For maturities of 20 to 30 years, the relative response of yields to long-maturity demand shocks ($\hat{\gamma}_\ell^{(\tau)}$) is over twice as large as the response of yields to short-maturity demand shocks ($\hat{\gamma}_s^{(\tau)}$). We

frequency market-based measure of the expected bid-to-cover before and after an auction. We return to the possibility of utilizing the bid-to-cover ratio to test the localization hypothesis in robustness checks.

can strongly (at the 0.1% level) reject the null of $\hat{\gamma}_s^{(\tau)}$ and $\hat{\gamma}_\ell^{(\tau)}$ being equal.

These results are consistent with the key predictions of our preferred habitat framework: during “normal” periods when financial risk-bearing capacity is high, demand shocks for short- and long-maturity securities have relatively similar impacts on the yield curve. During periods of financial distress when risk-bearing capacity is low, the impacts are more localized: the impact of short-maturity demand shocks are largest for short maturities, while the impact of long-maturity demand shocks peaks at the long end of the term structure. These results provide support for the view that during financial crises, arbitrageurs are less willing or able to integrate bond markets.¹⁶

The localization results are robust to a variety of alternative assumptions. In the interest of space, we provide summaries for a few key robustness specifications in this section. First, we explore the sensitivity of our results to using alternative measures of financial distress. Specifically, we consider two alternatives: i) an aggregate “intermediary capital ratio,” a market-based measure of financial distress (low intermediary capital ratios are associated with lower risk-bearing capacity) described in [He et al. \(2016\)](#); ii) a narrative-based measure of financial crisis from [Romer and Romer \(2017\)](#) (higher values of the crisis indicator are associated with lower risk-bearing capacity). Both of these alternatives generate results similar to our baseline findings (see Appendix Figures [B7](#) through [B11](#)). Second, our results are robust to using different cutoffs for separating auctions into short and long maturities. For example, when we use 10 years (rather than 7 years in the baseline) as the cut-off for long-maturity auctions, the results (Appendix Figure [B12](#)) still strongly support the localization hypothesis and, if anything, the point estimates for the “non-crisis” period are even more similar than in our baseline specification. Third, as we discussed above, the choice of the benchmark maturity τ^* is arbitrary in our framework. To verify that this choice is indeed immaterial for our results, we experiment with values other than $\tau^* = 3$ and find similar results (e.g. Appendix Figure [B13](#) reports estimates for $\tau^* = 6$). Fourth, our results are nearly identical when dropping auctions that occurred during the weeks of QE announcements (Appendix Figure [B14](#)).

Finally, we also considered an alternative regression specification to test the localization hypothesis. Our auction data provides a proxy for structural demand shocks: movements in the bid-to-cover ratio. However, the bid-to-cover ratio is only a crude proxy, because the value reported following an auction does not solely reflect new demand information revealed following the close of the auction. Nevertheless, it is informative to run

¹⁶Correlated shocks to demand could be an alternative explanation of localization effects. Note that correlated shocks alone do not negate the predictions of the model. However, if the correlation structure changes in crisis and demand shocks become *less* correlated across maturities, one may also rationalize stronger localization effects in crisis. We do not find evidence to support this explanation. Specifically, for each period (crisis sample period vs. non-crisis sample period), we have time series of bid-to-cover ratios for Treasury auctions with a given maturity. We estimate the correlation matrix of these time series for each period and test equality of the correlation matrices across the periods. We cannot reject equality of the matrices (p-value is 0.25).

the following regression:

$$D_t^{(\tau)} = \alpha^{(\tau)} + \nu_s^{(\tau)} \mathbf{I}(m_t = \text{short}) \tilde{\beta}_t + \nu_\ell^{(\tau)} \mathbf{I}(m_t = \text{long}) \tilde{\beta}_t + \varepsilon_t^{(\tau)}, \quad (20)$$

where $\tilde{\beta}_t$ is the residualized (“surprise”) bid-to-cover ratio following an auction at date t (controlling for its own four lags, as in Table 3). We further flip the sign of the bid-to-cover ratio, in order to make the estimates more comparable to our baseline specification. Note that unlike specification (19), the estimates $\hat{\nu}_s^{(\tau)}, \hat{\nu}_\ell^{(\tau)}$ measure the absolute response of the yield curve to the short and long demand factors (proxies), as opposed to the relative response. Hence, unlike the baseline specification (19), the formal test of the localization hypothesis is not as straightforward using specification (20) (recall that the localization hypothesis is about relative movements in yields across the term structure). Nevertheless, we see strong patterns of localization in the “crisis” estimates, but little evidence of localization in the “non-crisis” estimates. In the non-crisis subsample estimates (Panel A of Figure 9), the response to both short- and long-maturity demand follows a similar hump-shaped pattern: the response is increasing from short to intermediate maturities, peaking around $\tau = 5$ to $\tau = 10$ before declining (though there is some evidence that long demand shocks have larger effects on very long-maturity yields). On the other hand, the estimates from the crisis subsample (Panel B of Figure 9) exhibit significant differences across short and long estimates: the response to short demand shocks remains hump-shaped, but peaks for short maturities before quickly declining. Conversely, the response to long demand shocks increases almost without fail as the maturity increases, peaking at very long maturities.¹⁷

Since the mechanism for the market segmentation channel is the same regardless of the source of demand shifts (recall that the preferred habitat channel is about how private arbitrageurs absorb demand shifts rather than about the source of the demand shocks), our results already offer important lessons for central banks undertaking QE. For example, if the Fed is trying to decrease long-maturity Treasury rates relative to shorter-maturity rates, our findings suggest that QE policies that directly purchase long-maturity Treasuries should be effective during financial crises. Indeed, the Fed may have a menu of options in terms of where it can intervene in the maturity space to hit the yield at a target maturity. But if the Fed is trying to move the entire term structure of interest rates, during periods of high financial distress the Fed will have to be active in purchasing Treasuries throughout the yield curve.

¹⁷We can further refine our identification by focusing on variation in demand only due to indirect bidders (since as discussed above, these investors include foreign central banks and are more likely to have idiosyncratic demand). When we use the indirect bidder bid-to-cover ratio, we find similar results (Appendix Figure B15).

5 Implications for Quantitative Easing

In this section, we use our theoretical framework to make further progress in several directions. First, we use a calibrated version of our model to quantify the role of preferred habitat in rationalizing the response of asset prices to the QE announcement. Second, we use the model to evaluate the effectiveness of QE for macroeconomic stabilization purposes. Third, we consider alternative implementations of QE to inform policymakers about trade-offs associated with various designs of QE.

5.1 Model Calibration

We follow [Ray \(2019\)](#) and [Vayanos and Vila \(2021\)](#) and assume these functional forms:

$$\text{habitat elasticity function: } \alpha(\tau) = \alpha_0 \exp(-\alpha_1 \tau), \quad (21)$$

$$\text{habitat demand functions: } \theta^k(\tau) = \theta_0 \tau (\theta_1^k)^2 \exp(-\theta_1^k \tau), \quad (22)$$

$$\text{effective borrowing weights: } \eta(\tau) = \tau \eta_1^2 \exp(-\eta_1 \tau). \quad (23)$$

Equation (21) implies that the habitat investor elasticity with respect to (log) price is declining with maturity, and is single-peaked with respect to yields. Similarly, equations (22) and (23) imply that the demand factor and borrowing weights are single-peaked functions. In addition to improving numerical properties of the model, these exponential functional forms allow us some flexibility in capturing key modeling features, such as demand shocks targeted in specific areas of maturity space, without significantly increasing the dimensionality of the problem. Note that the functions $\theta^k(\tau)$ and effective borrowing weights $\eta(\tau)$ are parameterized such that they integrate to θ_0 and 1, respectively. Thus, the parameters α_0, θ_0 govern the overall size of the habitat elasticity and demand functions, while $\alpha_1, \theta_1^k, \eta_1$ govern the shape as a function of maturity: a lower value of these parameters imply that more of the weight of these functions lies at longer maturities.

The weighting function in the effective borrowing rate $\eta(\tau)$ is parameterized to match the fact that a large fraction of outstanding securities as well as volume in Treasury and corporate bond markets is concentrated at shorter-term maturities (1 year or less). Similar to [Ray \(2019\)](#), we set $\eta_1 = 2$, such that $\eta(\tau)$ peaks at 0.5 years and has an average value of 1 year.

To map the model to our estimates in the previous section, we assume there are three demand factors, corresponding to short- and long-maturity Treasury auctions, and a risky asset: $\beta_t^s, \beta_t^\ell, \tilde{\beta}_t$. In order to impose more discipline on the model, we assume that the habitat demand shocks are identical, except for the shape of the demand factor functions $\theta^s(\tau)$, $\theta^\ell(\tau)$, and $\tilde{\theta}(\tau)$. Specifically, we set $\theta_1^s = 0.5$, $\theta_1^\ell = 0.2$, and $\tilde{\theta}_1 = 0.5$ such that the short factor is concentrated in short maturities less than 5 years, while the long factor has more weight in intermediate and long maturities above 7 years, as in our regression

analysis in Section 4. We further assume that the habitat elasticity functions are identical for Treasuries and risky assets: $\alpha(\tau) = \tilde{\alpha}(\tau)$. We set the parameter $\alpha_1 = \tilde{\alpha}_1 = 0.1$ such that the habitat elasticity with respect to yields ($\equiv \tau \cdot \alpha(\tau)$) is maximized for the 10-year maturity, which is often taken as a key benchmark yield.

We also assume that the habitat demand factors are independent from one another, but may respond to the short rate (as in King (2019a)). For each demand factor $\beta_t^k \in \{\beta_t^s, \beta_t^\ell, \tilde{\beta}_t\}$, we have

$$d\beta_t^k = -(\kappa_\beta \beta_t^k + \phi_{r,\beta} r_t) dt + \sigma_\beta dB_{\beta^k,t},$$

where the parameters κ_β , $\phi_{r,\beta}$, and σ_β are identical for each demand factor.

Because both the habitat elasticity functions and demand functions enter the solution multiplicatively with risk aversion and demand shock volatility, they are only identified up to a scaling factor. Therefore, the remaining preferred habitat parameters to calibrate are $a \cdot \alpha_0$, $a \cdot \sigma_\beta \cdot \theta_0$, $a \cdot \phi_{r,\beta}$, and κ_β , which govern how the model deviates from risk-neutrality and how demand shocks propagate.¹⁸

We jointly estimate these habitat parameters and the more standard macro dynamics parameters in a moment-matching exercise. Following Vayanos and Vila (2021), we target volatility and cross-correlations of yields (levels and changes) for different maturities. Because our model includes risky assets and macroeconomic variables, we also target volatility and cross-correlations of these additional variables. Most importantly, we target the localization regression coefficients from Figure 8. We allow only the risk-adjusted parameters ($a \cdot \alpha_0$, $a \cdot \sigma_\beta \cdot \theta_0$, and $a \cdot \phi_{r,\beta}$) to be different in “crisis”, which we target to match the “crisis” localization regression coefficients from Figure 8. All other parameters are assumed to be the same across “crisis” and “non-crisis” periods. Given that the number of observations in the “non-crisis” period is vastly larger than the number of observations in the “crisis” period, we first estimate all of the parameters from the “non-crisis” sample. Appendix C describes how the moments are calculated in the model and mapped to the data.

Table 5 summarizes the results of this moment-matching exercise, which we use in the following numerical exercises. In short, our parameterized model not only picks up the qualitative features of the data but is also successful at matching the data quantitatively. For example, the model localization coefficients are close to the data localization coefficients in “crisis” and “non-crisis” periods (Figure 10).¹⁹ Thus, the model is well-suited for quantitative analyses.

¹⁸If shocks to quantity demand for Treasuries and risky assets can be measured directly across all periods, one can separately identify σ_β . Because such measures are not available, the literature (e.g., Vayanos and Vila (2021)) typically chooses some normalization, such as $\sigma_\beta = 1$. In our auction data, the bid-to-cover ratio captures this information partially; we return to this insight below when modeling QE.

¹⁹Appendix Figure B16 and Table B2 report the additional moments used in the calibration exercise.

5.2 Response of the Yield Curve to QE1

To assess the contribution of preferred habit theory to the observed reaction of yields to quantitative easing, we feed a “QE1” shock into our model, compute predicted responses of yields at different maturities, and compare predictions to actual changes in yields. In this exercise, we assume that QE1 does not resolve distress in the financial markets and thus we hold the model regime fixed at “crisis.” We focus on QE1 because it was arguably the “cleanest” LSAP shock: there are a clear set of policy announcement events, and the observed response to these events are unlikely to be plagued by anticipation issues relative to later rounds of QE. QE1 involved purchasing both Treasuries and mortgage-backed securities (MBS). Hence, we feed into the model a large purchase shock of risky and riskless assets. We discuss in detail how we mimic the actual QE1 shock in the model.

Persistence: We assume that this shock was completely unexpected (“MIT shock”), and that afterwards markets expected purchases to be unwound slowly and deterministically:

$$d\beta_t^{QE} = -\kappa_{QE}\beta_t^{QE} dt. \quad (24)$$

We set the inertia parameter $\kappa_{QE} = 0.2$. This magnitude roughly implies that markets expected the Fed to unwind its purchases somewhat faster than holding to maturity (more precisely, the half-life of the purchases is roughly 3.5 years). Ex-post, the MBS holdings roughly followed this process until the reintroduction of MBS purchases during QE3. On the other hand, the Treasuries purchased as part of the Fed’s QE programs were held on the balance sheet for a very long time, and holdings remained elevated well beyond that implied by our parameterization. However, this does not imply that markets expected this ex-ante.²⁰ We explore the sensitivity of this assumption below.

Composition: QE1 involved purchasing a total of roughly \$1.25 trillion mortgage-backed securities (MBS) and \$300 billion Treasuries, concentrated on intermediate and long-term maturity purchases (over 5 years).²¹ Given this focus, we set $\theta_1^{QE} = 0.35$, such that the model-implied QE1 purchases are of relatively long-term maturity but in between the maturities of the preferred habitat “short” and “long” factor described above. These purchases are split up such that roughly 80% of QE1 purchases are of the risky asset in the model, while the remaining 20% are of safe bonds, in order to match the fraction of actual MBS and Treasury purchases during QE1.

²⁰The actual purchases of MBS and Treasuries during QE1 were planned to take place over the 6 months following the March 2009 announcement. The FOMC statements during this time do not make any reference to selling these securities off, but state that the FOMC will “carefully monitor the size and composition of the Federal Reserve’s balance sheet in light of evolving financial and economic developments.” Eventually, the FOMC made clear their policy of Treasury reinvestment. For instance, in Chairman Bernanke’s July 2010 report to Congress, he stated that “the proceeds from maturing Treasury securities are being reinvested in new issues of Treasury securities with similar maturities.”

²¹In our analysis, we exclude purchases of agency debt (which accounts for a small fraction of the total purchases during QE1) given the complexities associated with the health of Freddie Mac and Fannie Mae.

Size: Matching the overall magnitude of QE1 requires a few additional steps. As discussed above, our calibration strategy does not separately identify the size of preferred habitat demand shifts and arbitrageur risk aversion. This allows us to compute the response of yields to a “unit” demand shock $\partial y_t^{(\tau)} / \partial \beta_t$. However, our moment-matching exercise provides no information about the dollar magnitude of a “unit” demand shock in the model, since we only can estimate the product $a \cdot \sigma_\beta \cdot \theta_0$. Our model is meant to capture all the volatility of demand shocks, not just those which occur during auctions. However, we can utilize additional information from Treasury auctions to pin down the dollar magnitude of demand shocks. From Table 3, a unit increase in the bid-to-cover for an auction of intermediate maturities moves yields by roughly 3 basis points. This movement in the bid-to-cover ratio corresponds to roughly \$30 billion, which we denote by $\Delta \beta_t^{(auc)}$. Hence, we have $\Delta \beta_t^{(auc)} \cdot \partial y_t^{(\tau)} / \partial \beta_t \approx 3bp$ and can use the model to solve for $\Delta \beta_t^{(auc)}$. Finally, since QE1 was roughly \$1.5 trillion, we have that $\Delta \beta^{(QE)} \approx 50 \times \Delta \beta_t^{(auc)}$.

Panel A of Figure 11 plots the cumulative change observed in the data and predicted in the model. We use the cumulative change in the yield curve reported in Krishnamurthy and Vissing-Jorgensen (2011) following the 5 major QE1 event dates as the empirical response of the yield curve to QE1. The remarkable consistency between the responses suggests that the actual market reaction to QE1 announcements is in line with the predictions of a preferred habitat model and the behavior of the market in response to observed shifts in private demand for Treasuries. This finding implies that the *net* effect of other channels of QE (e.g., inflation expectations, forward guidance, signaling) could be smaller than thought before.

5.3 Macroeconomic Effects of Quantitative Easing

While there is extensive research documenting the responses of financial markets to rounds of QE, little is known about how QE affected the broader economy because QE events are so infrequent. We cannot shed more light on this using regression analysis or similar tools, but we can use our calibrated model to quantify the macroeconomic effects of QE.

Panel B of Figure 11 shows that our baseline calibration implies that in terms of macroeconomic effects, QE1 increased output by roughly 0.7 percentage points, and inflation by 0.35 percentage points. These effects then monotonically fall towards zero over the next few years. Integrating over time, the cumulative effects are $\int_0^\infty E_0 [x_t] dt \approx 0.53$ percentage points and $\int_0^\infty E_0 [\pi_t] dt \approx 0.6$ percentage points. For comparison, under risk neutrality (that is, in a standard New Keynesian model), the cumulative effects of a 25 basis point cut in the policy rate with the same mean reversion $\kappa_r = 0.2$ as our QE1 shock are $\int_0^\infty E_0 [x_t] dt \approx 0.38$ percentage points and $\int_0^\infty E_0 [\pi_t] dt \approx 0.31$ percentage points. Hence, in our model, the stimulative effects of QE1 are comparable to a modest

(25-50 b.p.) but long-lasting conventional monetary policy shock.²²

5.4 Alternative Designs of Quantitative Easing

Can policymakers make QE more powerful? What are the potential downside risks of QE? To address these questions, we explore how variations in the implementation of large-scale asset purchases can influence the power of this tool to move output and inflation. Figure 12 shows how the dynamics of output change under the different sensitivity analyses.²³

Unwinding: One practical question for policymakers is how long central banks should hold assets accumulated during QE rounds. While this issue has been explored—but seemingly not resolved with a consensus recommendation (e.g., [Sims and Wu \(2020\)](#) and [Karadi and Nakov \(2020\)](#))—in models emphasizing reserve requirements/moral hazard constraints on banks as a key channel for QE, little is known in a preferred habitat macroeconomic context. To this end, we vary κ_{QE} in equation (24), which governs the unwinding process. Panel A of Figure 12 shows that the effects on output nearly double when comparing very fast and very slow unwinding (the x-axis reports results from $\kappa_{QE} \in (0.05, 1.0)$, implying a half-life of about three-quarters to fourteen years).

Intuitively, if the Fed were to make large purchases of assets but markets expect the Fed to quickly sell those securities back, we would not expect to observe large and long-term macroeconomic effects. Rather, it is the cumulative size of QE over time that matters. Hence, policymakers should be clear about how long the central bank expects to hold the securities on its balance sheet. To the extent that the policymaker is planning to unwind their asset holdings very slowly, providing a type of “forward guidance” regarding the expected path of purchases can potentially increase the immediate effectiveness of these policies if markets do not fully anticipate how long the QE program will last.

Finally, comparing the counter-factual “risky-only” and “Treasury-only” QE policies (the dashed orange and dotted blue lines), we observe the same pattern as a function of unwinding. However, for any degree of mean-reversion, the “risky-only” purchases have a larger effect on output than the “Treasury-only” purchases because “risky-only” purchases affect household borrowing rates directly.

²²From the perspective of our model there is little difference between a) the Fed buying assets (and thus reducing assets available to the private market) and b) the Treasury issuing less debt (and thus reducing assets available to the private market). Thus, while comparing our estimated effect of QE1 and actual data, one should keep in mind that the Treasury increased issuance of debt by approximately \$2.7 trillion between December 2008 and October 2010 (the duration of QE1) relative to the pre-crisis trend. The average maturity of debt issued over this period was 6.4 years. If we assume that this shock to the supply of government debt is as persistent as QE1 (i.e., debt is held to maturity), then QE1 was roughly offsetting the increased supply of Treasuries and the combined macroeconomic effect of changes in government debt due to fiscal and monetary policies was a wash.

²³Appendix Figure B17 reports the same exercises for the dynamics of inflation; we focus our discussion on the results for output, but the results for inflation are qualitatively very similar.

Risk Appetite: As we discussed above, the power of QE to affect yields at target maturities is high in crisis times and weak in non-crisis times. Consistent with this insight, Panel B of Figure 12 shows that the transmission is highly sensitive to the risk aversion of arbitrageurs. Given that our baseline calibration for “crisis” corresponds to the Great Recession, one has to have a financial crisis of truly unprecedented proportions to materially increase the power of QE-based tools. On the other hand, normal times are characterized by much lower values of risk aversion. As a result, the balance of risks appears to be somewhat one-sided: it is difficult to raise the power of QE beyond what was achieved during the Great Recession but it is relatively easy to reduce the power as soon as financial panics calm down. This logic suggests that QE is less effective as a “conventional” tool to the extent that “conventional” entails well-functioning financial markets. QE may remain in the central bankers’ toolkit, but should only be utilized during periods of financial distress. As in the previous sensitivity exercise, the counter-factual “risky-only” and “Treasury-only” QE policies have the same pattern as a function of risk aversion, but the “risky-only” purchases have a larger effect on output than the “Treasury-only” purchases.

Risky Asset Uncertainty: We next discuss how the transmission of QE depends on the riskiness of risky assets. Panel C of Figure 12 plots the long-run effect of QE on output as we increase σ_d from the baseline calibration. We find that the baseline QE policy has larger macroeconomic effects as risky assets become riskier. The intuition for this can be seen by examining the counter-factual “risky-only” and “Treasury-only” QE policies.

Unlike the previous sensitivity exercises, “risky-only” and “Treasury-only” QE policies act differently as a function of risky asset uncertainty. As risky asset uncertainty increases, the effect of risky asset purchases on output increases. However, the impact of Treasury purchases decreases. Intuitively, when risky asset payoff uncertainty is very low, Treasuries and risky assets are good substitutes (in the limit of no payoff risk, these two assets become perfect substitutes). In this case, “risky-only” and “Treasury-only” QE policies have similar effects on household borrowing rates, and therefore the transmission to macroeconomic variables will be similar. However, as risky asset uncertainty increases, Treasuries and risky assets become less substitutable. Now, “risky-only” QE policies are highly effective at moving household borrowing rates (and therefore have larger macroeconomic effects), while “Treasury-only” QE policies have smaller effects on household borrowing rates (and therefore have smaller macroeconomic effects).

QE Uncertainty: Recall that we assume QE was a one-off shock, completely unanticipated by markets. This may be an accurate representation of the first round of quantitative easing, but a decade later it is clear that large-scale asset purchases are here to stay. Hence, it is likely that markets now consider the possibility of future QE shocks. To model the recurrent nature of QE, we modify equation (24) and instead assume that QE

shocks are described by the following equation:

$$d\beta_t^{QE} = -\kappa_{QE}\beta_t^{QE} dt + \sigma_{QE} dB_{QE,t}. \quad (25)$$

Hence, whenever $\sigma_{QE} > 0$, QE shocks themselves may lead to additional macroeconomic volatility. Further, risk-averse arbitrageurs must hedge against QE risk, in addition to fundamental sources of risk in the economy.

Panel D of Figure 12 explores the change in long-run volatility of output and inflation change as a function of the volatility of QE shocks. $\sigma_{QE} = 0$ is our baseline estimate (marked by the vertical dotted line); the x-axis is the volatility of QE shocks relative to the volatility of habitat demand shocks $\frac{\sigma_{QE}}{\sigma_\beta}$; the y-axis is the the long-run variance of output. The results provide an important note of caution for central bankers: increased uncertainty regarding QE leads to increased macroeconomic volatility. In other words, although policymakers may desire the added flexibility of discretionary QE tools, the downside is that this increases the uncertainty surrounding these policy tools. By communicating clearly the expected path of QE purchases, policymakers should be able to reduce market uncertainty and prevent volatility spillovers from QE into the real economy. This provides support for the use of QE rules or forward guidance regarding asset purchases in the spirit of Ray (2019) and Greenwood et al. (2016).

6 Concluding Remarks

Quantitative easing (QE) programs are a massive policy experiment. The deployment of QE in response to the COVID-19 crisis is a testament to policymakers’ belief that the experiment worked. To understand which channels are responsible for the impact of QE on the macroeconomy, it is useful to unbundle these channels so that future policy can be designed to maximize the effectiveness of QE-like tools in crisis and non-crisis times. We focus on the “preferred habitat” channel, where due to market segmentation and limited arbitrage, interest rates for a given maturity range may be influenced by targeted buying or selling of assets within this range (“localization effect”).

We utilize Treasury auctions of government debt to identify Treasury demand shocks arising from changes in institutional investor demand to study how shocks in one maturity segment propagate to other segments, and how this propagation is affected by financial markets conditions. These shocks provide us with variation in demand for Treasuries that is unrelated to some prominent hypothesized channels of QE transmission (e.g., inflation expectations, forward guidance, or signaling) and instead allow us to focus on the role of preferred habitat mechanisms. Crucially, these mechanisms are dependent on how *private* agents in the market for Treasury debt absorb these demand shocks, regardless of the source of these shocks. We use this variation to discipline a general equilibrium model

that embeds financial markets with preferred habitat and use this model to assess the quantitative importance of preferred habit for QE rounds and alternative designs of QE.

We find that localization effects are stronger when markets are segmented (e.g. due to a crisis) than when markets are integrated. Through the lens of our model, we show that the magnitude of these localization effects is large enough to account for the entirety of interest rate movements in response to QE announcements, consistent with the view that QE programs worked mainly via market segmentation. Policy experiments in our calibrated model suggest that QE can be a useful policy tool in crises: a QE1 shock during crisis stimulates output and inflation by the magnitudes that roughly correspond to movements in response to a persistent 25-50 basis point cut in the policy rate during normal times. However, the effect of QE on asset prices (and hence the broader economy) weakens if the holding period of assets purchases by a central bank is short or financial markets are well-functioning; further, there is the risk that uncertainty about future QE rounds leads to excess macroeconomic volatility.

References

- Beetsma, R., Giuliodori, M., de Jong, F., and Widiyanto, D. (2016). Price effects of sovereign debt auctions in the euro-zone: The role of the crisis. *Journal of Financial Intermediation*, 25(C):30–53.
- Beetsma, R., Giuliodori, M., Hanson, J., and de Jong, F. (2018). Bid-to-cover and yield changes around public debt auctions in the euro area. *Journal of Banking & Finance*, 87(C):118–134.
- Bernanke, B. S. and Kuttner, K. N. (2005). What Explains the Stock Market’s Reaction to Federal Reserve Policy? *Journal of Finance*, 60(3):1221–1257.
- Bhattarai, S. and Neely, C. J. (2020). An analysis of the literature on international unconventional monetary policy. *FRB St. Louis Working Paper*, (2016-21C).
- Cahill, M. E., D’Amico, S., Li, C., and Sears, J. S. (2013). Duration risk versus local supply channel in Treasury yields: evidence from the Federal Reserve’s asset purchase announcements. Finance and Economics Discussion Series 2013-35, Board of Governors of the Federal Reserve System (U.S.).
- Cammack, E. B. (1991). Evidence on Bidding Strategies and the Information in Treasury Bill Auctions. *Journal of Political Economy*, 99(1):100–130.
- Campbell, J. R., Evans, C. L., Fisher, J. D., and Justiniano, A. (2012). Macroeconomic Effects of Federal Reserve Forward Guidance. *Brookings Papers on Economic Activity*, 43(1):1–80.
- Carlstrom, C. T., Fuerst, T. S., and Paustian, M. (2017). Targeting Long Rates in a Model with Segmented Markets. *American Economic Journal: Macroeconomics*, 9(1):205–242.
- Chen, H., Cúrdia, V., and Ferrero, A. (2012). The Macroeconomic Effects of Large-scale Asset Purchase Programmes. *Economic Journal*, 122(564):289–315.
- Chodorow-Reich, G. (2014). Effects of Unconventional Monetary Policy on Financial Institutions. *Brookings Papers on Economic Activity*, 45(1):155–227.

- Cúrdia, V. and Woodford, M. (2011). The central-bank balance sheet as an instrument of monetary policy. *Journal of Monetary Economics*, 58(1):54–79.
- D’Amico, S. and King, T. B. (2013). Flow and stock effects of large-scale treasury purchases: Evidence on the importance of local supply. *Journal of Financial Economics*, 108(2):425–448.
- Di Maggio, M., Kermani, A., and Palmer, C. J. (2020). How Quantitative Easing Works: Evidence on the Refinancing Channel. *Review of Economic Studies*, 87(3):1498–1528.
- Driessen, G. A. (2016). How treasury issues debt. *Congressional Research Service Report R40767*.
- Fieldhouse, A. J., Mertens, K., and Ravn, M. O. (2018). The Macroeconomic Effects of Government Asset Purchases: Evidence from Postwar U.S. Housing Credit Policy. *Quarterly Journal of Economics*, 133(3):1503–1560.
- Fleming, M. J. (2007). Who buys treasury securities at auction? *Federal Reserve Bank of New York Current Issues in Economics and Finance*, 13(1).
- Fleming, M. J. and Liu, W. (2016). Intraday pricing and liquidity effects of us treasury auctions.
- Forest, J. J. (2018). The Effect of Treasury Auction Results on Interest Rates: The 1990s Experience. Technical report, University of Massachusetts - Amherst.
- Garbade, K. D. (2007). The Emergence of Regular and Predictable as a Treasury Debt Management Strategy. *FRBNY Economic Policy Review*, (March):53–71.
- Garbade, K. D. and Ingber, J. F. (2005). The Treasury auction process: objectives, structure, and recent acquisitions. *Current Issues in Economics and Finance*, 11(Feb).
- Gertler, M. and Karadi, P. (2011). A model of unconventional monetary policy. *Journal of Monetary Economics*, 58(1):17 – 34. Carnegie-Rochester Conference Series on Public Policy: The Future of Central Banking April 16-17, 2010.
- Gorodnichenko, Y. and Ray, W. (2017). The Effects of Quantitative Easing: Taking a Cue from Treasury Auctions. NBER Working Papers 24122, National Bureau of Economic Research, Inc.
- Greenlaw, D., Hamilton, J. D., Harris, E., and West, K. D. (2018). A Skeptical View of the Impact of the Feds Balance Sheet. NBER Working Papers 24687, National Bureau of Economic Research, Inc.
- Greenwood, R., Hanson, S. G., and Vayanos, D. (2016). Forward Guidance in the Yield Curve: Short Rates versus Bond Supply. In Albagli, E., Saravia, D., and Woodford, M., editors, *Monetary Policy through Asset Markets: Lessons from Unconventional Measures and Implications for an Integrated World*, Central Banking, Analysis, and Economic Policies Book Series, pages 11–62. Central Bank of Chile.
- Greenwood, R. and Vayanos, D. (2014). Bond supply and excess bond returns. *Review of Financial Studies*, 27(3):663–713.
- Gürkaynak, R. S., Sack, B., and Wright, J. H. (2007). The U.S. Treasury yield curve: 1961 to the present. *Journal of Monetary Economics*, 54(8):2291 – 2304.
- Hamilton, J. D. and Wu, J. C. (2012). The Effectiveness of Alternative Monetary Policy Tools in a Zero Lower Bound Environment. *Journal of Money, Credit and Banking*, 44:3–46.
- He, Z., Kelly, B., and Manela, A. (2016). Intermediary asset pricing: New evidence from many asset classes. Working Paper 21920, National Bureau of Economic Research.
- He, Z. and Krishnamurthy, A. (2013). Intermediary Asset Pricing. *American Economic Review*, 103(2):732–770.

- Kaminska, I. and Zinna, G. (2020). Official demand for u.s. debt: Implications for u.s. real rates. *Journal of Money, Credit and Banking*, 52(2-3):323–364.
- Karadi, P. and Nakov, A. (2020). Effectiveness and addictiveness of quantitative easing. *Journal of Monetary Economics*.
- King, T. (2019a). Duration Effects in Macro-Finance Models of the Term Structure. Technical report.
- King, T. B. (2019b). Expectation and duration at the effective lower bound. *Journal of Financial Economics*, 134(3):736–760.
- Koijen, R. S., Koulischer, F., Nguyen, B., and Yogo, M. (2021). Inspecting the mechanism of quantitative easing in the euro area. *Journal of Financial Economics*, 140(1):1–20.
- Krishnamurthy, A. and Vissing-Jorgensen, A. (2011). The effects of quantitative easing on interest rates: Channels and implications for policy. *Brookings Papers on Economic Activity*, (2):215–265.
- Krishnamurthy, A. and Vissing-Jorgensen, A. (2012). The aggregate demand for Treasury debt. *Journal of Political Economy*, 120(2):233–267.
- Kuttner, K. N. (2001). Monetary policy surprises and interest rates: Evidence from the Fed funds futures market. *Journal of Monetary Economics*, 47(3):523–544.
- Kyle, A. S. and Xiong, W. (2001). Contagion as a Wealth Effect. *Journal of Finance*, 56(4):1401–1440.
- Li, C. and Wei, M. (2013). Term Structure Modeling with Supply Factors and the Federal Reserve’s Large-Scale Asset Purchase Programs. *International Journal of Central Banking*, 9(1):3–39.
- Lou, D., Yan, H., and Zhang, J. (2013). Anticipated and Repeated Shocks in Liquid Markets. *Review of Financial Studies*, 26(8):1891–1912.
- Martin, C. and Milas, C. (2012). Quantitative easing: a sceptical survey. *Oxford Review of Economic Policy*, 28(4):750–764.
- Ray, W. (2019). Monetary policy and the limits to arbitrage: Insights from a new keynesian preferred habitat model. Working paper.
- Romer, C. D. and Romer, D. H. (2017). New evidence on the aftermath of financial crises in advanced countries. *American Economic Review*, 107(10):3072–3118.
- Sims, E. and Wu, J. C. (2020). Evaluating central banks tool kit: Past, present, and future. *Journal of Monetary Economics*.
- Vayanos, D. and Vila, J. (2021). A Preferred-Habitat Model of the Term Structure of Interest Rates. *Econometrica*, 89(1):77–112.
- Wright, J. H. (2012). What does monetary policy do to long-term interest rates at the zero lower bound? *Economic Journal*, 122(564):F447–F466.

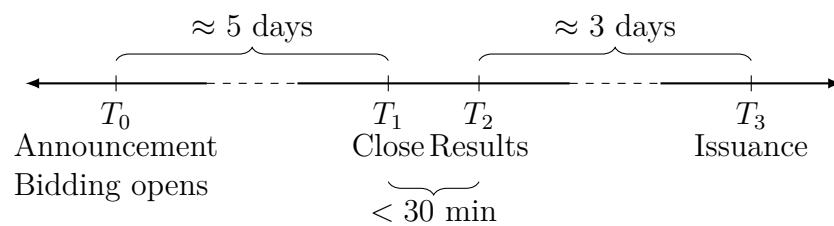


Figure 1: Auction Timing

Notes: Timeline of the events occurring during a representative Treasury auction.

August 03, 2011	202-504-3550	August 11, 2011	202-504-3550
TREASURY OFFERING ANNOUNCEMENT ¹		TREASURY AUCTION RESULTS	
Term and Type of Security	30-Year Bond	Term and Type of Security	30-Year Bond
Offering Amount	\$16,000,000,000	CUSIP Number	912810QSO
Currently Outstanding	\$0	Series	Bonds of August 2041
CUSIP Number	912810QSO	Interest Rate	3-3/4%
Auction Date	August 11, 2011	High Yield ¹	3.750%
Original Issue Date	August 15, 2011	Allotted at High	41.74%
Issue Date	August 15, 2041	Price	100.000000
Maturity Date	August 15, 2011	Accrued Interest per \$1,000	None
Dated Date	Bonds of August 2041	Median Yield ²	3.629%
Series	Determined at Auction	Low Yield ³	3.537%
Yield	Determined at Auction	Issue Date	August 15, 2011
Interest Rate	None	Maturity Date	August 15, 2041
Interest Payment Dates	February 15 and August 15	Original Issue Date	August 15, 2011
Accrued Interest from 08/15/2011 to 08/15/2011	None	Dated Date	August 15, 2011
Premium or Discount	Determined at Auction		
Minimum Amount Required for STRIPS	\$100		
Corpus CUSIP Number	912803DT7	Tendered	Accepted
Additional TINT(s) Due Date(s) and	August 15, 2041	Competitive	\$15,985,160,000
CUSIP Number(s)	912834KP2	Noncompetitive	\$14,855,600
Maximum Award	\$5,600,000,000	FIMA (Noncompetitive)	\$0
Maximum Recognized Bid at a Single Yield	\$5,600,000,000	Subtotal⁴	\$16,000,015,600⁵
NLP Reporting Threshold	\$5,600,000,000	SOMA	\$489,928,400
NLP Exclusion Amount	\$0	Total	\$16,489,944,000
Minimum Bid Amount and Multiples	\$100		
Competitive Bid Yield Increments ²	0.001%	Tendered	Accepted
Maximum Noncompetitive Award	\$5,000,000	Primary Dealer ⁶	\$10,921,532,000
Eligible for Holding in Treasury Direct Systems	Yes	Direct Bidder ⁷	\$3,119,654,000
Eligible for Holding in Legacy Treasury Direct	No	Indirect Bidder ⁸	\$1,943,974,000
Estimated Amount of Maturing Coupon Securities Held by the Public	\$24,430,000,000	Total Competitive	\$15,985,160,000
Maturing Date	August 15, 2011		
SOMA Holdings Maturing	\$2,205,000,000		
SOMA Amounts Included in Offering Amount	No		
FIMA Amounts Included in Offering Amount ³	Yes		
Noncompetitive Closing Time	12:00 Noon ET		
Competitive Closing Time	1:00 p.m. ET		

(b) Results

(a) Announcement

Figure 2: Example of Auction Press Releases

Notes: Press releases from the Treasury for an auction of 30-year bonds. Source: TreasuryDirect.

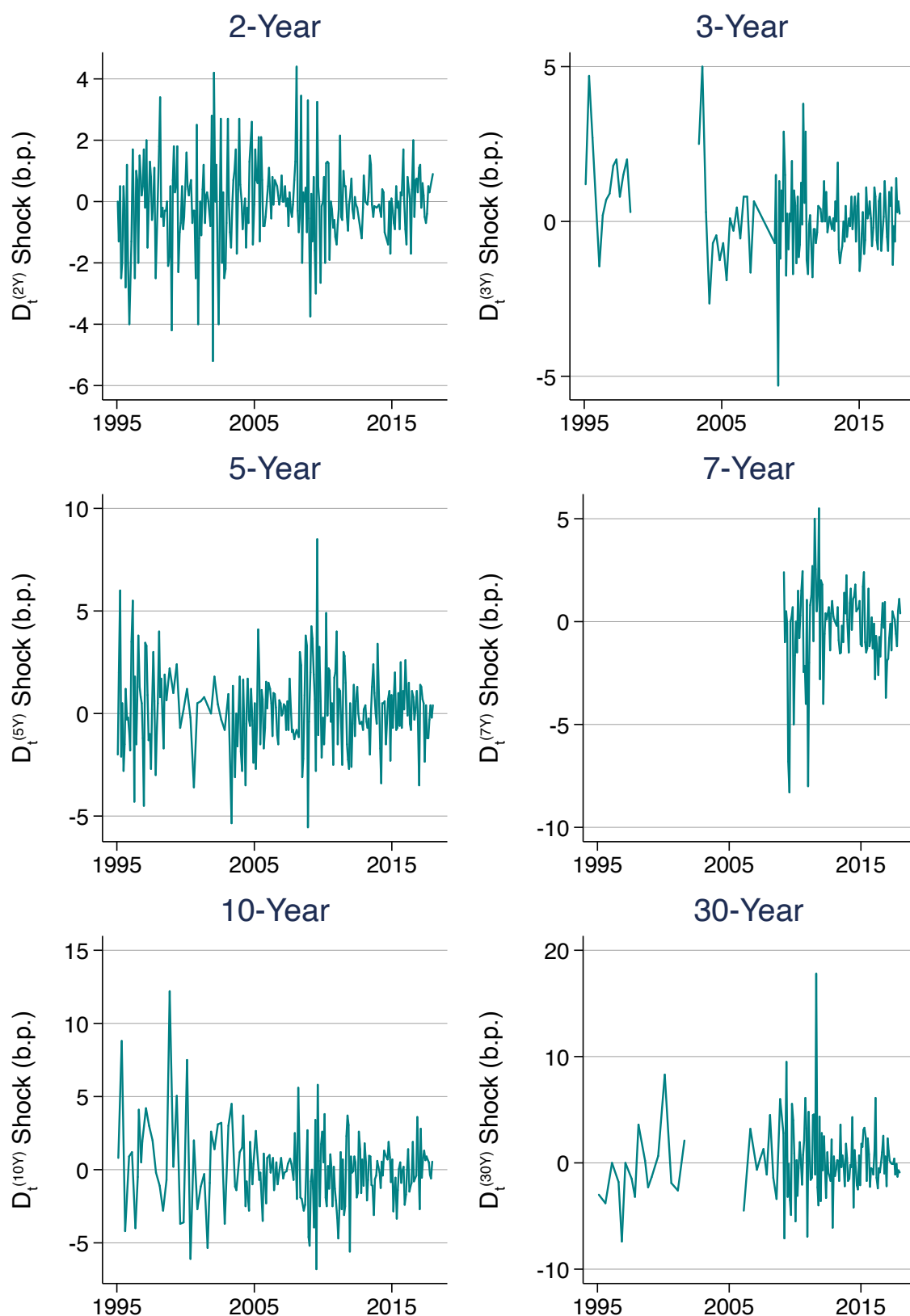


Figure 3: Time Series of Surprise Movements in Treasury Yields

Notes: Plots of the times series of intraday yield shocks following the close of Treasury auctions. Shocks $D_t^{(m)}$ are plotted separately for auctions of maturities $m = 2, 3, 5, 7, 10, 30$ years (in basis points). Gaps in the time series of 3-year, 7-year, and 30-year shocks correspond to temporary halts of newly issued securities of these maturities; see Figure B1.

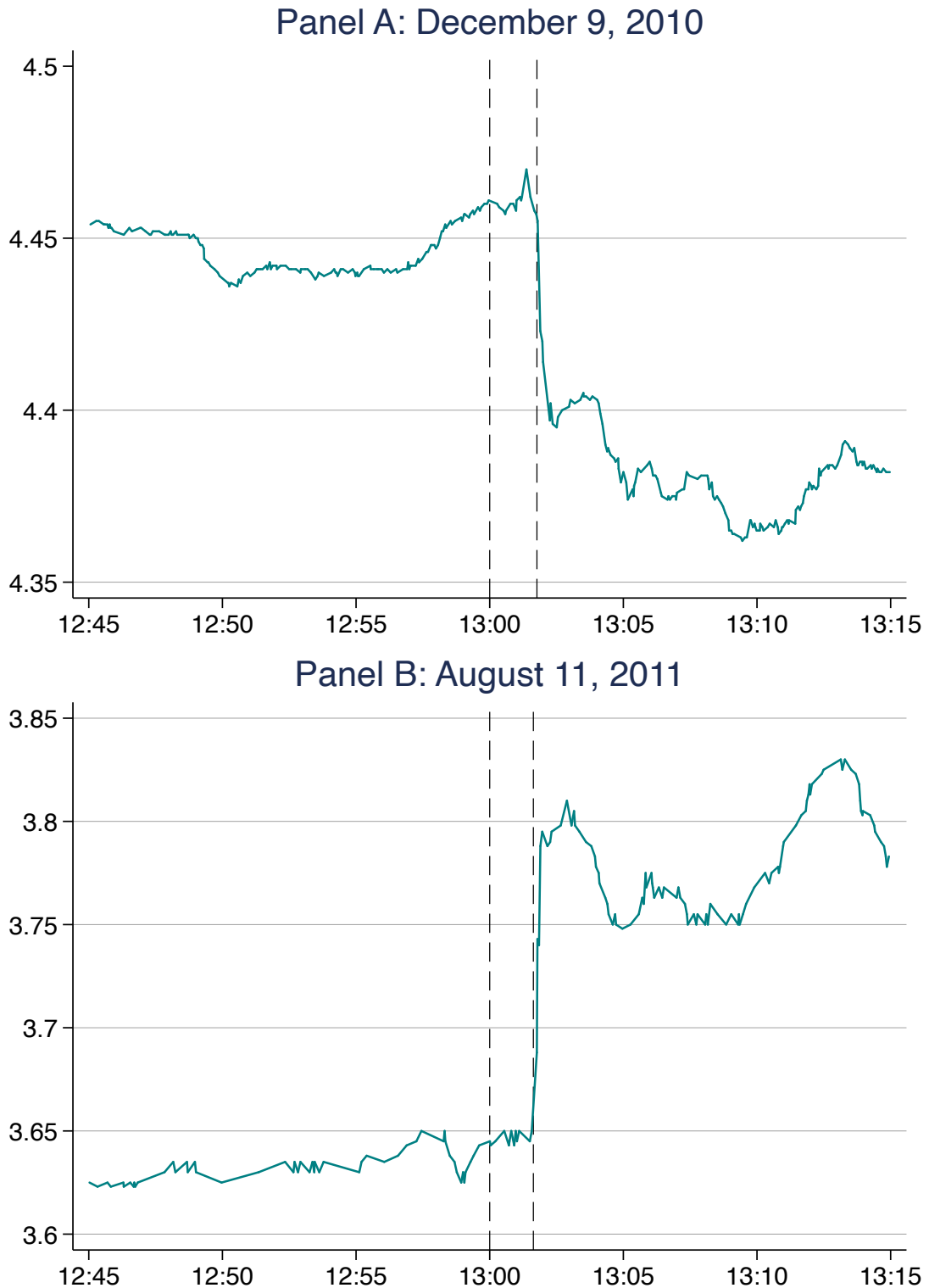


Figure 4: Intraday Treasury Yield Movements

Notes: Panel A plots intraday movements during the 30-year auction on December 9, 2010. An auction for reopened 30-year Treasury bonds closed at 1:00pm (first vertical line), and results were released shortly after (second vertical line). Immediately following the release, yields of the associated security in secondary-market trading fell sharply. Panel B plots intraday movements during the 30-year auction on August 11, 2011. An auction for newly-issued 30-year Treasury bonds closed at 1:00pm (first vertical line), and results were released shortly after (second vertical line). Immediately following the release, yields of the corresponding when-issued trading rose sharply

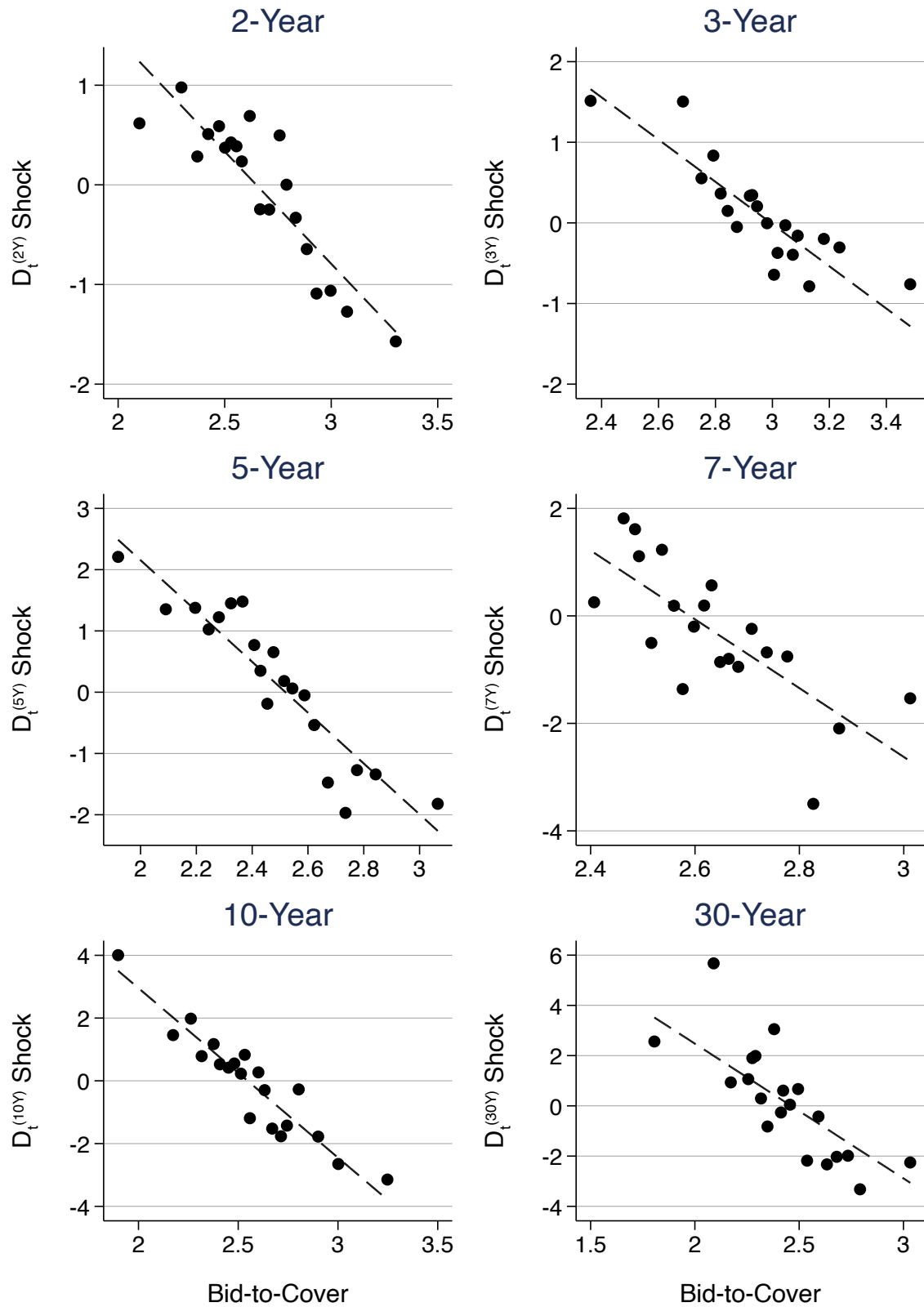


Figure 5: Demand Shocks and the Bid-to-Cover

Notes: Binned scatter plot examining the relationship between demand shocks and the bid-to-cover ratio across auctions. The bid-to-cover is the ratio of the dollar value of bids received to those accepted at a given auction. Four lags of the bid-to-cover are included; the residuals are plotted.

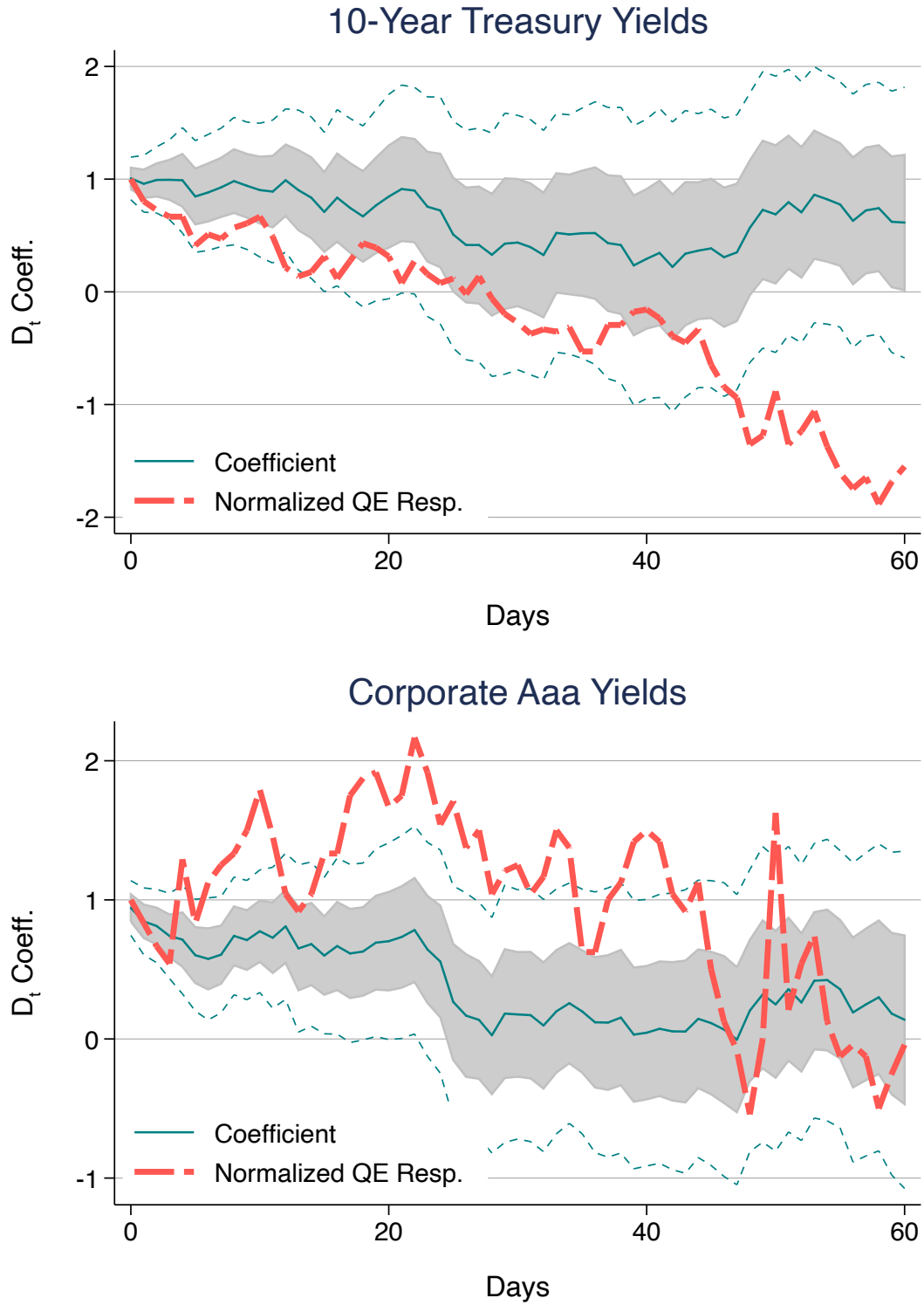


Figure 6: Long-Difference Response to Demand Shocks

Notes: Responses of 10-year Treasury spot rates (top panel) and Moody's Aaa yields (bottom panel) to demand shocks D_t (pooled across maturities). We compute "long-difference" regressions: on an auction date t , the dependent variable is $y_{t+h} - y_{t-1}$, the change h days after the auction relative to the day before the auction. The solid line plots the coefficients from regressions for $h = 0, \dots, 60$; the shaded region and dotted lines correspond to one- and two-standard error (Newey-West, 9 lags) confidence bands. The dashed line compares the long-horizon effects of the March 2009 QE1 FOMC announcement (normalized so that the impact on announcement is one).

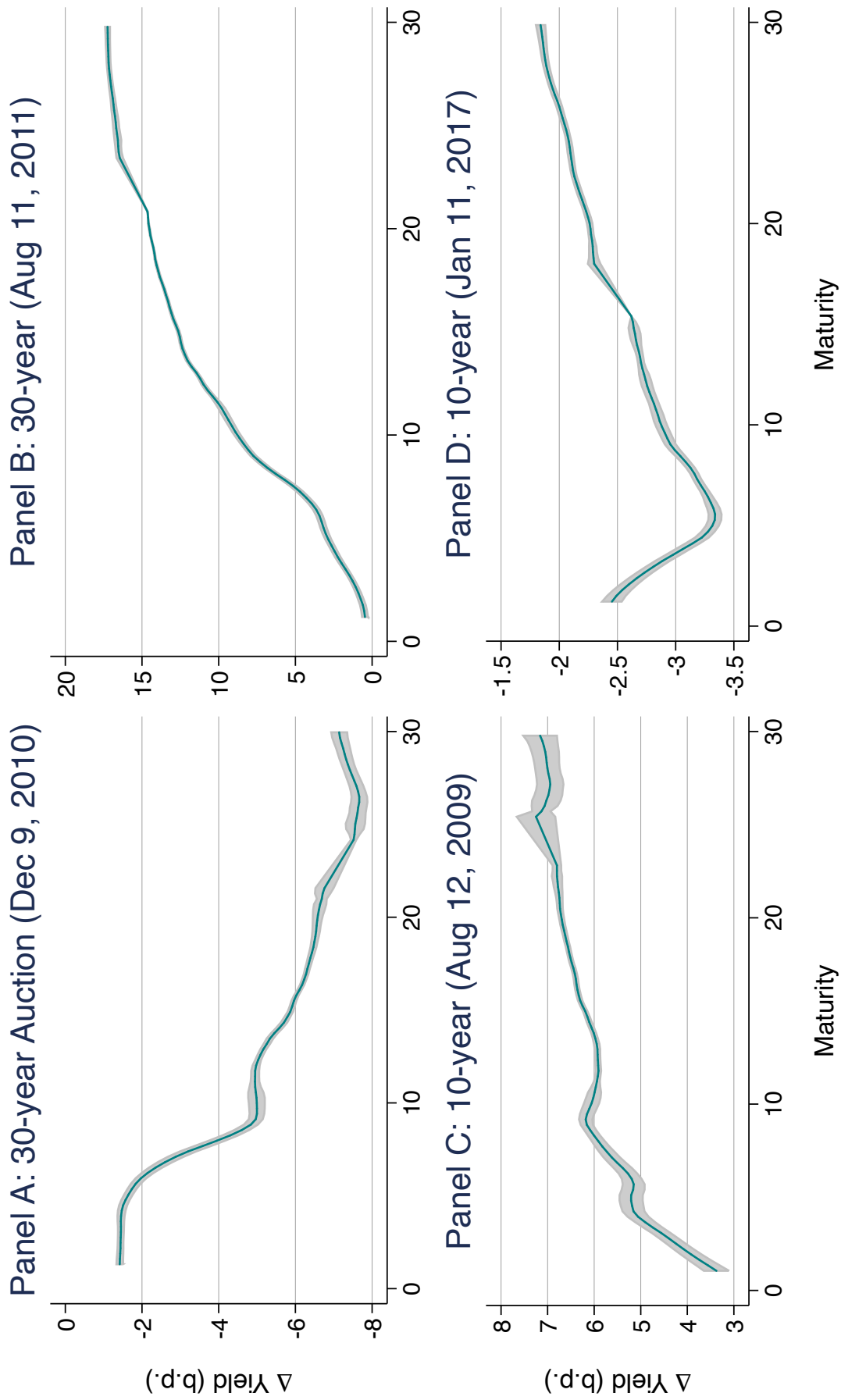


Figure 7: Changes in Yield Curves Following Treasury Auctions

Notes: Intraday changes in the yield curve following 30-year auctions on December 9, 2010 and August 11, 2011 (top panels) and following 10-year auctions on August 12, 2009 and January 11, 2017 (bottom panels). The change in yields (in basis points) are from all traded bills, notes, and bonds in the secondary market. The solid line represents the point estimates of local-mean smoothing regressions across maturities, while the shaded regions represent two standard error confidence intervals.

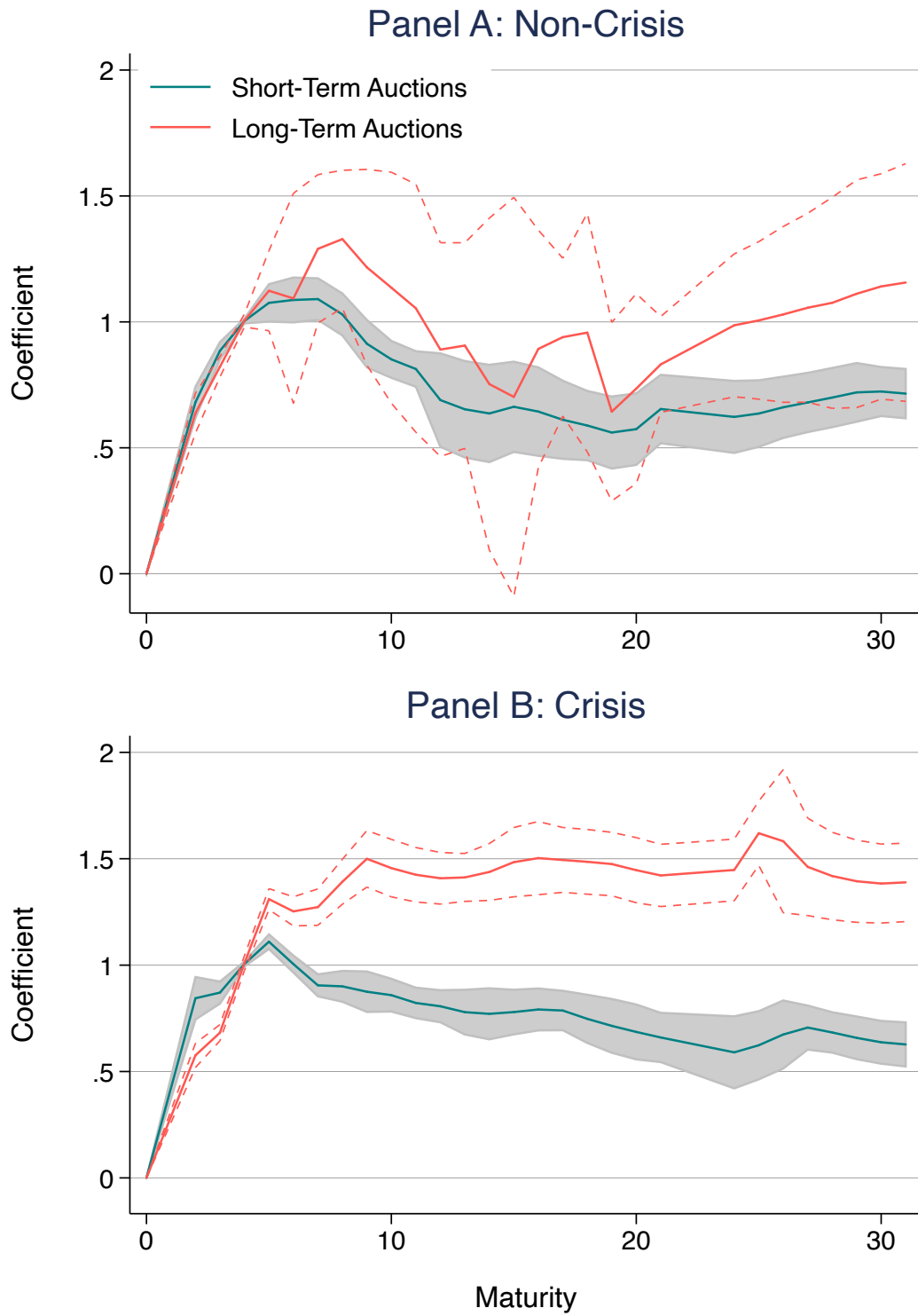


Figure 8: Localization Regression Results

Notes: Plots of the regression coefficients from regression equation (19). The top panel compares estimates from short- and long-maturity auctions during non-crisis periods; the bottom panel compares these estimates during crisis periods. 2 standard error (Newey-West, 9 lags) confidence intervals are included. Appendix Figure B6 reports p-values for the equality of estimates.

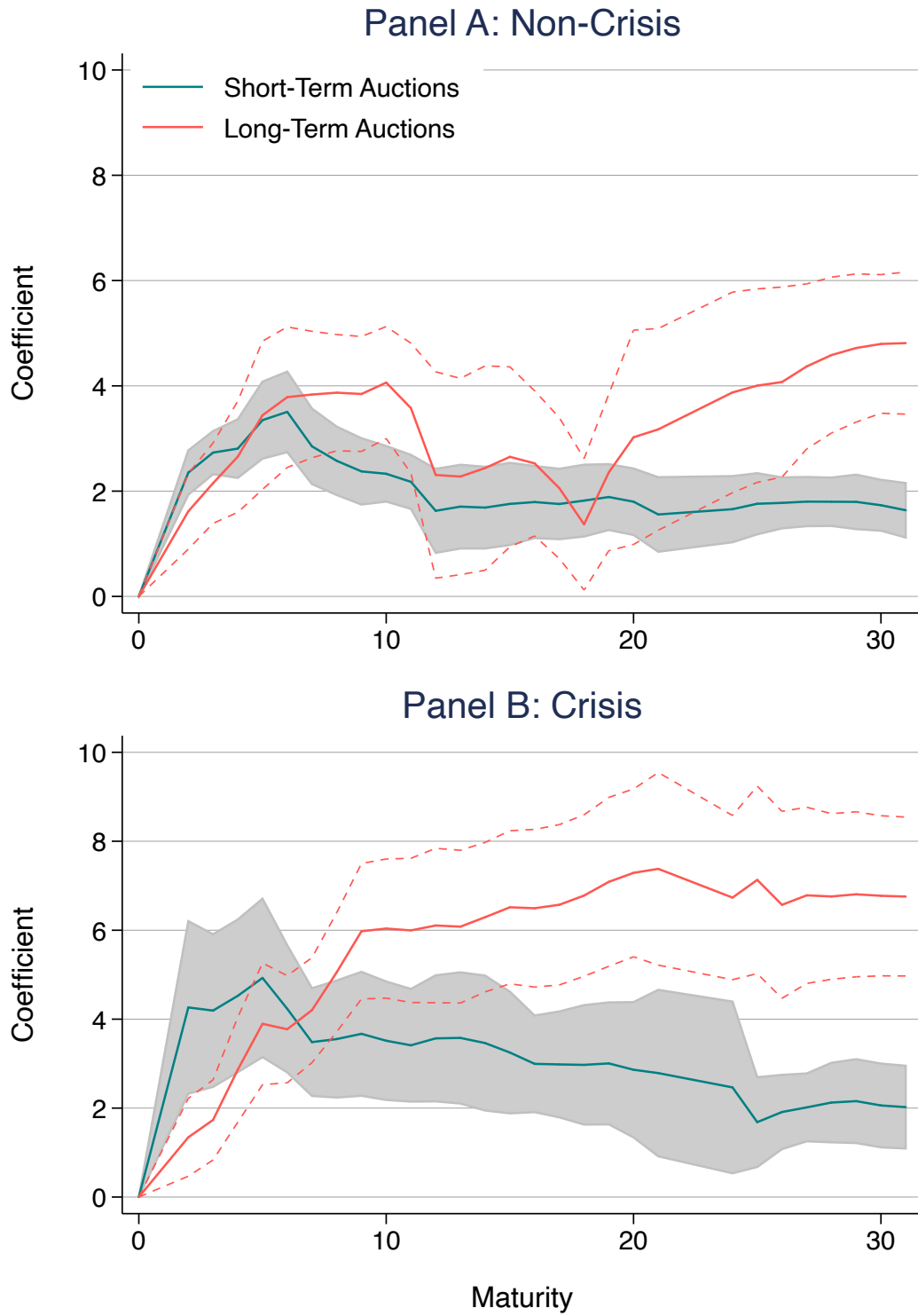


Figure 9: Localization Robustness: Bid-to-Cover

Notes: Estimates of the alternative localization regression equation (20), using the bid-to-cover ratio as a proxy of structural demand shocks (after controlling for its own four lags and flipping the sign). 2 standard error (Newey-West, 9 lags) confidence intervals are included.

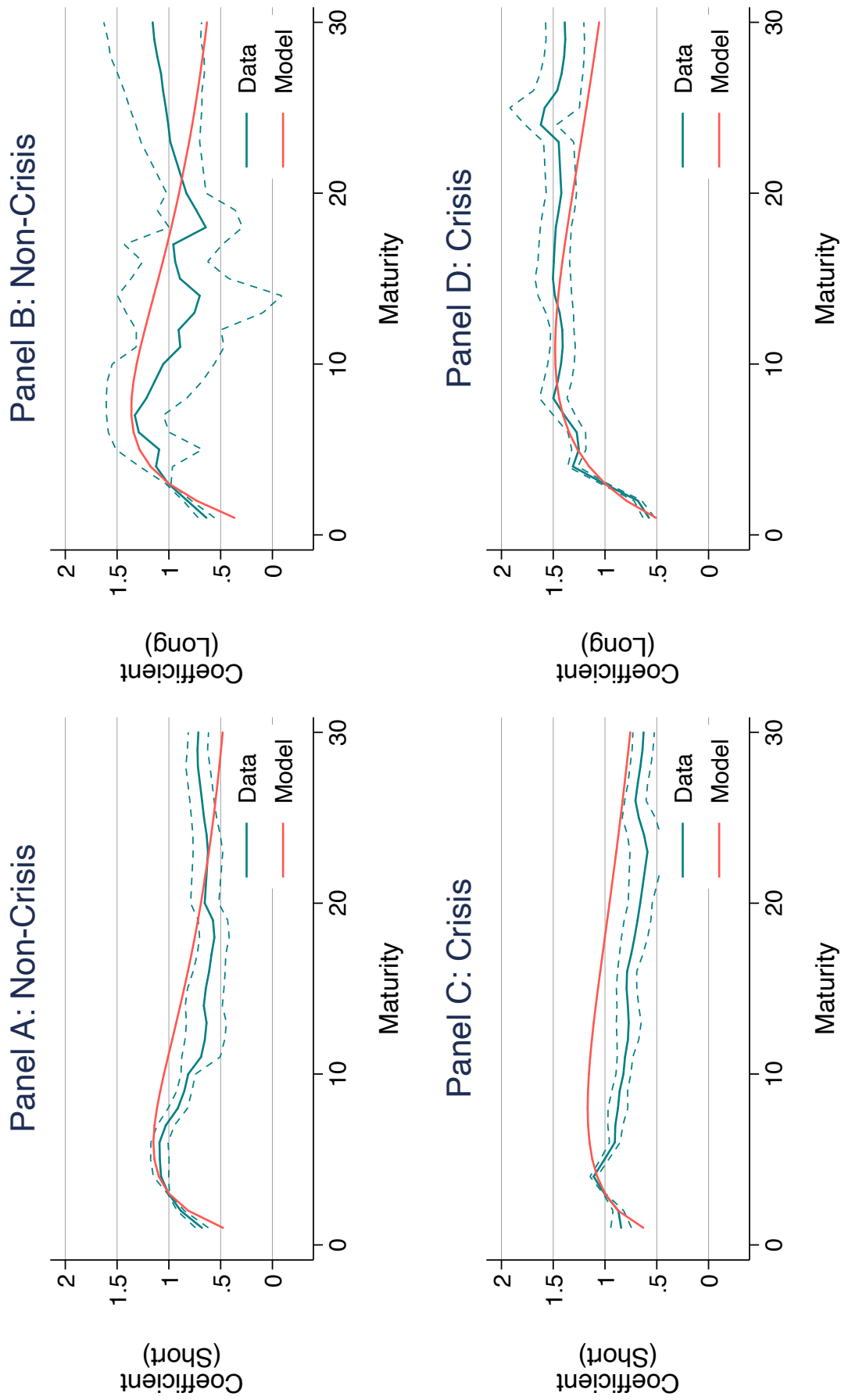


Figure 10: Model-Implied Localization Regression Coefficients

Notes: Model-implied coefficients from regression equation (19). The top panel plots the coefficients from the model calibrated to non-crisis periods, while the bottom panel plots the coefficients from the model calibrated to crisis periods.

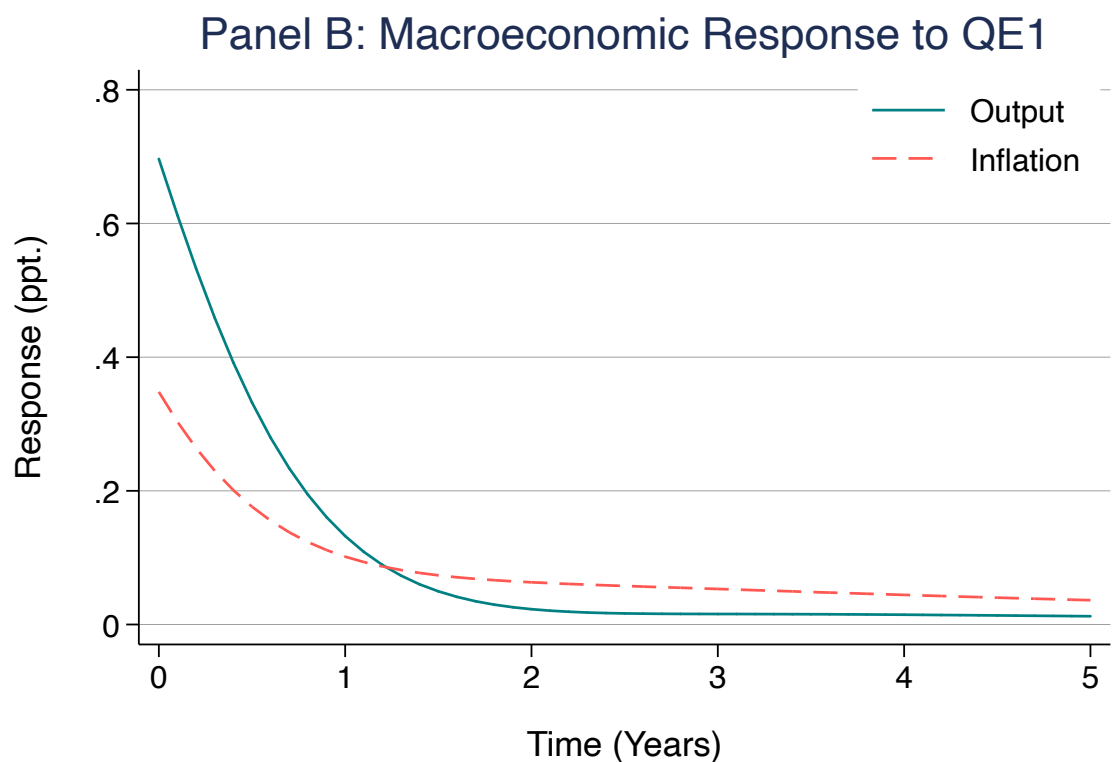
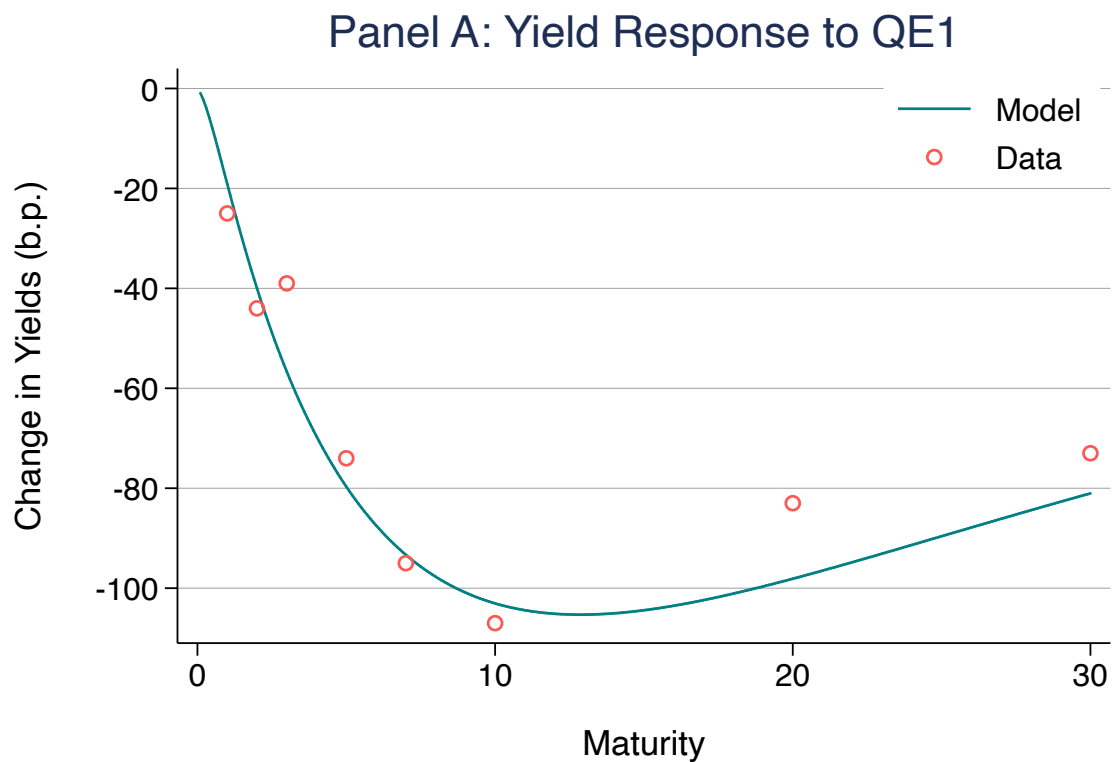


Figure 11: Model-Implied Response to QE1

Notes: Panel A compares the observed (cumulative) yield reactions and the model-implied change in yields following a QE1 shock. The empirical response is constructed as in [Krishnamurthy and Vissing-Jorgensen \(2011\)](#), and consists of the sum of the two-day changes in yields following all the major QE1 announcements. Panel B plots the model-implied IRF of output and inflation following QE1.

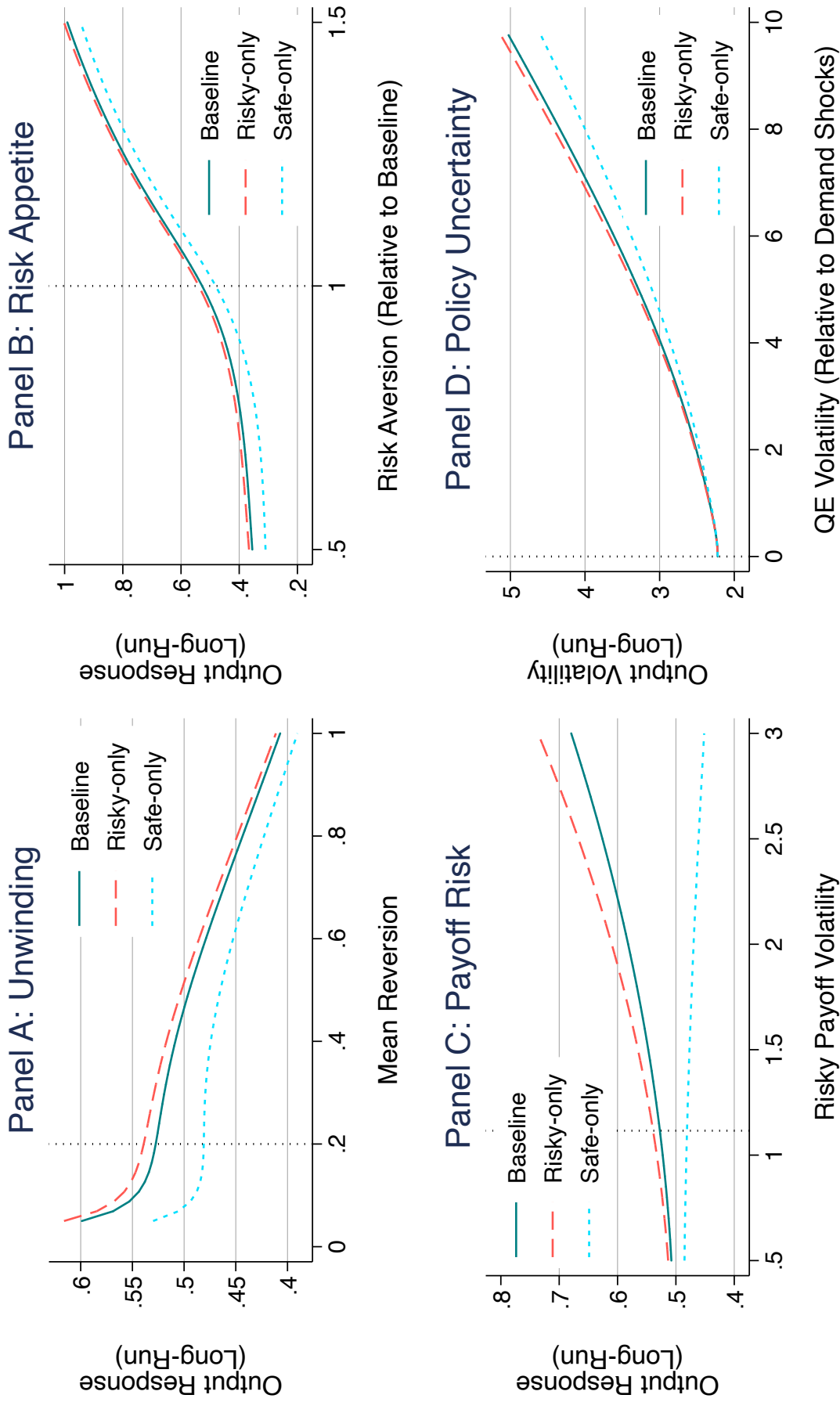


Figure 12: Policy Sensitivity Analysis: Output

Notes: Panel A plots the long-run impact of the QE shock in the model on output as a function of the mean reversion of the QE shock. Panel B plots the long-run impact of QE on output as a function of the long-run impact of QE on output as a function of risky asset payoff uncertainty. Panel C plots the change in long-run volatility of output as a function of the volatility of QE shocks. In each panel, the solid line corresponds to the baseline QE calibration. The dashed orange line shows results for a counter-factual QE policy which purchases risky assets only; the dotted blue line shows results for a counter-factual QE policy which purchases only Treasuries. Panel D reports the long-run volatility $Var[x_t]$ as a function of QE uncertainty. In all other panels, we summarize the effects of QE on output by reporting the cumulative effect following the QE shock $\int_0^\infty E_0[x_t] dt$ as a function of the QE parameters.

Table 1: Auction Summary Statistics

	Mean	Median	Std. Dev.	Min	Max
Offering Amount (billions)	22.51	22.00	8.99	5.00	44.00
Total Tendered (billions)	62.18	57.91	30.12	11.35	160.96
Term (Years)	8.09	5.00	8.60	2.00	30.25
High Yield	2.99	2.67	1.84	0.22	7.79
Bid-to-Cover	2.61	2.58	0.46	1.22	4.07
Bid-to-Cover by type [#]					
Direct Bidders	0.22	0.21	0.17	0.00	0.85
Indirect Bidders	0.53	0.53	0.17	0.03	1.05
Primary Dealers	1.93	1.88	0.34	0.98	3.12
Fraction Accepted by type [†]					
Depository Institutions	0.01	0.00	0.02	0.00	0.32
Individuals	0.01	0.00	0.02	0.00	0.19
Dealers	0.54	0.53	0.16	0.12	0.98
Pensions	0.00	0.00	0.01	0.00	0.21
Investment Funds	0.26	0.23	0.17	0.00	0.74
Foreign	0.19	0.18	0.09	0.00	0.61
Other	0.00	0.00	0.01	0.00	0.13

Notes: Summary statistics for Treasury note and bond auctions from 1995-2017. † indicates that the moments are computed for 2000 onward, the period for which these data are available. # indicates that the moments are computed from 2003 onward, the period for which these data are available.

Table 2: Treasury Yield Shocks Summary Statistics

	Mean	Med.	Std. Dev.	Min	Max	Obs.
Panel A: Auction shocks						
D_t	0.03	0.00	2.12	-8.30	17.80	1047
Panel B: Maturity						
$D_t^{(2Y)}$	-0.06	0.00	1.39	-5.20	4.40	256
$D_t^{(3Y)}$	0.15	0.10	1.32	-5.30	5.00	134
$D_t^{(5Y)}$	0.20	0.30	1.94	-5.55	8.50	233
$D_t^{(7Y)}$	-0.28	0.05	2.10	-8.30	5.50	106
$D_t^{(10Y)}$	-0.04	-0.05	2.55	-6.80	12.20	186
$D_t^{(30Y)}$	0.09	-0.15	3.28	-7.40	17.80	132
Panel C: Economic regime						
Expansion	0.03	0.00	2.03	-8.30	17.80	963
Recession	-0.07	-0.05	2.95	-7.10	9.50	84
Panel D: Monetary regime						
Non-ZLB	0.08	0.10	2.02	-7.40	12.20	563
ZLB	-0.03	0.00	2.23	-8.30	17.80	484
Panel E: Non-auction						
$\tilde{D}_t^{(2Y)}$	-0.07	0.00	1.32	-19.20	11.00	1225
$\tilde{D}_t^{(5Y)}$	-0.01	0.00	1.13	-17.40	12.90	1924
$\tilde{D}_t^{(10Y)}$	-0.01	0.00	1.03	-13.30	8.90	2151
$\tilde{D}_t^{(30Y)}$	0.01	0.00	0.92	-8.50	5.60	1914

Notes: Shocks $D_t = y_{t,post} - y_{t,pre}$ are the intraday change in Treasury yields before and after the close of an auction (in basis points). For newly issued securities, the yields are from when-issued trades. For reopened securities, the yields are from secondary-market trades. Panel B reports statistics for shocks $D_t^{(m)} = y_{t,post}^{(m)} - y_{t,pre}^{(m)}$ separately for major maturities $m = 2, 3, 5, 7, 10, 30$ years. Panels C and D report statistics separately for recessions/expansions and binding/non-binding ZLB periods, respectively. Panel E reports synthetic shocks on non-auction dates $\tilde{D}_t^{(m)} = y_{t,post}^{(m)} - y_{t,pre}^{(m)}$ using the same intraday windows around 1PM on non-auction dates. The yields are from secondary-market trades for on-the-run securities for maturities $m = 2, 5, 10, 30$ years.

Table 3: Demand Shocks and Measures of Demand

	(1) $D_t^{(2Y)}$	(2) $D_t^{(3Y)}$	(3) $D_t^{(5Y)}$	(4) $D_t^{(7Y)}$	(5) $D_t^{(10Y)}$	(6) $D_t^{(30Y)}$	(7) Pool D_t
Panel A: Total bid-to-cover ratio							
Bid-to-Cover	-0.57*** (0.15)	-0.91** (0.37)	-2.50*** (0.51)	-3.06*** (0.72)	-3.05*** (0.49)	-4.69*** (1.09)	-1.68*** (0.22)
Obs.	256	134	233	106	186	132	1047
R^2	0.06	0.11	0.20	0.09	0.26	0.20	0.12
Panel B: Expected and unexpected bid-to-cover							
Fitted	-0.03 (0.14)	-0.09 (0.37)	0.27 (0.62)	1.72 (2.44)	-0.40 (0.51)	-2.58 (1.89)	-0.11 (0.16)
Residual	-2.25*** (0.43)	-2.62*** (0.34)	-4.15*** (0.56)	-6.40*** (1.17)	-5.40*** (0.83)	-5.36*** (1.71)	-3.97*** (0.37)
Obs.	252	130	229	102	182	128	1023
R^2	0.22	0.26	0.34	0.22	0.43	0.22	0.26
Panel C: Bid-to-cover by bidder type							
Indirect	-4.72*** (0.62)	-3.01*** (0.71)	-8.82*** (1.24)	-13.22*** (1.71)	-8.38*** (0.90)	-15.79*** (2.68)	-8.42*** (0.84)
Direct	-2.51** (1.00)	-3.24*** (0.97)	-2.75 (1.78)	-4.88** (2.42)	-3.66** (1.63)	-6.38*** (1.91)	-3.61*** (0.72)
Primary	-0.42 (0.52)	-1.35** (0.61)	-2.97*** (0.77)	-0.09 (1.49)	-3.36*** (0.68)	-4.10** (1.73)	-2.22*** (0.42)
Obs.	159	117	168	102	146	111	803
R^2	0.46	0.39	0.48	0.59	0.50	0.53	0.39
Panel D: Fraction accepted by bidder type							
Invest. Fund	-6.61*** (1.37)	-6.33*** (1.48)	-9.78*** (1.94)	-15.10*** (2.70)	-9.62*** (1.65)	-17.83*** (4.40)	-10.49*** (1.17)
Foreign	-6.89*** (1.52)	-3.90** (1.60)	-10.43*** (2.04)	-16.35*** (2.56)	-9.61*** (2.41)	-17.56*** (5.15)	-9.50*** (1.15)
Misc.	-6.35** (2.88)	-6.87 (7.58)	-6.89*** (2.31)	3.92 (6.53)	11.98 (10.66)	-13.00** (6.44)	-6.88*** (2.12)
Obs.	197	117	181	102	160	115	872
R^2	0.27	0.22	0.30	0.49	0.31	0.41	0.24

Notes: Regressions of demand shocks $D_t^{(m)}$ on the bid-to-cover ratio and fractions accepted, total and broken up by bidder type. Columns (1)-(6) restrict the sample to include only auctions of maturities $m = 2, 3, 5, 7, 10, 30$ years; column (7) pools across all auctions. In Panels A, C, and D, four lags of the dependent variables are included but not reported; in Panel B, the fitted values and residuals of an AR(4) are both used as dependent variables. Newey-West (9 lags) standard errors in parentheses.

Table 4: Asset Price Reactions to Demand Shocks at Treasury Auctions

Asset type	Estimate	Std. Err.	Obs.	R^2	Sample
	(1)	(2)	(3)	(4)	(5)
Panel A: Corporate debt					
LQD	-3.93***	(0.15)	830	0.59	2002-2017
Corp. Aaa [†]	0.94***	(0.10)	1040	0.14	1995-2017
Corp. Baa [†]	0.96***	(0.10)	1040	0.15	1995-2017
Corp. C [†]	0.23	(0.39)	973	0.00	1997-2017
Panel B: Equities					
SPY	-0.23	(0.52)	1033	0.00	1995-2017
IWM	0.18	(0.58)	876	0.00	2000-2017
SP500 [†]	3.61	(2.74)	974	0.00	1995-2016
Russell 2000 [†]	6.26*	(3.25)	974	0.01	1995-2016
Panel C: Inflation and commodities					
GLD	-1.16***	(0.36)	775	0.02	2004-2017
GSCI [†]	-1.20	(2.74)	974	0.00	1995-2016
10Y Infl. Swap [†]	0.02	(0.08)	724	0.00	2004-2016
2Y Infl. Swap [†]	0.04	(0.17)	724	0.00	2004-2016
Panel D: Spreads and credit default swaps					
Aaa-Baa [†]	0.02	(0.03)	1040	0.00	1995-2017
LIBOR-OIS [†]	0.03	(0.04)	737	0.00	2003-2016
Auto CDS [†]	-0.60	(2.65)	733	0.00	2004-2016
Bank CDS [†]	-0.23	(0.16)	733	0.01	2004-2016
VIX [†]	-0.04	(0.03)	1040	0.00	1995-2017
Panel E: Federal funds futures					
1-Month Ahead [†]	0.03	(0.02)	1040	0.00	1995-2017
2-Month/1-Month Slope [†]	0.00	(0.01)	1040	0.00	1995-2017

Notes: Regressions of asset price changes on demand shocks D_t (pooled across maturities). [†] denotes daily series; otherwise, intraday changes are measured over the same window as auction demand shocks. Intraday changes are from ETFs that track securities or indices: LQD (corporate debt); SPY (S&P 500); IWM (Russell 2000); GLD (gold bullion). Daily series: Aaa, Baa, C (Moody's & BoA corporate debt yield indices); S&P 500, Russell 2000 (equity indices); GSCI (S&P Total Commodity Index); 10- and 2-year inflation swaps; Auto and Bank credit default swap indices; LIBOR-OIS (3-month USD LIBOR-Overnight Index Swap spread); VIX (implied volatility index); Federal funds futures (h -month ahead continuous contracts). Newey-West (9 lags) standard errors in parentheses.

Table 5: Model Calibration

Parameter	Value	[Crisis]	Description
Panel A: Macroeconomic Block			
σ_r	2.567		Monetary Policy Vol.
κ_r	1.082		Monetary Policy Inertia
σ_d	1.116		Risky Payoff Vol.
κ_d	0.879		Risky Payoff Inertia
$\sigma_{z,\pi}$	2.039		Cost-Push Shock Vol.
$\kappa_{z,\pi}$	0.802		Cost-Push Shock Inertia
$\sigma_{z,x}$	1.749		Agg. Demand Shock Vol.
$\kappa_{z,x}$	0.253		Agg. Demand Shock Inertia
δ	0.705		Nominal Rigidity
ϕ_π	3.096		Inflation Taylor Coeff.
ψ_x	0.393		Risky Payoff Output Coeff.
ρ	0.04		Discount Factor
ς^{-1}	1.0		Intertemporal Elasticity
Panel B: Financial Block			
κ_β	1.367		Demand Factor Inertia
$a \cdot \alpha_0$	0.008	[0.018]	Habitat Elasticity Size
$a \cdot \sigma_\beta \cdot \theta_0$	2.509	[5.123]	Demand Factor Size
$a \cdot \phi_{r,\beta}$	0.491	[4.620]	Demand Short Rate Response
θ_1^s	0.5		Short Treasury Factor Shape
θ_1^ℓ	0.2		Long Treasury Factor Shape
$\tilde{\theta}_1$	0.5		Risky Factor Shape
α_1	0.1		Habitat Elasticity Shape
η_1	2.0		Effective Borrowing Rate Shape
Panel C: QE1 Shock			
θ_1^{QE}	0.35		QE1 Shock Shape
κ_{QE}	0.2		QE1 Shock Intertia

Notes: Calibrated parameters used in the numerical simulations.

Appendix A Model Solution

This section characterizes the equilibrium of the model defined in Section 4. Conjecture an affine pricing structure as a function of the state variables: $-\log P_t^{(\tau)} = \mathbf{A}(\tau)^\top \mathbf{y}_t + C(\tau)$, $-\log \tilde{P}_t^{(\tau)} = \tilde{\mathbf{A}}(\tau)^\top \mathbf{y}_t + \tilde{C}(\tau)$, $\tilde{r}_t = \hat{\mathbf{A}}^\top \mathbf{y}_t + \hat{C}$. Then the economy evolves according to equation (14) (but note that the dynamics matrix Υ is a function of the effective borrowing rate coefficients $\hat{\mathbf{A}}$). So long as determinacy conditions are met (as in Ray (2019)), the state variables evolve according to

$$\mathbf{y}_t = -\Gamma(\mathbf{y}_t - \bar{\mathbf{y}}) dt + \boldsymbol{\sigma} d\mathbf{B}_t, \quad \mathbf{x}_t - \bar{\mathbf{x}} = \boldsymbol{\Omega}(\mathbf{y}_t - \bar{\mathbf{y}}), \quad (\text{A1})$$

$$\Gamma = \mathbf{Q}_{11}\mathbf{A}_1\mathbf{Q}_{11}^{-1}, \quad \boldsymbol{\Omega} = \mathbf{Q}_{21}\mathbf{Q}_{11}^{-1}, \quad (\text{A2})$$

where $\mathbf{Q}_{11}, \mathbf{A}_1$ (respectively, \mathbf{Q}_{21}) are the blocks of eigenvector and eigenvalue matrices of Υ from equation (14) associated with the state variables \mathbf{y}_t (respectively, jump variables \mathbf{x}_t).

Ito's Lemma then implies that $\frac{dP_t^{(\tau)}}{P_t^{(\tau)}} = \mu_t^{(\tau)} dt + \boldsymbol{\sigma}^{(\tau)} d\mathbf{B}_t$, where

$$\mu_t^{(\tau)} = \mathbf{A}'(\tau)^\top \mathbf{y}_t + C'(\tau) + \mathbf{A}(\tau)^\top \Gamma(\mathbf{y}_t - \bar{\mathbf{y}}) + \frac{1}{2} \mathbf{A}(\tau)^\top \Sigma \mathbf{A}(\tau), \quad \boldsymbol{\sigma}^{(\tau)} = -\mathbf{A}(\tau)^\top \boldsymbol{\sigma},$$

and $\Sigma = \boldsymbol{\sigma}\boldsymbol{\sigma}^\top$ (with analogous expressions for $\tilde{P}_t^{(\tau)}$).

Recall that $\tilde{r}_t \equiv \int_0^T \eta(\tau) E_t \frac{d\tilde{P}_t^{(\tau)}}{\tilde{P}_t^{(\tau)}} d\tau$. Hence, collecting terms that are linear in the state variables \mathbf{y}_t , we have

$$\hat{\mathbf{A}} = \int_0^T \eta(\tau) \left[\tilde{\mathbf{A}}'(\tau) + \Gamma^\top \tilde{\mathbf{A}}(\tau) \right] d\tau. \quad (\text{A3})$$

Then differentiating equation (4) with respect to holdings $X_t^{(\tau)}, \tilde{X}_t^{(\tau)}$ gives the optimality conditions of the arbitrageur:

$$\begin{aligned} \mu_t^{(\tau)} - r_t &= a \left[\int_0^T X_t^{(\tau)} \mathbf{A}(\tau) + \tilde{X}_t^{(\tau)} \tilde{\mathbf{A}}(\tau) d\tau \right]^\top \Sigma \mathbf{A}(\tau), \\ \tilde{\mu}_t^{(\tau)} - r_t &= a \left[\int_0^T X_t^{(\tau)} \mathbf{A}(\tau) + \tilde{X}_t^{(\tau)} \tilde{\mathbf{A}}(\tau) d\tau \right]^\top \Sigma \tilde{\mathbf{A}}(\tau). \end{aligned}$$

Substitute the market clearing conditions into the optimality conditions and collect terms that are linear in the state variables \mathbf{y}_t to get:

$$\begin{aligned} \mathbf{A}'(\tau) + \mathbf{M}\mathbf{A}(\tau) - \mathbf{e}_r &= \mathbf{0} \\ \tilde{\mathbf{A}}'(\tau) + \mathbf{M}\tilde{\mathbf{A}}(\tau) - \mathbf{e}_r &= \mathbf{0} \end{aligned}$$

where \mathbf{e}_r is a vector such that $\mathbf{e}_r^\top \mathbf{y}_t = r_t$, and

$$\begin{aligned} \mathbf{M} = \mathbf{\Gamma}^\top - a \int_0^T & [-\alpha(\tau)\mathbf{A}(\tau) + \mathbf{\Theta}(\tau)] \mathbf{A}(\tau)^\top \\ & + \left[-\tilde{\alpha}(\tau)\tilde{\mathbf{A}}(\tau) + \tilde{\mathbf{\Theta}}(\tau) \right] \tilde{\mathbf{A}}(\tau)^\top d\tau \mathbf{\Sigma}, \end{aligned} \quad (\text{A4})$$

where the functions $\mathbf{\Theta}(\tau)$, $\tilde{\mathbf{\Theta}}(\tau)$ stack the habitat demand functions $\theta^k(\tau)$, $\tilde{\theta}^k(\tau)$ into a vector. At maturity, the riskless bonds pay \$1 while the risky asset pays D_t , so the $\tau = 0$ prices are given by $P_t^{(0)} = 1$, $\tilde{P}_t^{(0)} = D_t$. Hence, we have the following initial conditions: $\mathbf{A}(0) = \mathbf{0}$, $\tilde{\mathbf{A}}(0) = -\mathbf{e}_d$, where \mathbf{e}_d is a vector such that $\mathbf{e}_d^\top \mathbf{y}_t = d_t$. Then assuming \mathbf{M} is diagonalizable and invertible, we can solve for the affine vector functions:

$$\mathbf{A}(\tau) = [\mathbf{I} - e^{-\mathbf{M}\tau}] \mathbf{M}^{-1} \mathbf{e}_i, \quad \tilde{\mathbf{A}}(\tau) = [\mathbf{I} - e^{-\mathbf{M}\tau}] \mathbf{M}^{-1} \mathbf{e}_i - e^{-\mathbf{M}\tau} \mathbf{e}_d. \quad (\text{A5})$$

Equilibrium is defined as the solution to the fixed point problem implicitly defined by equations (A3) and (A4). Given effective borrowing rate coefficients $\hat{\mathbf{A}}$, we recover $\mathbf{\Upsilon}$, and hence $\mathbf{\Gamma}$ through equation (A2). Given the matrix \mathbf{M} , we solve for the coefficient functions $\mathbf{A}(\tau)$, $\tilde{\mathbf{A}}(\tau)$ from equation (A5).

Online Appendix for
“Unbundling Quantitative Easing:
Taking a Cue from Treasury Auctions”

by Michael Droste, Yuriy Gorodnichenko, and Walker Ray

Appendix B Additional Figures and Tables

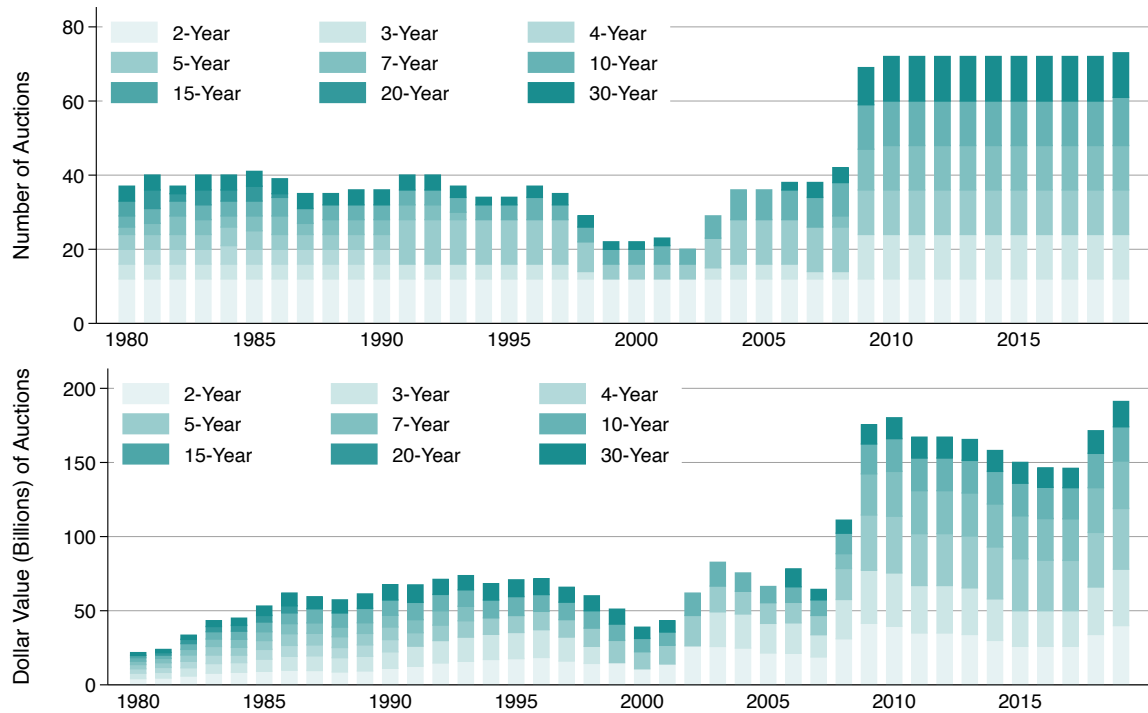


Figure B1: Number and Size of Auctions per Year

Notes: the number (top panel) and dollar value (bottom panel) of note and bond Treasury auctions per year by term length. The number of auctions temporarily fell in the late 1990s and early 2000s (during which time the Treasury ceased issuing 7- and 30-year securities). After the Great Recession, the number and size of auctions increased sharply. Since 2010, the Treasury has held auctions every month for maturities $m = 2, 3, 5, 7, 10, 30$ years.

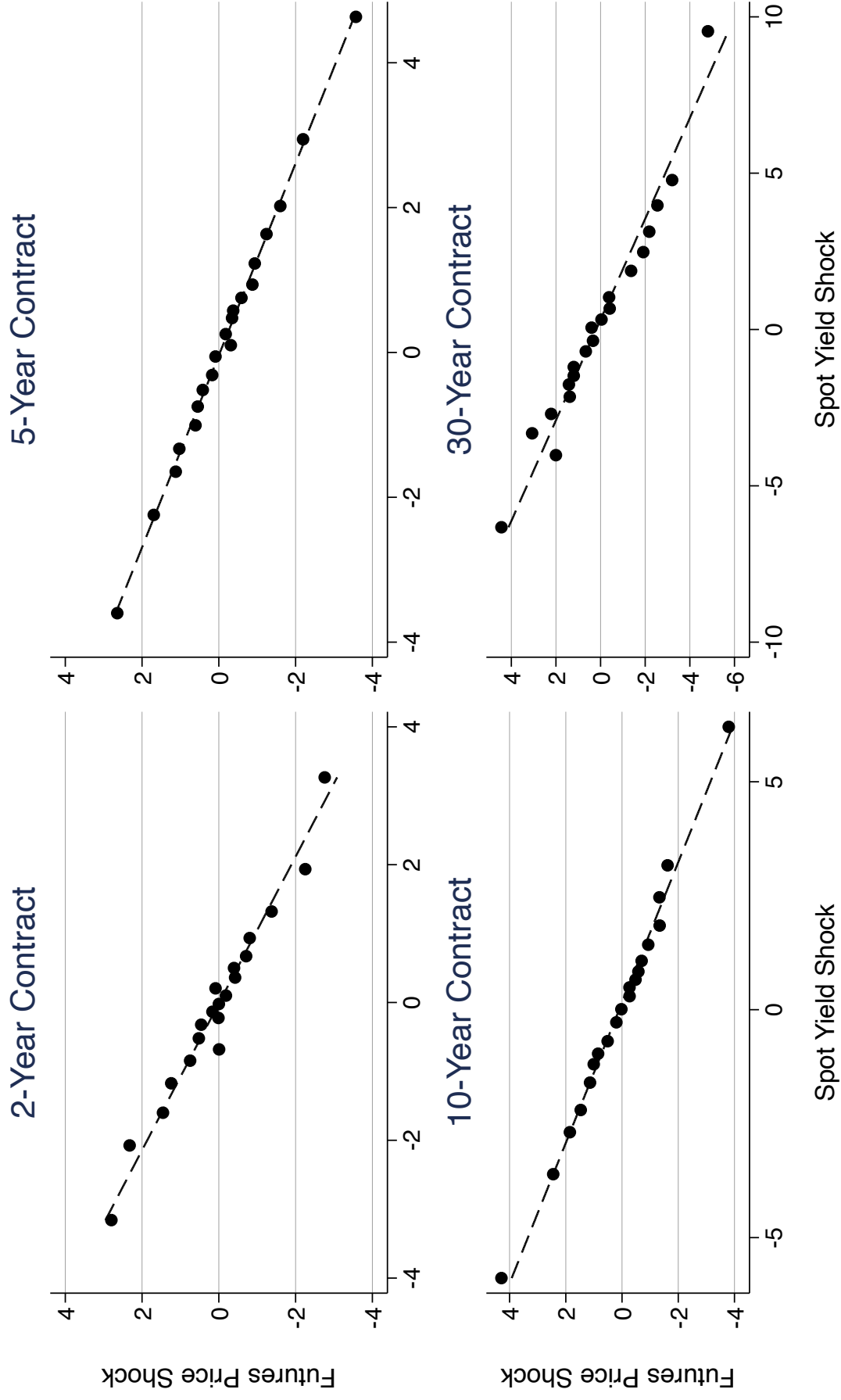


Figure B2: Demand Shock Comparison: Spot Yields and Futures

Notes: Comparison of intra-day changes in secondary market Treasury yields and Treasury futures, constructed using the same windows as described in equation (1). See [Gorodnichenko and Ray \(2017\)](#) for a detailed discussion of Treasury futures.

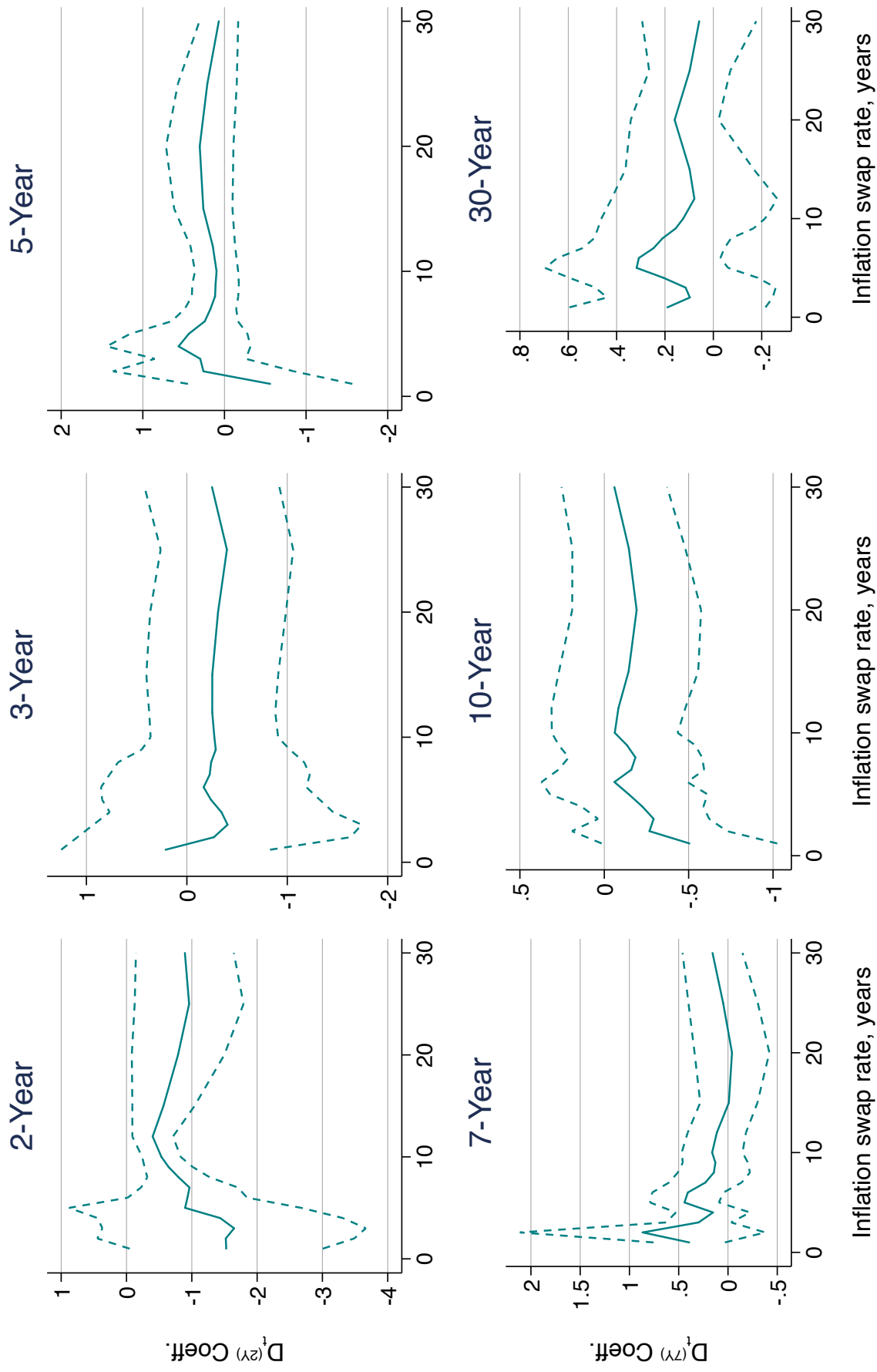


Figure B3: Inflation Swap Rates and Demand Shocks

Notes: Regressions of inflation swap rate changes on demand shocks $D_t^{(m)}$, run separately by maturities $m = 2, 3, 5, 7, 10, 30$ years. The solid line represents point estimates for inflation swaps of years $y = 1, \dots, 30$; dotted lines denote 2-standard error (Newey-West, 9 lags) confidence intervals.

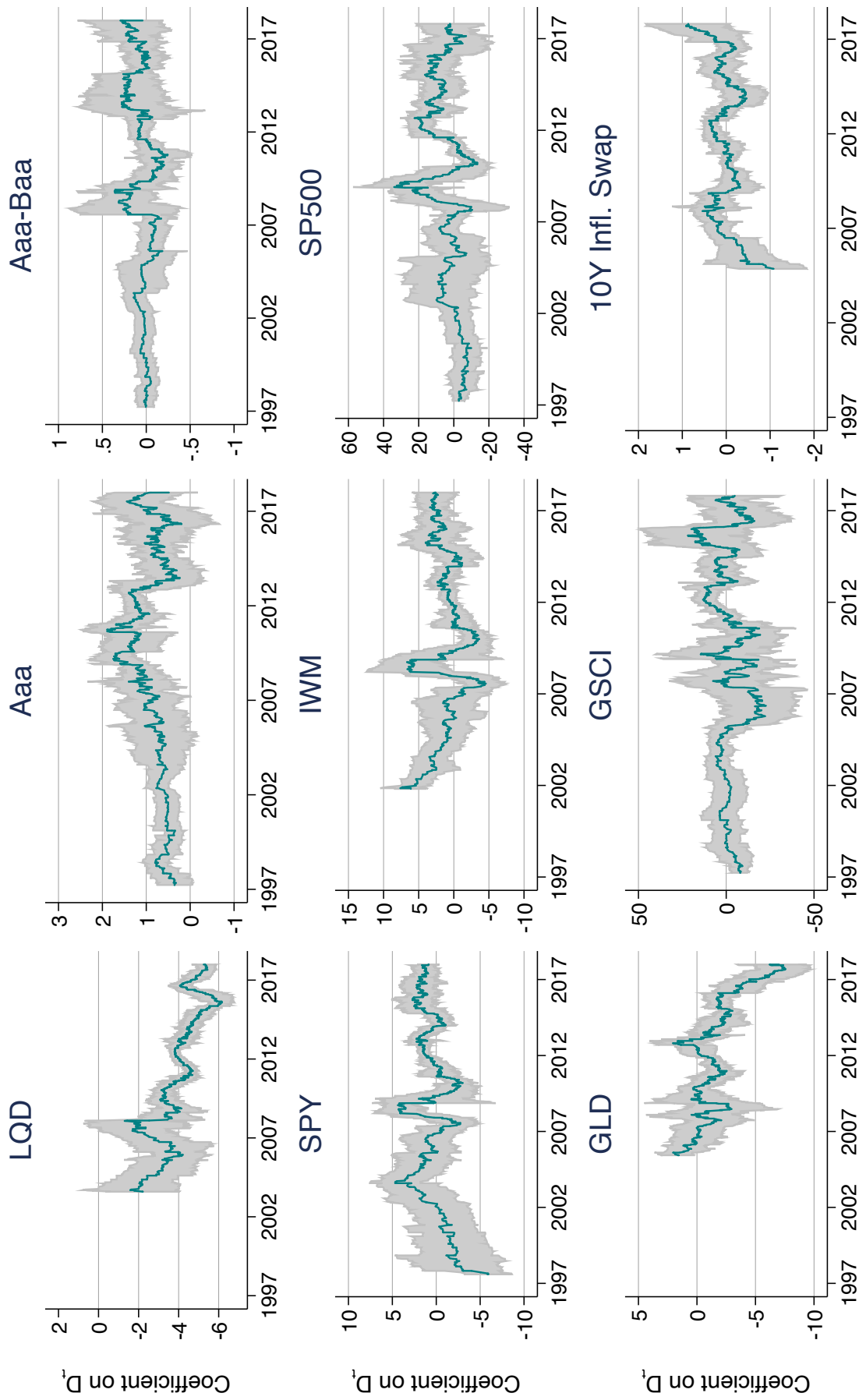


Figure B4: Rolling Regressions, Asset Prices

Notes: Rolling coefficient estimates of asset prices on auction demand shocks D_t (pooled across maturities). Each data point is from rolling estimates of the regressions reported in Table 4, using the 75 most recent auctions.

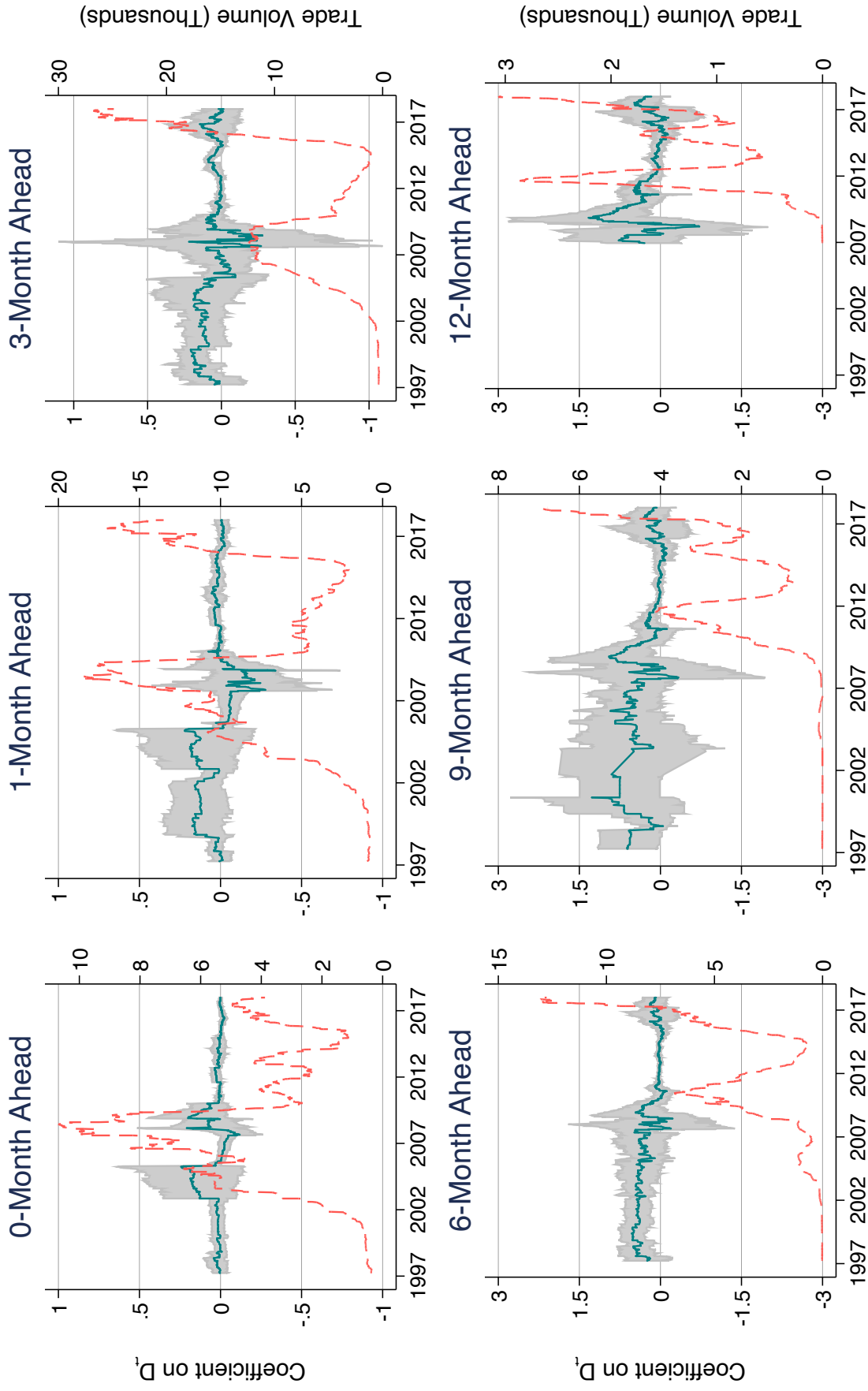


Figure B5: Rolling Regressions, Federal Funds Futures

Notes: Rolling coefficient estimates of h -month ahead expected federal funds rates on auction demand shocks D_t (pooled across maturities). Each data point presents rolling estimates using the 75 most recent auctions. The red line, indexed to the right y-axis, documents the average trade volume (in thousands) over the same 75-auction window

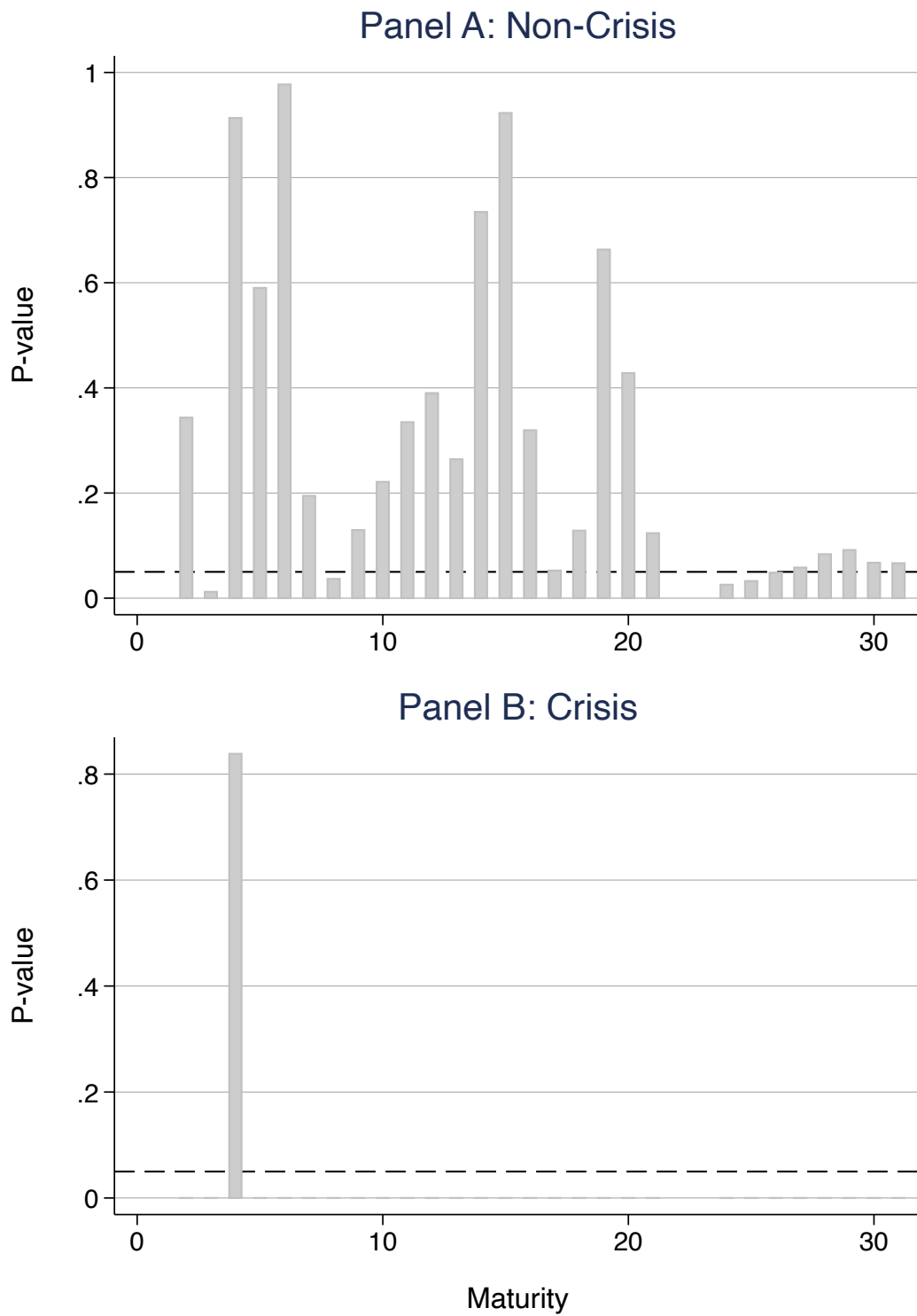


Figure B6: Model-Implied Preferred Habitat Coefficients, P-Values

Notes: P-values testing equality of coefficients from Figure 8.

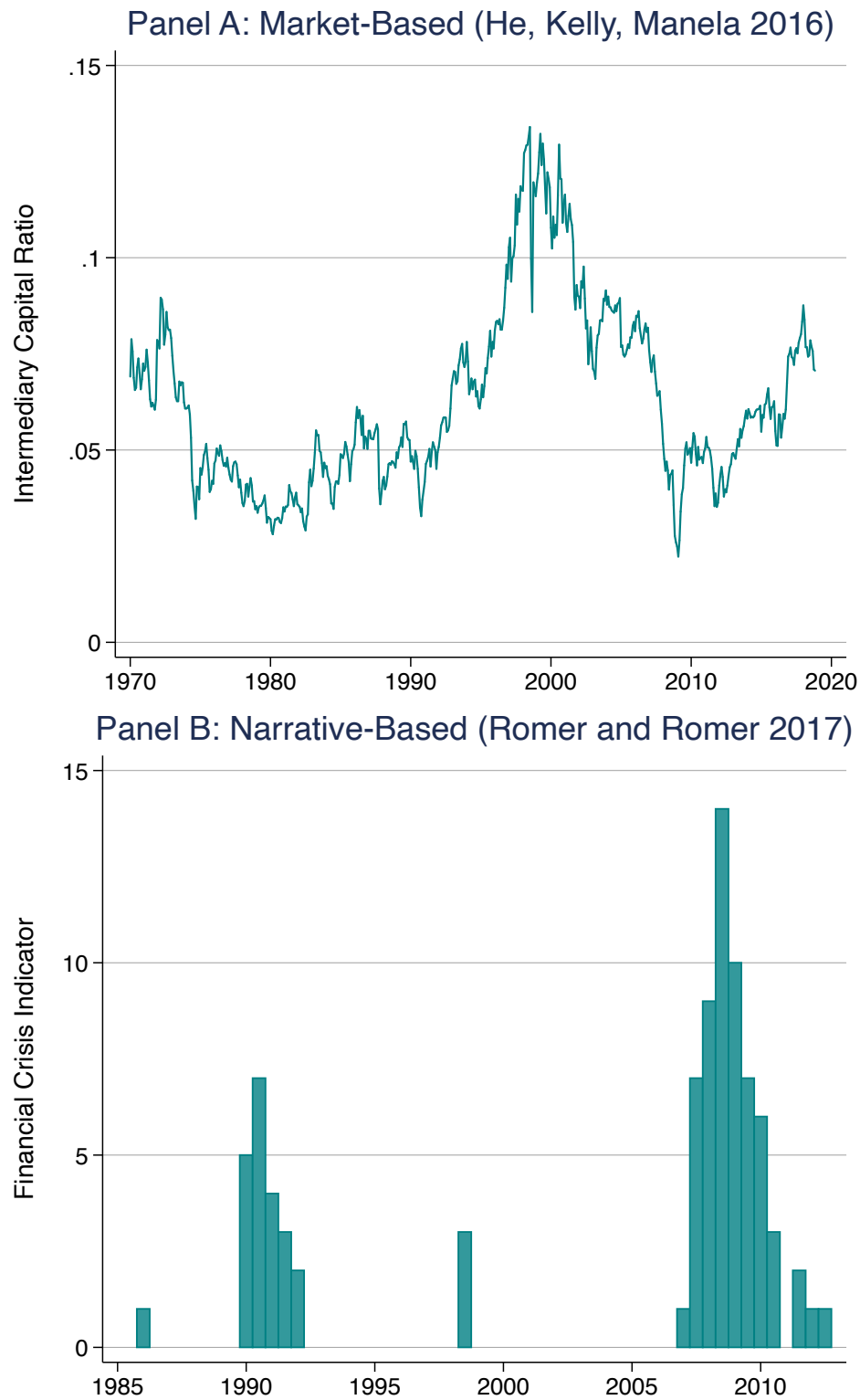
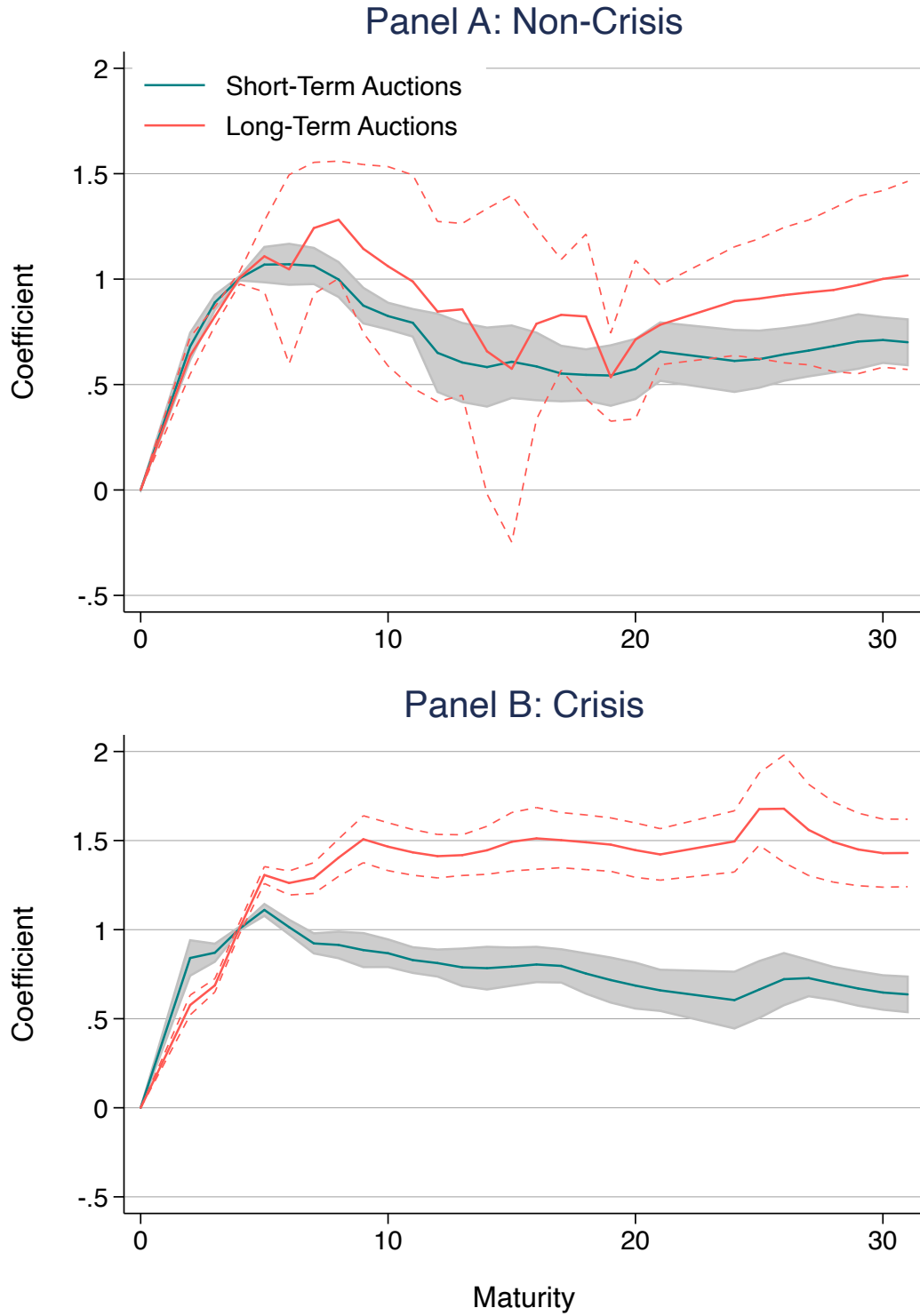


Figure B7: Alternative Measures of Financial Crises

Notes: Alternative measures of financial crises from [He et al. \(2016\)](#) (top panel) and [Romer and Romer \(2017\)](#) (bottom panel).



Notes: Estimates of regression equation (19), identifying financial crises as periods in which the aggregate capital ratio from He et al. (2016) is low (≤ 0.055).

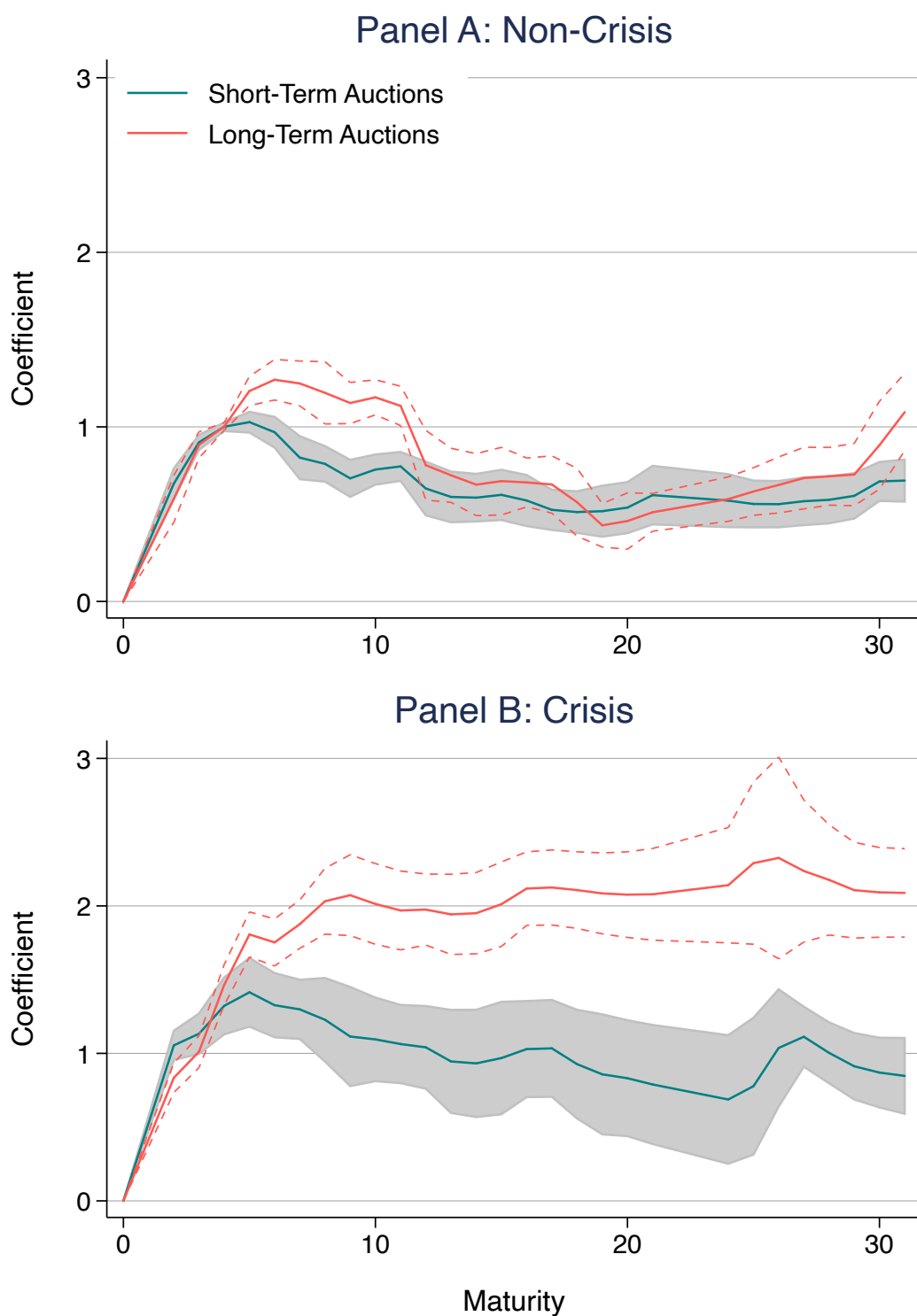
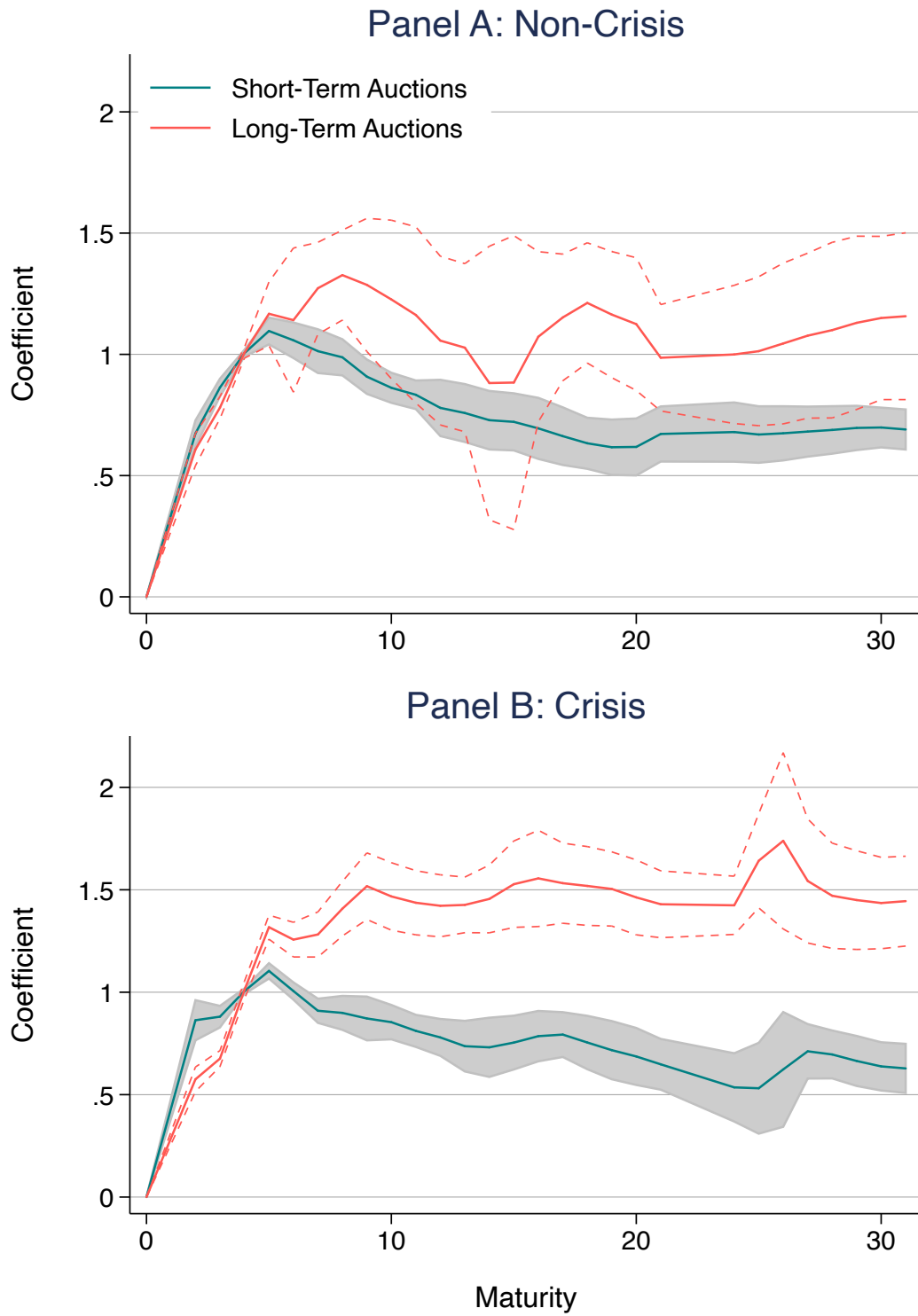


Figure B9: Localization Robustness: Market-Based Crises (Continuous)

Notes: Alternative specification of regression equation (19), where the crisis measure is treated as continuous (as measured by the aggregate capital ratio from He et al. (2016)). The measure is transformed to range from 0 to 1, and truncated so that values below 0.04 are set to 1 while values above 0.075 are set to 0.



Notes: Estimates of regression equation (19), identifying financial crises as periods identified by [Romer and Romer \(2017\)](#).

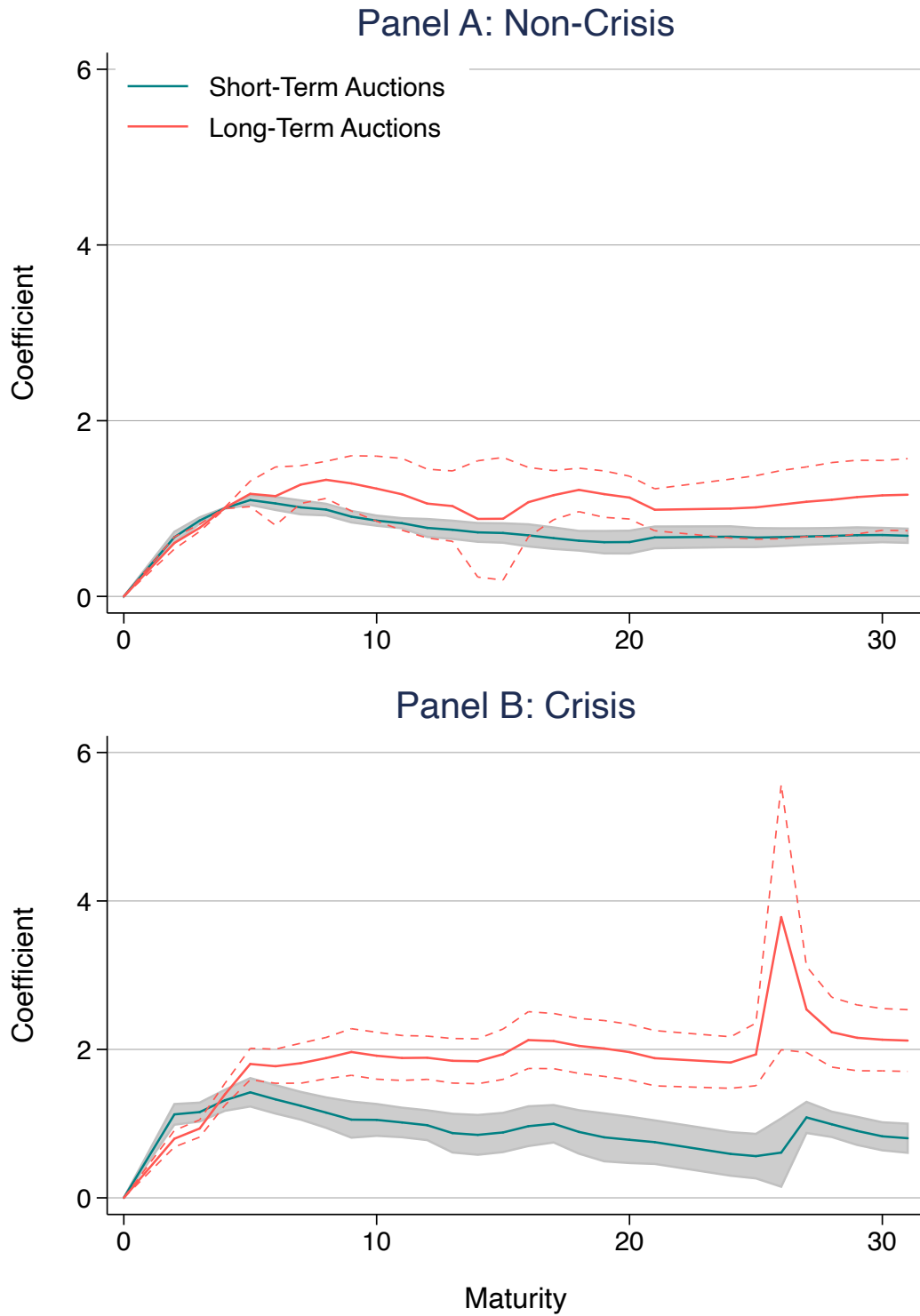


Figure B11: Localization Robustness: Narrative-Based Crises (Continuous)

Notes: Alternative specification of regression equation (19), where the crisis measure is treated as continuous (as measured by [Romer and Romer \(2017\)](#)). The measure is transformed to range from 0 to 1, and truncated so that values above 10 are set to 1.

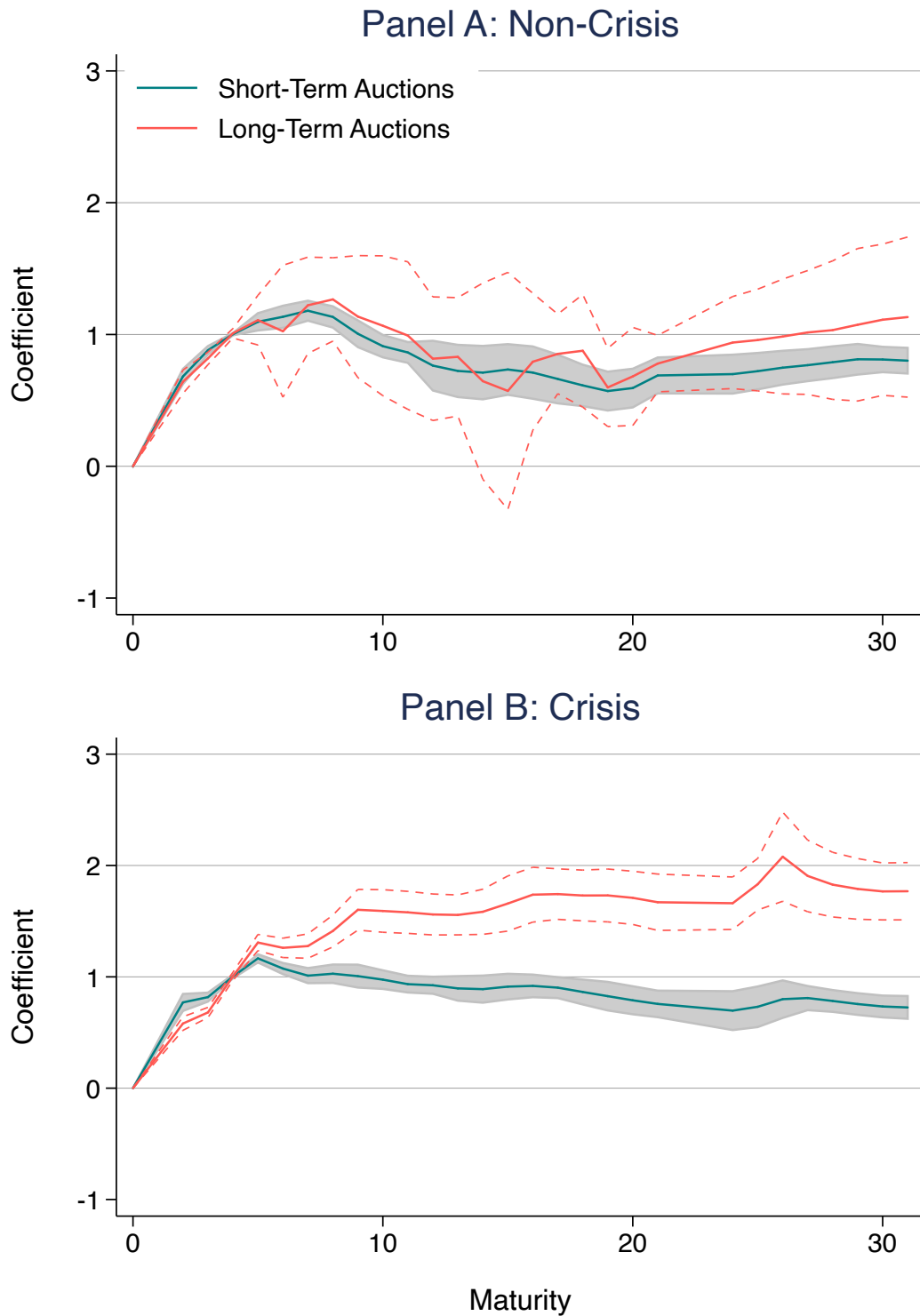


Figure B12: Localization Robustness: Long/Short Auctions

Notes: Estimates of regression equation (19), where short-maturity auctions are those with maturities 7 years or below, while long-maturity auctions are 10 years and above.

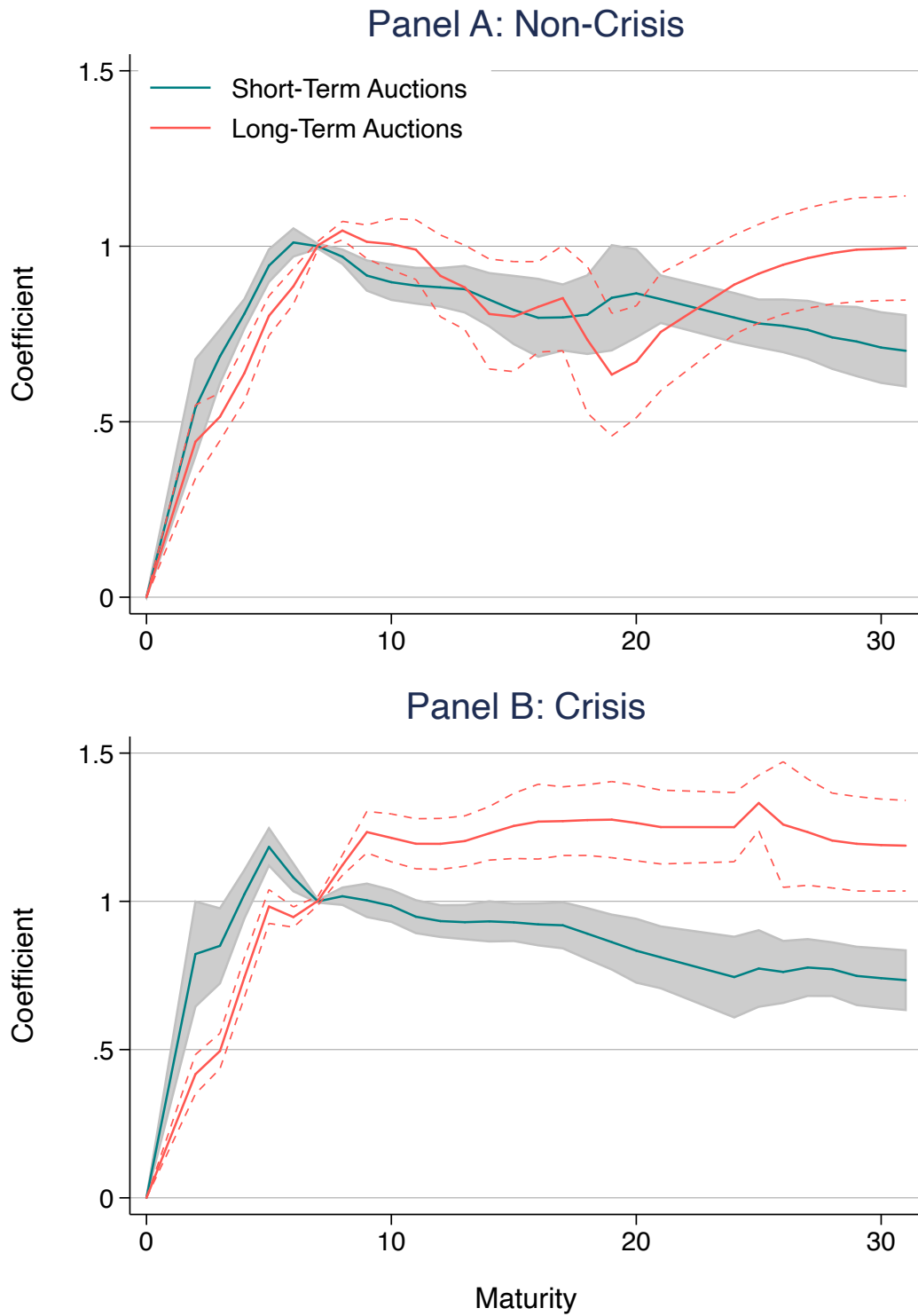


Figure B13: Localization Robustness: τ^*

Notes: Estimates of regression equation (19), where $\tau^* = 6$.

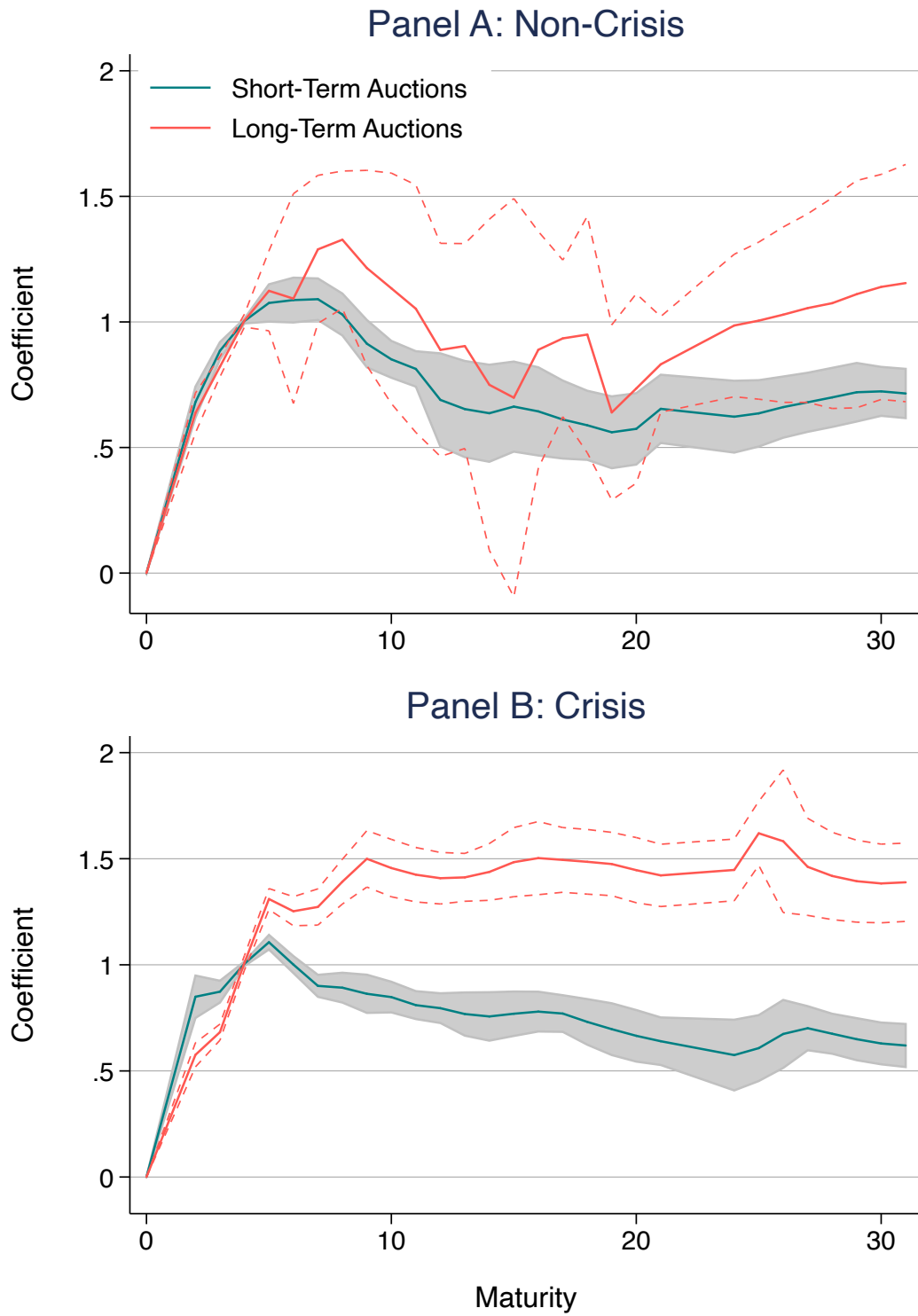


Figure B14: Localization Robustness: No QE Event Weeks

Notes: Estimates of regression equation (19), dropping auctions that occurred during the weeks of QE announcements.

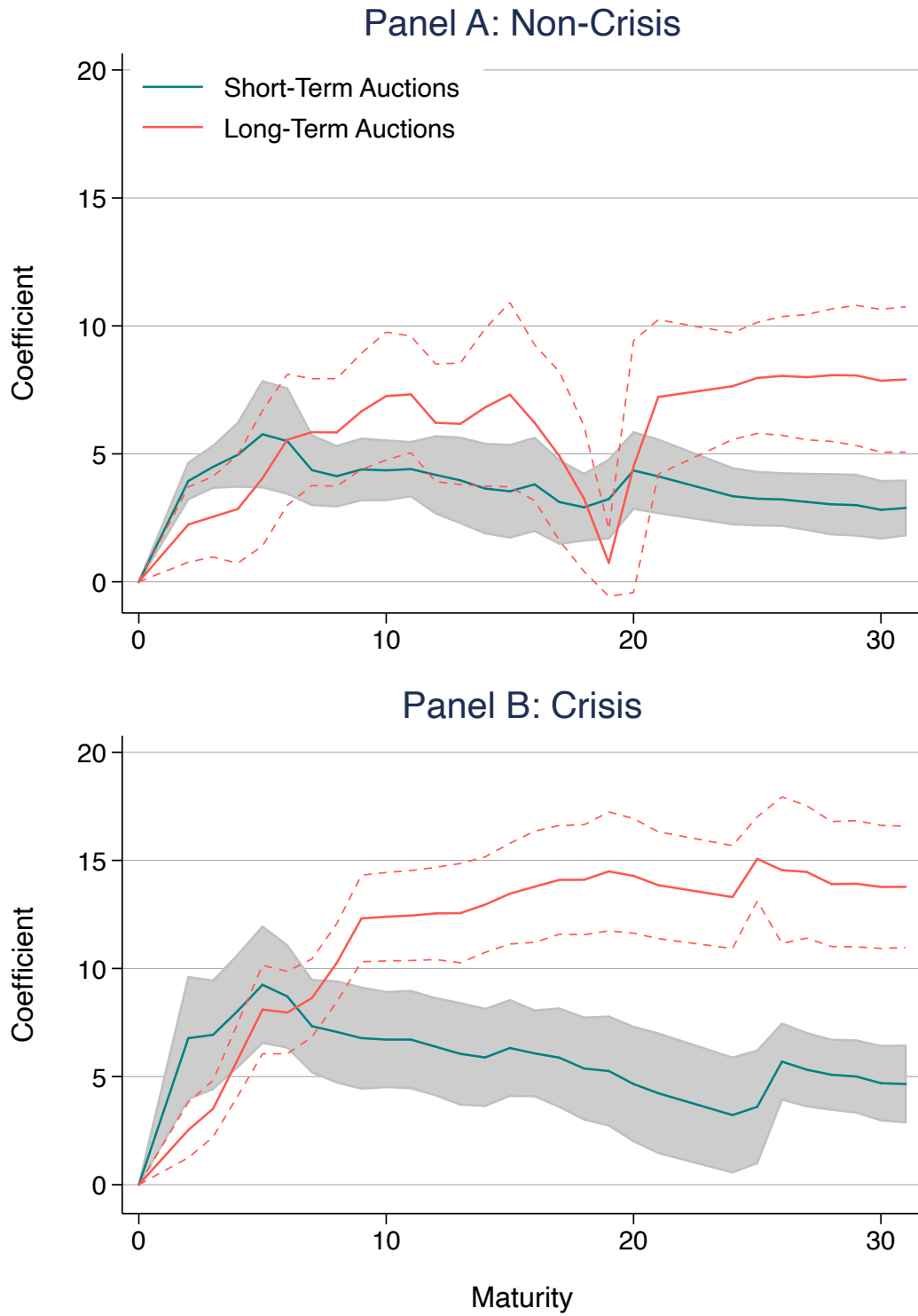


Figure B15: Localization Robustness: Bid-to-Cover, Indirect Bidders

Notes: Estimates of the alternative localization regression equation (20), using the bid-to-cover ratio of indirect bidders only as a proxy of structural demand shocks (after controlling for its own four lags and flipping the sign).

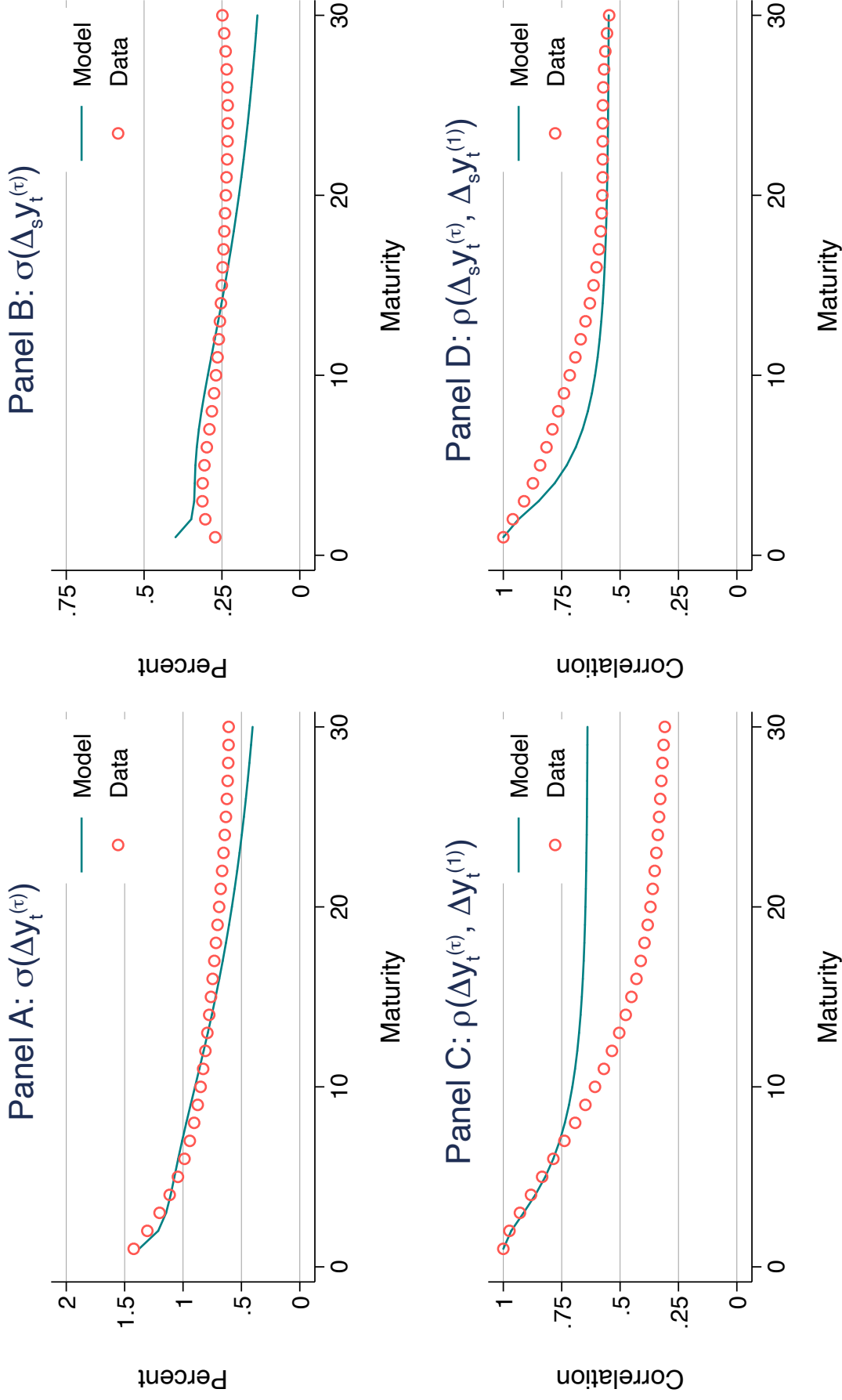


Figure B16: Targeted Moments as a Function of Maturity

Notes: comparison of targeted moments in the model (solid lines) with the data (scatter points). The targeted moments are regression coefficients across the term structure (maturity is on the x-axis): Fama-Bliss coefficients (left column) and Campbell-Shiller coefficients (right column), during periods of non-crisis (top row) and crisis (bottom row).

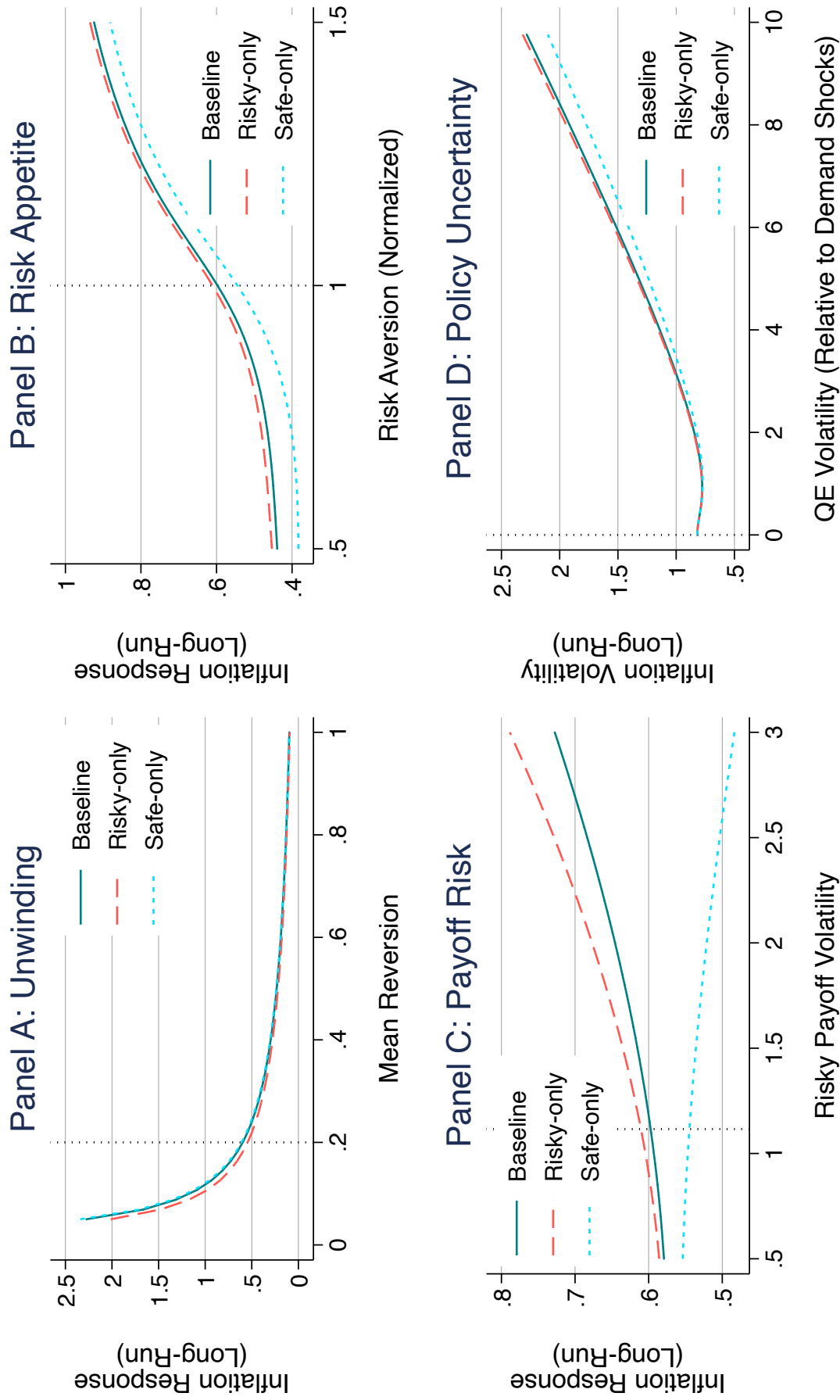


Figure B17: Policy Sensitivity Analysis: Inflation

Notes: The top-left panel plots the long-run impact of the QE shock in the model on inflation as a function of the mean reversion of the QE shock. The top-right panel plots the long-run impact of QE on inflation as a function of arbitrageur risk aversion. The bottom-left panel plots the change in long-run volatility of inflation as a function of the volatility of QE shocks. In each panel, the solid line corresponds to the baseline QE calibration. The dashed orange line shows results for a counter-factual QE policy which purchases risky assets only; the dotted blue line shows results for a counter-factual QE policy which purchases only Treasuries.

Table B1: Asset Price Reactions to Demand Shocks (IV Specification)

Asset type	Estimate (1)	Std. Err. (2)	Obs. (3)	F-stat (4)	Sample (5)
Panel A: Corporate debt					
LQD	-4.25***	(0.33)	826	92.2	2002-2017
Corp. Aaa [†]	1.10***	(0.15)	1016	147.5	1995-2017
Corp. Baa [†]	1.14***	(0.14)	1016	147.5	1995-2017
Corp. C [†]	0.36	(0.47)	969	134.6	1997-2017
Panel B: Equities					
SPY	-1.04	(0.68)	1020	145.9	1995-2017
IWM	-0.84	(0.94)	872	108.0	2000-2017
SP500 [†]	1.65	(4.24)	950	142.0	1995-2016
Russell 2000 [†]	5.45	(4.40)	950	142.0	1995-2016
Panel C: Inflation and commodities					
GLD	-1.63***	(0.58)	771	67.1	2004-2017
GSCI [†]	-5.80	(3.99)	950	142.0	1995-2016
10Y Infl. Swap [†]	0.04	(0.13)	720	67.1	2004-2016
2Y Infl. Swap [†]	0.09	(0.33)	720	67.1	2004-2016
Panel D: Spreads and credit default swaps					
Aaa-Baa [†]	0.04	(0.06)	1016	147.5	1995-2017
LIBOR-OIS [†]	0.22	(0.15)	733	70.8	2003-2016
Auto CDS [†]	1.72	(2.66)	729	69.5	2004-2016
Bank CDS [†]	-0.40	(0.26)	729	69.5	2004-2016
VIX [†]	0.05	(0.06)	1016	147.5	1995-2017
Panel E: Federal funds futures					
1-Month Ahead [†]	0.01	(0.05)	1016	147.5	1995-2017
2-Month/1-Month Slope [†]	0.00	(0.02)	1016	147.5	1995-2017

Notes: The table repeats the regressions from Table 4, but instruments the demand shocks D_t with the surprise component of the bid-to-cover ratio. First-stage F-statistics are reported in column (3). Newey-West (9 lags) standard errors in parentheses.

Table B2: Targeted Moments

Target Moment	Data	Model
$\sigma(y_t^{(1)})$	1.993	1.978
$\sigma(\tilde{y}_t^{(1)} - y_t^{(1)})$	0.542	0.549
$\sigma(\pi_t)$	0.973	0.882
$\sigma(x_t)$	1.992	1.996
$\sigma(\Delta y_t^{(1)})$	1.423	1.376
$\sigma(\Delta(\tilde{y}_t^{(1)} - y_t^{(1)}))$	0.615	0.617
$\sigma(\Delta\pi_t)$	0.900	0.935
$\sigma(\Delta x_t)$	2.190	2.137
$\sigma(\Delta_s y_t^{(1)})$	0.272	0.399
$\sigma(\Delta_s(\tilde{y}_t^{(1)} - y_t^{(1)}))$	0.258	0.218
$\sigma(\Delta_s \pi_t)$	0.232	0.362
$\sigma(\Delta_s x_t)$	0.499	0.745
$\rho(y_t^{(1)}, \pi_t)$	0.549	0.615
$\rho(\tilde{y}_t^{(1)} - y_t^{(1)}, x_t)$	-0.171	-0.158
$\rho(\pi_t, x_t)$	0.268	0.271

Notes: comparison of targeted moments in the model and the data. The targeted moments are volatility and correlations across short-term rates and macroeconomic variables. Δ denotes a 1-year change, while Δ_s denote a 1-month change. $\sigma(\cdot)$ denotes standard deviation (reported in percentage points), while $\rho(\cdot, \cdot)$ denotes correlation.

Appendix C Additional Model Details

C.1 Numerical Solution: Laplace Transforms

Using the functional forms assumed in Section 5, we can solve the model by assuming that $T \rightarrow \infty$ and using Laplace transforms

The differential equations (A5) are characterize the coefficient functions $\mathbf{A}(\tau), \tilde{\mathbf{A}}(\tau)$. Define the Laplace transform $\mathcal{A}(s) \equiv \mathcal{L}\{\mathbf{A}(\tau)\}(s)$. Then equation (A5) implies:

$$\begin{aligned} s\mathcal{A}(s) + \mathbf{M}\mathcal{A}(s) - \frac{1}{s}\mathbf{e}_i &= \mathbf{0} \\ \implies \mathcal{A}(s) &= [s\mathbf{I} + \mathbf{M}]^{-1} \left[\frac{1}{s}\mathbf{e}_i \right] \end{aligned}$$

using the fact that $\mathbf{A}(0) = \mathbf{0}$. Similarly, we have

$$\begin{aligned} s\tilde{\mathcal{A}}(s) + \mathbf{e}_d + \mathbf{M}\tilde{\mathcal{A}}(s) - \frac{1}{s}\mathbf{e}_i &= \mathbf{0} \\ \implies \tilde{\mathcal{A}}(s) &= [s\mathbf{I} + \mathbf{M}]^{-1} \left[\frac{1}{s}\mathbf{e}_i - \mathbf{e}_d \right] \end{aligned}$$

using the fact that $\tilde{\mathbf{A}}(0) = -\mathbf{e}_d$.

Note that the derivative with respect to the Laplace parameter s is given by

$$\begin{aligned} \mathcal{A}'(s) &= [s\mathbf{I} + \mathbf{M}]^{-1} \left[-\frac{1}{s^2}\mathbf{e}_i - \mathcal{A}(s) \right] \\ \tilde{\mathcal{A}}'(s) &= [s\mathbf{I} + \mathbf{M}]^{-1} \left[-\frac{1}{s^2}\mathbf{e}_i - \tilde{\mathcal{A}}(s) \right] \end{aligned}$$

Additionally, define $\mathbf{X}(\tau) \equiv \mathbf{A}(\tau)\mathbf{A}(\tau)^\top$. Note that from equation (A5) we can write

$$\begin{aligned} \mathbf{A}'(\tau)\mathbf{A}(\tau)^\top + \mathbf{A}(\tau)\mathbf{A}'(\tau)^\top + \mathbf{M}\mathbf{X}(\tau) + \mathbf{X}(\tau)\mathbf{M}^\top - \mathbf{e}_i\mathbf{A}(\tau)^\top - \mathbf{A}(\tau)\mathbf{e}_i^\top &= \mathbf{0} \\ \iff \mathbf{X}'(\tau) + \mathbf{M}\mathbf{X}(\tau) + \mathbf{X}(\tau)\mathbf{M}^\top - \mathbf{e}_i\mathbf{A}(\tau)^\top - \mathbf{A}(\tau)\mathbf{e}_i^\top &= \mathbf{0} \end{aligned}$$

Define the Laplace transform $\mathcal{X}(s) \equiv \mathcal{L}\{\mathbf{X}(\tau)\}(s)$. Then we have

$$\left[\frac{1}{2}s\mathbf{I} + \mathbf{M} \right] \mathcal{X}(s) + \mathcal{X}(s) \left[\frac{1}{2}s\mathbf{I} + \mathbf{M} \right]^\top = \mathbf{e}_i\mathcal{A}(s)^\top + \mathcal{A}(s)\mathbf{e}_i^\top$$

since $\mathbf{X}(0) = \mathbf{0}$. This is a Lyapunov equation. A sufficient condition for a unique solution $\mathcal{X}(s)$ is if all the eigenvalues of $\left[\frac{1}{2}s\mathbf{I} + \mathbf{M} \right]$ have positive real parts.

Analogously, define $\tilde{\mathbf{X}}(\tau)$ and $\tilde{\mathcal{X}}(s)$, and the same steps as above imply

$$\left[\frac{1}{2}s\mathbf{I} + \mathbf{M} \right] \tilde{\mathcal{X}}(s) + \tilde{\mathcal{X}}(s) \left[\frac{1}{2}s\mathbf{I} + \mathbf{M} \right]^\top = \mathbf{e}_i\tilde{\mathcal{A}}(s)^\top + \tilde{\mathcal{A}}(s)\mathbf{e}_i^\top + \mathbf{e}_d\mathbf{e}_d^\top$$

since $\tilde{\mathbf{X}}(0) = (-\mathbf{e}_d)(-\mathbf{e}_d^\top) = \mathbf{e}_d\mathbf{e}_d^\top$.

With this notation, we have that

$$\begin{aligned}\int_0^T \alpha(\tau; \alpha_0, \alpha_1) \mathbf{A}(\tau) \mathbf{A}(\tau)^\top d\tau &= \alpha_0 \mathcal{X}(\alpha_1) \\ \int_0^T \theta(\tau; \theta_0, \theta_1) \mathbf{A}(\tau)^\top d\tau &= -\theta_0 \theta_1^2 \mathcal{A}'(\theta_1)^\top\end{aligned}$$

and similarly for terms involving $\tilde{\mathbf{A}}(\tau)$.

With a slight abuse of notation, define the following matrices:

$$\begin{aligned}\mathcal{X} &\equiv \alpha_0 \mathcal{X}(\alpha_1) \\ \tilde{\mathcal{X}} &\equiv \tilde{\alpha}_0 \tilde{\mathcal{X}}(\tilde{\alpha}_1) \\ \mathcal{Y} &\equiv \begin{bmatrix} \vdots \\ -\theta_{0k} \theta_{1k}^2 \mathcal{A}'(\theta_{1k})^\top \\ \vdots \end{bmatrix} \\ \tilde{\mathcal{Y}} &\equiv \begin{bmatrix} \vdots \\ -\tilde{\theta}_{0k} \tilde{\theta}_{1k}^2 \tilde{\mathcal{A}}'(\tilde{\theta}_{1k})^\top \\ \vdots \end{bmatrix}\end{aligned}$$

All of these matrices are implicitly determined by \mathbf{M} . Hence we can write the equation characterizing \mathbf{M} , equation (A4), as the solution of a root-finding problem:

$$\begin{aligned}F(\mathbf{M}) &= \mathbf{0} \\ F(\mathbf{M}) &= \mathbf{\Gamma}^\top - a \left\{ \mathcal{Y} - \mathcal{X} + \tilde{\mathcal{Y}} - \tilde{\mathcal{X}} \right\} \mathbf{\Sigma} - \mathbf{M}\end{aligned}$$

C.2 Moment-Matching Exercise

We estimate the unknown parameters to minimize the distance between the model-implied and empirical moments. Collecting the unknown parameters into a vector $\boldsymbol{\rho}$, we estimate the model by choosing $\hat{\boldsymbol{\rho}}$ to minimize the weighted sum of square residuals:

$$L(\boldsymbol{\rho}) = \sum_{n=1}^N w_n (\hat{m}_n - m_n(\boldsymbol{\rho}))^2,$$

where $\{\hat{m}_n\}_n$ represents the moments from the data, and $\{m_n(\boldsymbol{\rho})\}_n$ the model-implied counterparts as a function of the calibration parameters. The terms w_n represent the weights placed on each target moment. We set the weight to one for moments which are not a function of maturity, and to $1/\mathcal{N}_T$ for moments that are a function of maturity, where \mathcal{N}_T is the number of maturities. In order to compute second moments in the model,

note that the long-run variance and auto-covariance of the state is given by

$$\begin{aligned} Var[\mathbf{y}_t] &= vec^{-1} [(\mathbf{\Gamma} \oplus \mathbf{\Gamma})^{-1} vec(\mathbf{\Sigma})] \equiv \mathbf{\Sigma}^\infty \\ Cov[\mathbf{y}_{t+s}, \mathbf{y}_t] &= \exp(-\mathbf{\Gamma}s) \mathbf{\Sigma}^\infty \end{aligned}$$

and computing covariances of any model object is immediate due to the linearity in the model. For instance, the standard deviation of 10-year yields is given by

$$\sqrt{Var[y_t^{(10)}]} = \frac{1}{10} \sqrt{\mathbf{A}(10)^\top \mathbf{\Sigma}^\infty \mathbf{A}(10)}$$

We target the following set of moments:

- The volatility of 1-year Treasury yields, 1-year Corporate-Treasury spread, output gap, and inflation (in levels, 1-year changes, and 1-month changes).
- The correlation of inflation and the 1-year Treasury yield, the correlation of output gap and 1-year Corporate-Treasury spread, and the correlation of inflation and the output gap (in levels).
- The volatility of the entire term structure of Treasury yields (1-year changes and 1-month changes).
- The correlation of the entire term structure of Treasury yields and the 1-year Treasury yields (1-year changes and 1-month changes).
- The localization regression coefficients from Figure 8.

Besides the localization regression coefficients, the data is monthly. Inflation is defined as the year-over-year log change in the Personal Consumption Expenditure price index. The output gap is defined as the cyclical component of Industrial Production using an HP filter. Zero-coupon Treasury yields are from [Gürkaynak et al. \(2007\)](#). Zero-coupon corporate bond yields are from the Treasury’s “HQM” data. We utilize the HQM data in order to capture the borrowing rates which are important for macroeconomic activity; however, these rates reflect relatively safe corporate rates. We explore the sensitivity of the model to different levels of payoff risk. Besides the localization regression coefficients, moments are computed starting in 1986, the start of the availability of 30-year zero-coupon Treasury yields in the [Gürkaynak et al. \(2007\)](#) data.

C.3 Localization Proofs

Definitions and terminology: In order to compare the effects of demand factors j and k , we compare their relative effects on bond prices. Suppose demand factor k is more concentrated on long-maturity bonds compared to demand factor j ($\theta_1^j > \theta_1^k$). Consider

the effect of factor k on long-maturity bonds relative to its own effects on short-maturity bonds. If this relative movement is the same as factor j , then we say that demand factors have “global” effects on the yield curve. If instead the relative effect of factor k on long-maturity bonds is larger than that of factor j (and similarly, the relative effect of factor j on short-maturity bonds is larger than that of factor k), we say that demand factors have “local” effects on the yield curve.

We formalize this logic as follows. Let

$$\mathcal{B}_j(s, t) \equiv \frac{\mathcal{A}_j(s)}{\mathcal{A}_j(t)} \quad (\text{C1})$$

This vector is the weighted average response of bond prices with Laplace frequency parameter s , relative to the weighted average response of bond prices with Laplace frequency parameter t . The weights in the Laplace transform are given by $e^{-s\tau}$, so $s > t$ implies that $\mathcal{A}_j(s)$ has more weight on short-maturity bonds than $\mathcal{A}_j(t)$. Hence, if $s > t$ and $\mathcal{B}_j(s, t) > \mathcal{B}_k(s, t)$, then we have that the j -demand factor has a relatively larger impact on short-maturity yields, compared to the k -demand factor. If $s < t$ and $\mathcal{B}_j(s, t) > \mathcal{B}_k(s, t)$, then we have that the j -demand factor has a relatively larger impact on long-maturity yields, compared to the k -demand factor.

Hence, demand factors have “global” effects if $\mathcal{B}_j(s, t) = \mathcal{B}_k(s, t)$ for all demand factors j, k and frequency weights s, t . Demand factors have “local” effects if $\mathcal{B}_j(s, t) > \mathcal{B}_k(s, t)$ for demand factors j, k such that $\theta_1^j > \theta_1^k$ and frequency weights $s > t$.

Before stating and proving our results formally, we preview and discuss the results. Proposition 1 shows that demand shocks have global effects when arbitrageurs approach risk-neutrality ($a \rightarrow 0$) or when demand factors are risk-free ($\sigma_\beta = 0$). Proposition 1 further shows that the first-order effects of increasing risk aversion do not lead to a localization of demand shocks. That is, in a neighborhood around $a = 0$, increasing risk aversion does change the global nature of demand shocks.

Proposition 2 shows that the second-order effects of increasing risk aversion increase the localization of demand shocks. That is, for large enough values of risk aversion $a \gg 0$, demand shocks become localized. Proposition 2 also shows that with infinite risk aversion, demand shocks become fully localized. Note that this is a “discontinuous” result; the model is no longer arbitrage-free.

Assumptions:

1. The “general equilibrium” effects of imperfect arbitrage are not too large near $a = 0$: $\lim_{a \rightarrow 0} d^n/da^n (\mathbf{\Gamma}) \approx 0$.
2. The state dynamics and correlation matrices are diagonal: $\mathbf{\Gamma} = \text{diag} \left[\dots \ \gamma_{j,j} \ \dots \right]$ and $\mathbf{\Sigma} = \text{diag} \left[\dots \ \sigma_{j,j}^2 \ \dots \right]$.

3. Demand factors are identical besides the location of $\theta(\tau)^k$. That is, $\theta_0^j = \theta_0^k$, $\gamma_{j,j} = \gamma_{k,k}$, and $\sigma_{j,j}^2 = \sigma_{k,k}^2$ for $j, k > 1$.
4. There are no risky asset habitat demand traders: $\tilde{\alpha}(\tau) = 0$ and $\tilde{\theta}(\tau) = 0$.

Assumption 1 and 2 are for analytical tractability (and for instance hold trivially in partial equilibrium models such as Vayanos and Vila (2021)). Note that Assumption 1 does not imply that demand factors have no macroeconomic implications, but only assumes that changes in risk aversion in a neighborhood around risk-neutrality do not lead to changes in the dynamics of the model. Assumption 3 implies that besides the location in maturity space, demand factors are symmetric. Assumption 4 is also for tractability, and allows us to focus only on localization effects across maturities.

In order to simplify notation, define $\lim_{a \rightarrow 0} \frac{d^n}{da^n}(x) \equiv d_0^n x$ for any model object x . Assumption 1 implies that as $a \rightarrow 0$,

$$\begin{aligned}\mathbf{M} &\rightarrow \mathbf{\Gamma}^\top \\ d_0 \mathbf{M} &= \{\mathcal{X} - \mathcal{Y}\} \mathbf{\Sigma} \\ d_0^n \mathbf{M} &= n \{d_0^{n-1} \mathcal{X} - d_0^{n-1} \mathcal{Y}\} \mathbf{\Sigma}\end{aligned}$$

and hence we can recursively solve for all derivatives with respect to a at $a = 0$.

With these assumptions, we have that as $a \rightarrow 0$, \mathbf{M} is also diagonal and so is $s\mathbf{I} + \mathbf{M}$. To simplify notation, define the vector and matrix equations

$$[\mathbf{g}(s)]_i \equiv \frac{1}{s + \gamma_{i,i}}, \quad [\mathbf{G}(s)]_{i,j} \equiv \frac{1}{s + \gamma_{i,i} + \gamma_{j,j}} \quad (\text{C2})$$

and note that Assumption 3 implies that for all $j, k, m, n > 1$:

$$\mathbf{g}_j(s) = \mathbf{g}_k(s), \quad \mathbf{G}_{j,k}(s) = \mathbf{G}_{m,n}(s)$$

Using this notation, we have that

$$\lim_{a \rightarrow 0} \mathcal{A}(s) \equiv \mathcal{A}^0(s) = \frac{1}{s} \cdot \mathbf{g}(s) \circ \mathbf{e}_r = \left[\frac{1}{s(s+\gamma_{11})} \quad 0 \quad \dots \quad 0 \right]^\top \quad (\text{C3})$$

$$\lim_{a \rightarrow 0} \mathcal{A}'(s) \equiv \mathcal{A}^{0'}(s) = -\mathbf{g}(s) \circ \left[\frac{1}{s^2} \mathbf{e}_r + \mathcal{A}(s) \right] = \left[-\frac{2s+\gamma_{11}}{s^2(s+\gamma_{11})^2} \quad 0 \quad \dots \quad 0 \right]^\top \quad (\text{C4})$$

where \circ denotes the Hadamard (element-wise) product. Further,

$$d_0^n \mathcal{A}(s) = -\mathbf{g}(s) \circ \sum_{k=0}^{n-1} \binom{n}{k} d_0^{n-k} \mathbf{M} d_0^k \mathcal{A}(s) \quad (\text{C5})$$

$$d_0^n \mathcal{A}'(s) = -\mathbf{g}(s) \circ \left(d_0^n \mathcal{A}(s) + \sum_{k=0}^{n-1} \binom{n}{k} d_0^{n-k} \mathbf{M} d_0^k \mathcal{A}'(s) \right) \quad (\text{C6})$$

We also can characterize the limit of $\mathcal{X}(s)$:

$$\lim_{a \rightarrow 0} \mathcal{X}(s) \equiv \mathcal{X}^0(s) = \mathbf{G}(s) \circ (\mathbf{e}_r \mathcal{A}(s)^\top + \mathcal{A}(s) \mathbf{e}_r^\top) \quad (\text{C7})$$

and recursively the derivatives are found from:

$$\mathbf{d}_0^n \mathcal{X}(s) = \mathbf{G}(s) \circ \left(\mathbf{e}_r \mathbf{d}_0^n \mathcal{A}(s)^\top + \mathbf{d}_0^n \mathcal{A}(s) \mathbf{e}_r^\top \sum_{k=0}^{n-1} (\mathbf{d}_0^{n-k} \mathbf{M} \mathbf{d}_0^k \mathcal{X}(s) + \mathbf{d}_0^k \mathcal{X}(s) \mathbf{d}_0^{n-k} \mathbf{M}^\top) \right) \quad (\text{C8})$$

In particular, equations (C4) and (C7) imply:

$$\begin{aligned} \lim_{a \rightarrow 0} [\mathcal{X}]_{i,j} &= \begin{cases} 2\alpha_0 \mathcal{A}_1^0(\alpha_1) \mathbf{G}_{1,1}(\alpha_1) & \text{if } i = j = 1 \\ 0 & \text{otherwise} \end{cases} \\ \lim_{a \rightarrow 0} [\mathcal{Y}]_{i,j} &= \begin{cases} -\theta_0^j (\theta_1^j)^2 \mathcal{A}_1^{0'}(s) & \text{if } i > 1, j = 1 \\ 0 & \text{otherwise} \end{cases} \\ \Rightarrow [\mathbf{d}_0 \mathbf{M}]_{i,j} &= \begin{cases} 2\sigma_{1,1}^2 \alpha_0 \mathcal{A}_1^0(\alpha_1) \mathbf{G}_{1,1}(\alpha_1) & \text{if } i = j = 1 \\ \sigma_{1,1}^2 \theta_0^j (\theta_1^j)^2 \mathcal{A}_1^{0'}(s) & \text{if } i > 1, j = 1 \\ 0 & \text{otherwise} \end{cases} \end{aligned}$$

So $\mathbf{d}_0 \mathbf{M}$ is zero everywhere except the first column, which we denote $\mathbf{d}_0 \mathbf{M}_1$. Then

$$\mathbf{d}_0 \mathcal{A}(s) = -\mathbf{g}(s) \circ \mathbf{d}_0 \mathbf{M}_1 \cdot \mathcal{A}_1^0(s) \quad (\text{C9})$$

$$\mathbf{d}_0 \mathcal{A}'(s) = -\mathbf{g}(s) \circ \mathbf{d}_0 \mathbf{M}_1 \circ (\mathcal{A}_1^{0'}(s) - \mathbf{g}(s) \cdot \mathcal{A}_1^0(s)) \quad (\text{C10})$$

and

$$\mathbf{d}_0^2 \mathcal{A}(s) = -\mathbf{g}(s) \circ (\mathbf{d}_0^2 \mathbf{M}_1 \cdot \mathcal{A}_1^0(s) + 2\mathbf{d}_0 \mathbf{M}_1 \cdot \mathbf{d}_0 \mathcal{A}_1^0(s)) \quad (\text{C11})$$

$$\mathbf{d}_0^2 \mathcal{A}'(s) = -\mathbf{g}(s) \circ (\mathbf{d}_0^2 \mathbf{M}_1 \cdot (\mathcal{A}_1^{0'}(s) - \mathbf{g}_1(s) \mathcal{A}_1^0(s)) + 2\mathbf{d}_0 \mathbf{M}_1 \cdot (\mathbf{d}_0 \mathcal{A}_1^{0'}(s) - \mathbf{g}_1(s) \mathbf{d}_0 \mathcal{A}_1^0(s))) \quad (\text{C12})$$

The following Lemma derives some useful algebraic properties of the model.

Lemma 1. *For $n \geq 2$, the ratio*

$$\frac{\mathbf{d}_0^n \mathcal{A}_j(s)}{\mathbf{d}_0 \mathcal{A}_j(s)} = n \frac{\mathbf{d}_0^{n-1} \mathcal{A}_1(s)}{\mathcal{A}_1^0(s)} + \frac{\mathbf{d}_0^n \mathbf{M}_{j,1}}{\mathbf{d}_0 \mathbf{M}_{j,1}} + \frac{\sum_{k=1}^{n-2} \binom{n}{k} [\mathbf{d}_0^{n-k} \mathbf{M} \mathbf{d}_0^k \mathcal{A}(s)]_j}{\mathbf{d}_0 \mathbf{M}_{j,1} \mathcal{A}_1^0(s)} \quad (\text{C13})$$

Proof. We have that

$$\frac{\mathbf{d}_0^n \mathcal{A}_j(s)}{\mathbf{d}_0 \mathcal{A}_j(s)} = \frac{[\sum_{k=0}^{n-1} \binom{n}{k} \mathbf{d}_0^{n-k} \mathbf{M} \mathbf{d}_0^k \mathcal{A}(s)]_j}{\mathbf{d}_0 \mathbf{M}_{j,1} \mathcal{A}_1^0(s)}$$

Since $d_0 \mathbf{M}$ is zero everywhere besides the first column, we have that $d_0 \mathbf{M} \mathbf{x}(s) = d_0 \mathbf{M}_1 \cdot \mathbf{x}_1(s)$ for any vector function $\mathbf{x}(s)$. Hence

$$\frac{[d_0 \mathbf{M} d_0^n \mathcal{A}(s)]_j}{d_0 \mathbf{M}_{j,1} \mathcal{A}_1^0(s)} = \frac{d_0^n \mathcal{A}_1(s)}{\mathcal{A}_1^0(s)}$$

which is independent of j .

Since $\mathcal{A}^0(s)$ is zero everywhere besides the first element, we have that $\mathbf{Q} \mathcal{A}^0(s) = \mathbf{Q}_1 \cdot \mathcal{A}_1^0(s)$ for any matrix \mathbf{Q} , where \mathbf{Q}_1 is the first column of \mathbf{Q} . Hence

$$\frac{[d_0^n \mathbf{M} \mathcal{A}^0(s)]_j}{d_0 \mathbf{M}_{j,1} \mathcal{A}_1^0(s)} = \frac{d_0^n \mathbf{M}_{j,1}}{\mathbf{M}_{j,1}}$$

which is independent of s .

In particular, equation (C13) implies that for $n = 2$, the ratio is additively separable in the demand factor index j and the Laplace frequency weight s .

□

Proposition 1 (“Global” Demand Shocks). *Demand shocks have “global” effects under (near) risk-neutrality, or when demand is risk-free.*

(a) *For any demand factors j, k and Laplace frequency parameters s, t , we have that*

$$\lim_{a \rightarrow 0} (\mathcal{B}_j(s, t) - \mathcal{B}_k(s, t)) = 0$$

(b) *Assume $\Sigma_{j,j} = 0$ for all demand factors j (but $\sigma_r^2 > 0$ and $a > 0$). For any demand factors j, k and Laplace frequency parameters s, t , we have that*

$$\mathcal{B}_j(s, t) = \mathcal{B}_k(s, t)$$

(c) *For any demand factors j, k and Laplace frequency parameters s, t , we have that*

$$\lim_{a \rightarrow 0} \frac{d}{da} (\mathcal{B}_j(s, t) - \mathcal{B}_k(s, t)) = 0$$

Proof. (a) For $j > 1$, $\mathcal{A}_j(s) = 0$ when $a = 0$, so apply L'Hopital's rule to equation (C1):

$$\lim_{a \rightarrow 0} \mathcal{B}_j(s, t) = \frac{d_0 \mathcal{A}_j(s)}{d_0 \mathcal{A}_j(t)} \tag{C14}$$

Equation (C9) implies that the ratio

$$\frac{d_0 \mathcal{A}_j(s)}{d_0 \mathcal{A}_j(t)} = \frac{\mathbf{g}_j(s) \mathcal{A}_1^0(s)}{\mathbf{g}_j(t) \mathcal{A}_1^0(t)}$$

and from Assumption 3, $\mathbf{g}_j(s) = \mathbf{g}_k(s)$ for any $j > 1, k > 1$. Hence

$$\frac{d_0 \mathcal{A}_j(s)}{d_0 \mathcal{A}_j(t)} = \frac{d_0 \mathcal{A}_k(s)}{d_0 \mathcal{A}_k(t)}$$

and the result follows.

A useful corollary of this result that $\lim_{a \rightarrow 0} \mathcal{B}_j(s, t) > 0$, since $\mathcal{A}_1(s) > 0$ and $\mathbf{g}(s) > 0$ (element-wise).

- (b) When demand is risk-free, Σ is zero everywhere except for the first element (equal to σ_r^2). Hence, we have that

$$a \cdot \{\mathcal{X} - \mathcal{Y}\} \Sigma = a\sigma_r^2 \cdot \begin{bmatrix} \mathcal{X}_1 - \mathcal{Y}_1 & \mathbf{0} & \dots & \mathbf{0} \end{bmatrix}$$

where $\mathcal{X}_1, \mathcal{Y}_1$ are the first columns of \mathcal{X} and \mathcal{Y} . Since Γ is diagonal, for any $a > 0$, $\mathbf{M} \equiv \Gamma^\top + a \cdot \{\mathcal{X} - \mathcal{Y}\} \Sigma$ is zero everywhere except the first column and diagonal. Therefore, the $j > 1$ element of $\mathcal{A}(s)$ is given by

$$\begin{aligned} \mathcal{A}_j(s) &= \frac{1}{s} [(s\mathbf{I} + \mathbf{M})^{-1}]_{j,1} = \frac{a\sigma_r^2(\mathcal{Y}_{j,1} - \mathcal{X}_{j,1})}{s(s + \gamma_{j,j})(s + \gamma_{1,1} + a\sigma_r^2\mathcal{X}_{1,1})} \\ \implies \mathcal{B}_j(s, t) &= \frac{t(t + \gamma_{j,j})(t + \gamma_{1,1} + a\sigma_r^2\mathcal{X}_{1,1})}{s(s + \gamma_{j,j})(s + \gamma_{1,1} + a\sigma_r^2\mathcal{X}_{1,1})} \end{aligned}$$

Then the result follows since $\gamma_{j,j} = \gamma_{k,k}$ for $j, k > 1$ (by Assumption 3).

- (c) Differentiating equation (C1) (and applying L'Hopital's rule and removing terms equal to zero in the limit) gives

$$d_0 \mathcal{B}_j(s, t) = \frac{d_0^2 \mathcal{A}_j(s) d_0 \mathcal{A}_j(t) - d_0^2 \mathcal{A}_j(t) d_0 \mathcal{A}_j(s)}{2 d_0 \mathcal{A}_j(t)^2}$$

Equation (C14) and the corollary from the proof of (a) implies

$$\lim_{a \rightarrow 0} \mathcal{B}_j(s, t) = \frac{d_0 \mathcal{A}_j(t)}{d_0 \mathcal{A}_j(s)} = \frac{d_0 \mathcal{A}_k(t)}{d_0 \mathcal{A}_k(s)} = \lim_{a \rightarrow 0} \mathcal{B}_k(s, t) > 0$$

Hence

$$\begin{aligned} \frac{d_0 \mathcal{A}_j(t)}{d_0 \mathcal{A}_j(s)} d_0 \mathcal{B}_j(s, t) &= \frac{1}{2} \left(\frac{d_0^2 \mathcal{A}_j(s)}{d_0 \mathcal{A}_j(s)} - \frac{d_0^2 \mathcal{A}_j(t)}{d_0 \mathcal{A}_j(t)} \right) \\ \frac{d_0 \mathcal{A}_j(t)}{d_0 \mathcal{A}_j(s)} d_0 \mathcal{B}_k(s, t) &= \frac{1}{2} \left(\frac{d_0^2 \mathcal{A}_k(s)}{d_0 \mathcal{A}_k(s)} - \frac{d_0^2 \mathcal{A}_k(t)}{d_0 \mathcal{A}_k(t)} \right) \end{aligned}$$

From the Lemma 1, we have that

$$\frac{1}{2} \frac{d_0^2 \mathcal{A}_j(s)}{d_0 \mathcal{A}_j(s)} = \frac{1}{2} \frac{d_0^2 \mathbf{M}_{j,1}}{d_0 \mathbf{M}_{j,1}} + \frac{d_0 \mathcal{A}_1(s)}{\mathcal{A}_1^0(s)}$$

which is additively separable in terms which are a function of j and s . The result follows. \square

Proposition 2 (“Localized” Demand Shocks). *Demand shocks have “local” effects far from risk-neutrality, and are fully localized under infinite risk aversion.*

(a) Suppose $\Sigma_{j,j} > 0$. For any demand factors j, k and Laplace frequency parameters s, t , we have that

$$\lim_{a \rightarrow 0} \operatorname{sgn} \frac{d^2}{da^2} (\mathcal{B}_j(s, t) - \mathcal{B}_k(s, t)) = \operatorname{sgn}(s - t)(\theta_1^j - \theta_1^k)$$

(b) When risk aversion $a = \infty$:

$$\frac{d \log P_t^{(\tau)}}{d\beta_t^k} = \frac{\theta^k(\tau)}{\alpha(\tau)}, \quad \frac{d \log P_t^{(\tau)}}{dr_t} = 0$$

Proof. (a) Differentiating equation (C1) (and applying L’Hopital’s rule and removing terms equal to zero in the limit) gives

$$\begin{aligned} d_0^2 \mathcal{B}_j(s, t) = & \frac{1}{6 d_0 \mathcal{A}_j(t)^3} (3 d_0^2 \mathcal{A}_j(t)^2 d_0 \mathcal{A}_j(s) - 3 d_0^2 \mathcal{A}_j(s) d_0^2 \mathcal{A}_j(t) d_0 \mathcal{A}_j(t) + \\ & 2 d_0^3 \mathcal{A}_j(s) d_0 \mathcal{A}_j(t)^2 - 2 d_0^3 \mathcal{A}_j(t) d_0 \mathcal{A}_j(t) d_0 \mathcal{A}_j(s)) \end{aligned}$$

Using the results from Prop 1, we can scale and rewrite as

$$\begin{aligned} \frac{d_0 \mathcal{A}_j(t)}{d_0 \mathcal{A}_j(s)} d_0^2 \mathcal{B}_j(s, t) &= \frac{1}{3} \left(\frac{d_0^3 \mathcal{A}_j(s)}{d_0 \mathcal{A}_j(s)} - \frac{d_0^3 \mathcal{A}_j(t)}{d_0 \mathcal{A}_j(t)} \right) + \frac{1}{2} \left(\frac{d_0^2 \mathcal{A}_j(t)}{d_0 \mathcal{A}_j(t)} \right) \left(\frac{d_0^2 \mathcal{A}_j(t)}{d_0 \mathcal{A}_j(t)} - \frac{d_0^2 \mathcal{A}_j(s)}{d_0 \mathcal{A}_j(s)} \right) \\ \frac{d_0 \mathcal{A}_j(t)}{d_0 \mathcal{A}_j(s)} d_0^2 \mathcal{B}_k(s, t) &= \frac{1}{3} \left(\frac{d_0^3 \mathcal{A}_k(s)}{d_0 \mathcal{A}_k(s)} - \frac{d_0^3 \mathcal{A}_k(t)}{d_0 \mathcal{A}_k(t)} \right) + \frac{1}{2} \left(\frac{d_0^2 \mathcal{A}_k(t)}{d_0 \mathcal{A}_k(t)} \right) \left(\frac{d_0^2 \mathcal{A}_j(t)}{d_0 \mathcal{A}_j(t)} - \frac{d_0^2 \mathcal{A}_j(s)}{d_0 \mathcal{A}_j(s)} \right) \end{aligned}$$

and note that the final parenthetical term in each expression is identical (from Prop 3).

Focusing on the third-order terms, from Lemma 1 we have that

$$\frac{1}{3} \frac{d_0^3 \mathcal{A}_j(s)}{d_0 \mathcal{A}_j(s)} = \frac{d_0^2 \mathcal{A}_1(s)}{\mathcal{A}_1^0(s)} + \frac{1}{3} \frac{d_0^3 \mathbf{M}_{j,1}}{\mathbf{M}_{j,1}} + \frac{[d_0^2 \mathbf{M} d_0 \mathcal{A}(s)]_j}{d_0 \mathbf{M}_{j,1} \mathcal{A}_1^0(s)}$$

The final term in the sum can be written

$$\frac{[\mathrm{d}_0^2 \mathbf{M} \mathrm{d}_0 \mathcal{A}(s)]_j}{\mathrm{d}_0 \mathbf{M}_{j,1} \mathcal{A}_1^0(s)} = \sum_{m=1}^J \left[\frac{[\mathrm{d}_0^2 \mathbf{M}]_{j,m}}{\mathrm{d}_0 \mathbf{M}_{j,1}} \right] \cdot \left[\frac{\mathrm{d}_0 \mathcal{A}_m(s)}{\mathcal{A}_1^0(s)} \right] \equiv \mathbf{u}_j^\top \mathbf{v}(s)$$

and hence

$$\frac{1}{3} \left(\frac{\mathrm{d}_0^3 \mathcal{A}_j(s)}{\mathrm{d}_0 \mathcal{A}_j(s)} - \frac{\mathrm{d}_0^3 \mathcal{A}_j(t)}{\mathrm{d}_0 \mathcal{A}_j(t)} \right) - \frac{1}{3} \left(\frac{\mathrm{d}_0^3 \mathcal{A}_k(s)}{\mathrm{d}_0 \mathcal{A}_k(s)} - \frac{\mathrm{d}_0^3 \mathcal{A}_k(t)}{\mathrm{d}_0 \mathcal{A}_k(t)} \right) = [\mathbf{u}_j - \mathbf{u}_k]^\top [\mathbf{v}(s) - \mathbf{v}(t)]$$

Further, from Lemma 1,

$$\begin{aligned} \left(\frac{\mathrm{d}_0^2 \mathcal{A}_j(t)}{\mathrm{d}_0 \mathcal{A}_j(t)} - \frac{\mathrm{d}_0^2 \mathcal{A}_k(t)}{\mathrm{d}_0 \mathcal{A}_k(t)} \right) &= \frac{\mathrm{d}_0^2 \mathbf{M}_{j,1}}{\mathrm{d}_0 \mathbf{M}_{j,1}} - \frac{\mathrm{d}_0^2 \mathbf{M}_{k,1}}{\mathrm{d}_0 \mathbf{M}_{k,1}} \\ &\equiv [\mathbf{u}_j - \mathbf{u}_k]_1 \\ \frac{1}{2} \left(\frac{\mathrm{d}_0^2 \mathcal{A}_j(t)}{\mathrm{d}_0 \mathcal{A}_j(t)} - \frac{\mathrm{d}_0^2 \mathcal{A}_j(s)}{\mathrm{d}_0 \mathcal{A}_j(s)} \right) &= \frac{\mathrm{d}_0 \mathcal{A}_1(t)}{\mathcal{A}_1^0(t)} - \frac{\mathrm{d}_0 \mathcal{A}_1(s)}{\mathcal{A}_1^0(s)} \\ &\equiv -[\mathbf{v}(s) - \mathbf{v}(t)]_1 \end{aligned}$$

Therefore, we have that

$$\frac{\mathrm{d}_0 \mathcal{A}_j(t)}{\mathrm{d}_0 \mathcal{A}_j(s)} \left(\mathrm{d}_0^2 \mathcal{B}_j(s, t) - \mathrm{d}_0^2 \mathcal{B}_k(s, t) \right) = \sum_{m=2}^J [\mathbf{u}_j - \mathbf{u}_k]_m [\mathbf{v}(s) - \mathbf{v}(t)]_m$$

Dealing with each vector separately: first, we have that

$$\begin{aligned} \mathbf{v}(s) &= \frac{\mathrm{d}_0 \mathcal{A}(s)}{\mathcal{A}_1^0(s)} = -\mathbf{g}(s) \circ \mathrm{d}_0 \mathbf{M}_1 \\ \implies \mathbf{v}(s) - \mathbf{v}(t) &= -\mathrm{d}_0 \mathbf{M}_1 \circ (\mathbf{g}(s) - \mathbf{g}(t)) \end{aligned}$$

Next, the j, m element of $\mathrm{d}_0^2 \mathbf{M}$ is

$$[\mathrm{d}_0^2 \mathbf{M}]_{j,m} = (\alpha_0 [\mathrm{d}_0 \mathbf{X}]_{j,m} + \theta_0^j (\theta_1^j)^2 \mathrm{d}_0 \mathcal{A}'_m(\theta_1^j)) \sigma_{m,m}^2$$

(and recall that $\theta_0^1 = 0$). We have that

$$\begin{aligned} \frac{[\mathrm{d}_0 \mathbf{X}]_{j,m}}{\mathrm{d}_0 \mathbf{M}_{j,1}} &= \begin{cases} -(\mathbf{g}_j(\alpha_1) \mathcal{A}_1^0(\alpha_1) + \mathcal{X}_{1,1}^0(\alpha_1)) \mathbf{S}_{j,1}(\alpha_1) & \text{if } m = 1 \\ 0 & \text{otherwise} \end{cases} \\ &= \frac{[\mathrm{d}_0 \mathbf{X}]_{k,m}}{\mathrm{d}_0 \mathbf{M}_{k,1}} \end{aligned}$$

where the second equality follows from Assumption 3.

Recall $d_0 \mathbf{M}_{j,1} = \sigma_r^2 \theta_0^j (\theta_1^j)^2 [d_0 \mathcal{A}'(\theta_1^j)]_1$, hence we can write

$$\begin{aligned} -\frac{\theta_0^j (\theta_1^j)^2}{d \mathbf{M}_{j,1}} d_0 \mathcal{A}'(\theta_1^j) &= -d_0 \mathbf{M}_1 \circ \mathbf{g}(\theta_1^j) \circ \left(1 + \mathbf{g}(\theta_1^j) \frac{\theta_1^j}{1 + \theta_1^j \mathbf{g}_1(\theta_1^j)} \right) \\ &\equiv -d_0 \mathbf{M}_1 \circ \mathbf{h}(\theta_1^j) \end{aligned}$$

Therefore,

$$[\mathbf{u}_j - \mathbf{u}_k] = -d_0 \mathbf{M}_1 \circ (\mathbf{h}(\theta_1^j) - \mathbf{h}(\theta_1^k))$$

which implies

$$[\mathbf{u}_j - \mathbf{u}_k] \circ [\mathbf{v}(s) - \mathbf{v}(t)] = (d_0 \mathbf{M}_1)^2 \circ (\mathbf{h}(\theta_1^j) - \mathbf{h}(\theta_1^k)) \circ (\mathbf{g}(s) - \mathbf{g}(t))$$

Hence, the sign of any element of the above vector is determined by the (element-wise) behavior of the functions \mathbf{g}, \mathbf{h} . From equation (C2), the function $\mathbf{g}_m(s)$ is decreasing in s for any element m . Further,

$$\begin{aligned} \mathbf{h}_m(x) &= \frac{3x^2 + 2(\gamma_{m,m} + \gamma_{1,1}) + \gamma_{m,m}\gamma_{1,1}}{(x + \gamma_{m,m})^2(2x + \gamma_{1,1})} \\ \implies \mathbf{h}'_m(x) &= -\frac{2x(x + \gamma_{1,1})(\gamma_{1,1} + \gamma_{m,m} + 3x)}{(x + \gamma_{m,m})^3(2x + \gamma_{1,1})^2} \end{aligned}$$

so $\mathbf{h}_m(x)$ is also decreasing in x for any element m . Thus, we have that

$$\text{sgn} [(\mathbf{h}_m(\theta_1^j) - \mathbf{h}_m(\theta_1^k)) \cdot (\mathbf{g}_m(s) - \mathbf{g}_m(t))] = \text{sgn}(\theta_1^j - \theta_1^k) \cdot (s - t)$$

and therefore the sum over the $m \geq 2$ elements has the same sign. The result follows.

- (b) If $a = \infty$, arbitrageurs invest their entire wealth in the risk-free rate and hence hold no long-maturity bonds: $X_t^{(\tau)} = 0$ for all τ and t . Thus market clearing implies that habitat investors also take zero positions: $Z_t^{(\tau)} = 0$. Thus, the results follow from differentiating equation (6) with respect to any demand factor β_t^k or short rate r_t and setting to zero.

□

Appendix D Data Appendix

This data appendix briefly describes the data sources used in our paper.

Treasury auctions: Information on the dates and details of treasury auctions is freely available from TreasuryDirect.gov. Data on announcements and results are available starting in 1979. Data on amounts accepted and tendered by bidder are available since 2003. Allotment by investor class begins in 2000.

Bond data: We obtain intraday secondary market data on U.S. Treasuries through GovPX, a dataset maintained by NEX Data. This data can be obtained through Wharton Research Data Services (WRDS) by subscription, and can be purchased by individuals or subscribing research institutions. A previous version of this paper used intraday Treasury futures to construct our shock series. This data is available for purchase directly from the Chicago Mercantile Exchange (CME). Our GovPX data covers the period 1995 through 2017. Zero-coupon Treasury yields are from [Gürkaynak et al. \(2007\)](#). Zero-coupon corporate bond yields are from the Treasury’s “HQM” data, available from FRED.

Federal funds futures: We make use of federal funds futures, which are traded on the Chicago Mercantile Exchange. This data can be purchased directly through CME, or as part of a subscription to a data repository that provides it. Refinitiv Datastream provides data on federal funds futures traded on the Chicago Mercantile Exchange since 1994.

Asset prices: Daily historical data on inflation swaps, commodity prices, spreads, and credit default swaps are obtained through an institutional subscription to Refinitiv Datastream. Individual researchers may also purchase access to Datastream. Intraday historical data on equities (LQD, SPY, IWM, GLD in Table 4) are derived from the NYSE Trades and Quotes (TAQ) database, which is available to individual or institutional subscribers in WRDS. The coverage of these series varies, and is shown in the right-most column of Table 4.

Macroeconomic aggregates: Data on macroeconomic variables (industrial production and PCE inflation) were downloaded from FRED.